

Optimal Application Conditions for Variable Temperature Solvent Injection into Sands and Carbonates for Heavy-Oil and Bitumen Recovery

by

Hector Leyva Gomez

A thesis submitted in partial fulfillment of the requirements for the degree of

Doctor of Philosophy

in

Petroleum Engineering

Department of Civil and Environmental Engineering
University of Alberta

© Hector Leyva Gomez, 2016

Abstract

Steam injection is the most common technique in heavy-oil/bitumen recovery. However, the emission of greenhouse gases into the atmosphere, its water requirements, and excessive operational cost associated entail finding alternative solutions. One approach is combining steam and solvent injection by taking advantage of steam injection, preheating the reservoir for a more effective solvent recovery application. In this case, the performance of subsequent solvent injection strictly depends on the temperature and pressure in the reservoir. Recent experimental studies on superheated solvent injection showed that solvent in the gas formed near the saturation line yields an optimal recovery, minimizing the asphaltene precipitation and maximizing the recovery. This research investigates this process through a numerical modeling exercise and experiments under solvent injection to formulate the optimal pressure and temperature conditions for different reservoir conditions and hydrocarbon solvents.

We first report the results of numerical simulation of previous laboratory experiments performed elsewhere, in which heavy-oil was exposed to solvent vapours at high temperatures. The injection of propane into sand packs or consolidated sandstones at elevated temperatures was simulated and a sensitivity analysis was carried out to identify the key parameters in the processes. Our results and observations showed that exist a critical temperature that yields a maximum recovery and its value depends on the solvent considered and the pressure and temperature of the experiment.

Next, a hypothetical field scale numerical model was constructed and the key parameters identified during the aforementioned sensitivity analysis were incorporated. Then, injection process was simulated for a two-horizontal injection/production pattern. An optimization study

was performed to identify the relative contributions of the effective parameters (pressure, temperature, and injection rate) and to propose an optimal application scheme using genetic algorithm. The critical pressure and temperature yielding maximum production and highest profit considering solvent retrieval were defined for different injection rates and application scenarios.

Finally, we conducted a series of dynamic experiments in which liquid solvent (propane, heptane, and distilled oil) was injected into heavy oil saturated artificially fractured Berea sandstone, Indiana limestone, and naturally fracture vuggy carbonate samples with and without pre-thermal injection. To account for the effect of wettability on the process, experiments with Berea sandstone were repeated on the samples exposed to wettability alteration (more oil-wet) process.

During the experiments, hot solvent was injected continuously through artificially fractured cores followed by hot water (or steam injection) phase. The optimal temperatures for heavy oil recovery and solvent retrieval, in the subsequent hot water injection, for each kind of rock sample and type of solvent were determined. Our results showed that heavy oil recovery increase was due not only to temperature but also to the solvent carbon number. When the temperature is higher than the saturation curve, the recovery decreases and the lightest component of the heavy oil are dragged out the core by the gas stream. Additionally, it was observed that for a successful solvent retrieval by hot water injection, temperature of water should be equal to or higher than the saturation temperature of liquid solvent, retained in the rock matrix.

This thesis is dedicated to

Cecilia, Eduardo, Mónica and Jorge

This thesis is because of you!

Acknowledgements

I would like to thank Dr. Tayfun Babadagli for sharing his precious time, patience and knowledge with me through my PhD studies. It was an honor being part of the Enhanced Oil and Gas Recovery and Reservoir Characterization Research Group. Thanks to all the former and current members (colleagues, technicians and assistants) of this group.

My gratitude to Dr. Rodolfo G. Camacho Velázquez for his mentorship: Also, to Martín Velázquez Franco, for sharing his expertise and advice.

My deepest appreciation to PEMEX Exploración y Producción for giving me the opportunity to study a PhD as well as Conacyt-Sener-Hidrocarburos Fund for providing the financial support. Thanks to México.

This research was financially supported by Dr. Tayfun Babadagli's NSERC Industrial Research in Unconventional Oil Recovery (industrial partners were Schlumberger, CNRL, SUNCOR, Touchstone Exploration (Petrobank), Sherritt Oil, PEMEX, Statoil, Husky Energy, Saudi Aramco and APEX Eng.) and NSERC Discovery Grant (No: RES0011227). CMG also provided the software that was intensively used in this research.

I give thanks to my wonderful wife, Cecilia. Her encouragement and unconditional support contributed to making this possible. Also, thanks to my kids, Eduardo, Mónica and Jorge for giving me the joy of living.

I want to give thanks to J. Ramón Mayorquín Ruíz and his family for being wonderful friends. And last but not the least to Francisco Javier Argüelles-Vivas who filled my days with laughter.

Thanks God for allowing me share these new experiences with my family and friends.

TABLE OF CONTENTS

Chapter 1 : Introduction.....	1
1.1 Introduction.....	2
1.2 Literature review.....	3
1.3 Statement of the problem and objectives.....	6
1.4 Solution methodology.....	7
1.5 Outline.....	8
1.6 References.....	9
Chapter 2: Numerical Simulation of Heavy-Oil/bitumen Recovery by Solvent Injection at Elevated Temperatures	12
2.1 Summary.....	13
2.2 Introduction.....	13
2.3 Statement of the problem.....	16
2.4 Description of the model.....	16
2.4.1 History matching.....	19
2.4.2 Prediction of recovery factor	25
2.5 Analysis of the results.....	28
2.6 Up-scaling to field conditions.....	30
2.7 Conclusions and recommendations	32
2.8 Nomenclature.....	33
2.9 References.....	33
Chapter 3 : High -Temperature Solvent Injection for Heavy-Oil Recovery from Oil Sands: Determination of Optimal Application Conditions through Genetic Algorithm.....	36
3.1 Summary.....	37

3.2 Introduction.....	37
3.3 Description of the problem and solution methodology	38
3.4 Reservoir model.....	39
3.5 Objective function.....	46
3.6 Results and discussion	48
3.7 Conclusions.....	58
3.8 Nomenclature.....	59
3.9 References.....	60

Chapter 4 : Hot Solvent Injection for Heavy Oil/Bitumen Recovery from Fractured Reservoirs: An Experimental Approach to Determine Optimal Application Conditions ... 63

4.1 Summary.....	64
4.2 Introduction.....	64
4.3 Description of the problem and solution methodology	65
4.4 Experimental setup and procedures	66
4.5 Results.....	72
4.6 Conclusions.....	84
4.7 Nomenclature.....	85
4.8 References.....	85

Chapter 5 : Heavy Oil/Bitumen Recovery from Fracture Carbonates by Hot-Solvent Injection: An Experimental Approach to Determine Optimal Application Conditions 89

5.1 Summary.....	90
5.2 Introduction.....	90
5.3 Description of the problem and solution methodology	92
5.4 Experimental setup and procedures	92

5.5 Results.....	100
5.6 Analysis of results.....	104
5.7 Conclusions.....	112
5.8 Nomenclature.....	113
5.9 References.....	114
5.10Appendix.....	116
Chapter 6 : Summary, Contributions and recomendations.....	121
6.1 Summary of the research	122
6.2 Scientific and practical contributions to the literature and industry	123
6.3 Suggested future work	125

LIST OF TABLES

Table 2-1. Summary of the experimental details reported by Pathak et al. (2010, 2011a-b).	18
Table 2-2. Heavy oil composition.....	19
Table 2-3. Values of MSC for simulation using Propane.....	25
Table 2-4. Values of MSC for simulation using Butane.....	25
Table 2-5. Scaling of soaking time and core height, reported by Pathak et al. (2010, 2011a-b), and from simulation.	31
Table 3-1. Main parameters used in the simulation model.....	41
Table 3-2. Parameters to be optimized.	43
Table 3-3. Genetic algorithm configuration.....	46
Table 3-4. Costs considered in the objective function.....	48
Table 3-5. Best combination of parameters yielding maximum economic benefit injecting propane.....	51
Table 3-6. Best combination of parameters yielding maximum economic benefit injecting butane.....	51
Table 3-7. Solvent cost	55
Table 4-1. Oil and core properties.	68
Table 4-2. Heptane composition.....	70
Table 5-1. Oil and core properties.	94
Table 5-2. Heptane composition.....	95
Table 5-3. Naphtha composition.....	95
Table 5-4. Normal boiling point for some alkanes (Ahmed 1989).....	112

LIST OF FIGURES

Figure 1-1. Methodology proposed for this study	8
Figure 2-1. Grid model used for the simulation.....	17
Figure 2-2. Viscosity model used to match the data of the oil produced in the previous experiments provided by Pathak et al. (2010).	20
Figure 2-3. Oil accumulated in the collecting area and average pressure for a particular case....	20
Figure 2-4. Oil recovered and pressure for experiments in which the drainage valve was opened.	20
Figure 2-5. Match of the experiments given in Table 2-1 at 1500 kPa.	21
Figure 2-6. Match of the experiments given in Table 2-1 at 54 °C.....	21
Figure 2-7. Match of the experiments given in Table 2-1 at 53 °C.....	21
Figure 2-8. Match of the experiments given in Table 2-1 at 52 °C.....	21
Figure 2-9. Match of the experiments given in Table 2-1 at different pressures.....	22
Figure 2-10. Match of the experiments given in Table 2-1 at 98 °C.....	22
Figure 2-11. Flow restriction factor (FRF) and its trend, used to match the experiments with propane.....	22
Figure 2-12. Flow restriction factor (FRF) and its trend, used to match the experiments with butane.....	22
Figure 2-13. Reaction rate factor (RR) and its trend, used to match the experiments with propane.	23
Figure 2-14. Reaction rate (RR) factor and its trend, used to match the experiments with butane.	23
Figure 2-15. Final oil drained using propane at 500, 1650 and 1830 kPa.	26
Figure 2-16. Final oil drained using Butane at 1500, 1650 and 1830 kPa.....	26
Figure 2-17. Final drained oil into region 2 using propane as a solvent, for 1500 kPa and three different core heights and temperatures.....	26

Figure 2-18. Final drained into region 2 oil using butane as a solvent, for 1500 kPa and three different core heights and temperatures.	26
Figure 2-19. Total solids precipitated in the system vs. time. Propane at 1500 kPa at three different temperatures and heights.	26
Figure 2-20. Total solids precipitated in the system vs. time using butane at 1500 kPa at three different temperatures and heights.	26
Figure 2-21. Total drained oil into region 2. Propane at 1500 kPa and its saturation temperature for three different core heights at 100 min.	27
Figure 2-22. Total drained oil into region 2. Propane at 1650 kPa and its saturation temperature for three different core heights at 100 min.	27
Figure 2-23. Total drained oil into region 2. Propane at 1830 kPa and its saturation temperature for three different core heights at 100 min.	27
Figure 2-24. Total drained oil into region 2. Butane at 1500 kPa and its saturation temperature for three different core heights at 60 min.	27
Figure 2-25. Total drained oil into region 2. Butane at 1650 kPa and its saturation temperature for three different core heights at 60 min.	27
Figure 2-26. Total drained oil into region 2. Butane at 1830 kPa and its saturation temperature for three different core heights at 60 min.	27
Figure 2-27. Total asphaltene precipitated and produced with drained oil. Propane as a solvent for 1500 kPa and three different core heights.	28
Figure 2-28. Total asphaltene precipitated and produced with drained oil. Butane as a solvent for 1500 kPa and three different core heights.	28
Figure 3-1. Entire well pattern and half well pattern used in the study showing the grid model of 70×1×50 cells and the two horizontal wells.	40
Figure 3-2. Restriction factor, adapted from Leyva and Babadagli (2011).	42
Figure 3-3. Frequency of solid precipitation, adapted from Leyva and Babadagli (2011).	42
Figure 3-4. Continuous injection with simultaneous production scheme.	44
Figure 3-5. Intermittent injection scheme with simultaneous and continuous production.	44

Figure 3-6. Alternated injection production scheme with simultaneous and continuous production.	45
Figure 3-7. Injection-soaking-production scheme.	45
Figure 3-8. Progress of the main parameters during the optimization processes of scheme No. 1, injecting propane.	50
Figure 3-9. Progress of the main parameters during the optimization processes of scheme No. 2, injecting propane.	50
Figure 3-10. Progress of the main parameters during the optimization processes of scheme No. 3, injecting propane.	50
Figure 3-11. Progress of the main parameters during the optimization processes of scheme No. 4, injecting propane.	50
Figure 3-12. Progress of the main parameters during the optimization processes of scheme No. 4, injecting propane.	50
Figure 3-13. Progress of the main parameters during the optimization processes of scheme No. 2, injecting butane.	50
Figure 3-14. Progress of the main parameters during the optimization processes of scheme No. 3, injecting butane.	51
Figure 3-15. Progress of the main parameters during the optimization processes of scheme No. 4, injecting butane.	51
Figure 3-16. Economic benefit and RF injecting for propane. Note that MRF and Gross profit are negative.	52
Figure 3-17. Economic benefit and RF injecting butane. Note that MRF and Gross profit are negative.	54
Figure 3-18 Breakeven point for propane.	56
Figure 3-19 Breakeven point for butane.	56
Figure 3- 20. Maximum economic benefit with 100% solvent retrieved.	56
Figure 4-1. Artificial fractures in sandstone cores, used in the experiments.	67
Figure 4-2. Experimental setup.	69
Figure 4-3. Comparison of recovery factor for experiments performed at 21°C.	71
Figure 4-4. Comparison of recovery factor for experiments performed at 21°C.	71

Figure 4-5. Comparison of recovery factor for experiments performed at 45 and 90°C for core and heptane, respectively	71
Figure 4-6. Oil recovery factor at 100°C from a core in horizontal position.....	73
Figure 4-7. Oil accumulation at the bottom of the core, inside the sleeve at the outlet of the sleeve.....	73
Figure 4-8. Oil diluted produced from experiment performed at 45°C. Water-wet rock matrix..	74
Figure 4-9. Solvent retrieval for experiment performed at 45°C. Water-wet rock matrix.	74
Figure 4-10. Oil diluted produced from experiment at 70°C. Water-wet rock matrix.	75
Figure 4-11. Solvent retrieval for experiment at 70°C. Water-wet rock matrix.....	75
Figure 4-12. Oil diluted produced from experiment at 100°C. Water-wet rock matrix.	75
Figure 4-13. Solvent retrieval for experiment at 100°C. Water-wet rock matrix.....	75
Figure 4-14. Oil diluted produced from experiment at 130°C. Water-wet rock matrix.	75
Figure 4-15. Solvent retrieval for experiment at 130°C. Water-wet rock matrix.....	75
Figure 4-16. Oil diluted produced from experiment at 45°C using oil-wet rock matrix.....	76
Figure 4-17. Solvent retrieval for experiment at 45°C using oil-wet rock matrix.....	76
Figure 4-18. Oil diluted produced from experiment at 70°C using oil-wet rock matrix.....	76
Figure 4-19. Solvent retrieval for experiment at 70°C using oil-wet rock matrix.....	76
Figure 4-20. Oil diluted produced from experiment at 100°C using oil-wet rock matrix.....	76
Figure 4-21. Solvent retrieval for experiment at 100°C using oil-wet rock matrix.....	76
Figure 4-22. Oil diluted produced from experiment at 130°C using oil-wet rock matrix.....	77
Figure 4-23. Solvent retrieval for experiment at 130°C using oil-wet rock matrix.....	77
Figure 4-24. Oil recovery from all experiments, expressed as % of OOIP for different temperatures.....	79
Figure 4-25. Oil recovery from rock matrix from all experiments. Note that oil from fracture space is not included.	79

Figure 4-26. Oil diluted produced from experiments using Berea sandstone (water-wet).....	81
Figure 4-27. Solvent retrieval for experiments using Berea sandstone (oil-wet) treated chemically.....	81
Figure 4-28. Density at 25°C of oil produced from Berea sandstone cores in vertical position. .	82
Figure 4-29. Density at 25°C of oil produced from oil-wet Berea sandstone cores in vertical position.....	82
Figure 4-30. Percentage of solvent retrieval vs. temperature. Cumulative values shown include both solvent from the oil diluted and condensate from the solvent vapour.	83
Figure 5-1. Bioclastic wackestone cores with moldic porosity, open fractures, and partially sealed from a Mexican outcrop field.	93
Figure 5-2. Cores after saturation processes: a) Indiana limestone core after joint the four sections with bonding putty. b) Naturally fracture carbonate core before joint the four sections with bonding putty.	94
Figure 5-3. Experimental set up used to perform experiments with either heptane or naphtha at low pressure.	96
Figure 5-4. Experimental set up used to perform experiments with either propane at high pressure.	97
Figure 5-5. Pressure and temperature conditions for experiments performed with propane and heptane.	98
Figure 5-6. Pressure and temperature conditions for experiments performed with naphtha.	98
Figure 5-7. Oil produced from experiment performed at 70°C with Indiana limestone and heptane.	101
Figure 5-8. Solvent retrieval for experiment performed at 70°C with Indiana limestone and heptane.	101
Figure 5-9. Oil recovered from experiments performed with heptane and Indiana limestone. .	101
Figure 5-10. Solvent retrieved from experiments performed with heptane and Indiana limestone.	101

Figure 5-11. Oil recovered from experiments performed with naphtha and Indiana limestone.	102
Figure 5-12. Solvent retrieved from experiments performed with naphtha and Indiana limestone.	102
Figure 5-13. Oil recovered from experiments performed with propane and Indiana limestone.	103
Figure 5-14. Solvent retrieved from experiments performed with propane and Indiana limestone.	103
Figure 5-15. Fluid produced during experiment performed at 21°C at a lower injection rate and low temperature. Note the oil traces at the bottom of test tube.	103
Figure 5-16. Fluids produced during experiment performed at 35°C. Solvent injected in liquid form.	103
Figure 5-17. Oil recovered from experiments performed with heptane and distilled oil, naturally vuggy fracture carbonate cores.	104
Figure 5-18. Solvent retrieved from experiments performed with heptane and distilled oil, naturally vuggy fracture carbonate cores.	104
Figure 5-19. Oil recovery factor from experiments with heptane at different temperatures. Indiana limestone and naturally fracture carbonate and heptane. Previous results from Leyva and Babadagli (2014) for Berea sandstone has been included.	105
Figure 5-20. Oil recovery factor from experiments with naphtha at different temperatures. Indiana limestone, naturally fracture carbonate, and heptane.	107
Figure 5-21. Oil recovery factor from experiments with propane at different temperatures with Indiana limestone.	108
Figure 5-22. Core after injecting heptane at 73°C showing zones that apparently were not saturated with heavy oil.	109
Figure 5-23. Trapped oil, after experiment with distillate oil at 90°C.	109
Figure 5-24. Core after injecting naphtha, showing asphaltene deposited on fractures.	110
Figure 5-25. Solvent retrieved from heptane, experiments with Indiana limestone and naturally fracture carbonate.	111

Figure 5-26. Solvent retrieved from naphtha experiments with Indiana limestone and naturally fracture carbonate.....	111
Figure 5-27. Solvent retrieved from propane experiments with Indiana limestone.	112
5-A1. Oil produced from experiment performed at 90°C with Indiana limestone and heptane.	116
5-A2. Solvent retrieval for experiment performed at 90°C with Indiana limestone and heptane.	116
5-A3. Oil produced from experiment performed at 100°C with Indiana limestone and heptane.	116
5-A4. Solvent retrieval for experiment performed at 100°C with Indiana limestone and heptane.	116
5-A5. Oil produced from experiment performed at 120°C with Indiana limestone and heptane.	117
5-A6. Solvent retrieval for experiment performed at 120°C with Indiana limestone and heptane.	117
5-A7. Oil produced from experiment performed at 21.5°C with Indiana limestone and naphtha.	117
5-A8. Solvent retrieval for experiment performed at 21.5°C with Indiana limestone and naphtha.	117
5-A9. Oil produced from experiment performed at 45°C with Indiana limestone and naphtha.	117
5-A10. Solvent retrieval for experiment performed at 45°C with Indiana limestone and naphtha.	117
5-A11. Oil produced from experiment performed at 70°C with Indiana limestone and naphtha.	118
5-A12. Solvent retrieval for experiment performed at 70°C with Indiana limestone and naphtha.	118
5-A13. Oil produced from experiment performed at 90°C with Indiana limestone and naphtha.	118

5-A14. Solvent retrieval for experiment performed at 90°C with Indiana limestone and naphtha.	118
5-A15. Oil produced from experiment performed at 100°C with Indiana limestone and naphtha.	118
5-A16. Solvent retrieval for experiment performed at 100°C with Indiana limestone and naphtha.	118
5-A17. Oil diluted and produced solvent retrieved from experiment performed at 22°C with Indiana limestone and liquid propane.	119
5-A18. Solvent retrieval for experiment performed at 35°C with Indiana limestone and liquid propane.....	119
5-A19. Oil produced and solvent retrieved from experiment performed at 35°C with Indiana limestone and liquid propane.	119
5-A20. Oil produced and solvent retrieval for experiment performed at 55°C with Indiana limestone and gaseous propane.....	119
5-A21. Oil produced and solvent retrieved from experiment performed at 60°C with Indiana limestone and gaseous propane.....	119
5-A22. Oil recovered from experiment performed at 95 °C with naturally fractured carbonate sample and heptane.	120
5-A23. Solvent retrieval for experiment performed at 95°C with naturally fractured carbonate sample and heptane.	120
5-A24. Oil produced from experiment performed at 73°C with Naturally fractured carbonate sample and naphtha.	120
5-A25. Solvent retrieval for experiment performed at 73°C with Naturally fractured carbonate sample and naphtha.....	120

Chapter 1: Introduction

1.1 Introduction

Steam Assisted Gravity Drainage (SAGD) was introduced by Butler in the early 1980s and is currently used in many field projects in Canada to recover bitumen (Government of Alberta 2011). This process requires large volumes of water for steam generation, resulting in costly post production water treatment. Thomas (2007) reported that water consumption for steam generation ranged from 200 to 500 ton/m³ of bitumen. Consequentially, the emission of CO₂ from burning natural gas to heat the water becomes a critical factor in designing steam injection processes. Due to these limitations and concerns, several thermal and non-thermal alternative techniques to SAGD that involve solvent injection have been proposed like VAPEX (Butler and Mokrys 1991, 1993). Vapour Extraction (VAPEX) is a non-thermal technique in which a gaseous solvent is injected from an upper horizontal injection well into a heavy-oil reservoir. Then, the production is enhanced by the reduction of the oil viscosity due to the diffusion of solvent into the heavy-oil. In contrast, Steam Alternating Solvent (SAS) is a process in which the steam and solvent are injected alternately (Zhao 2004). According to preliminary estimations by Li and Mamora (2011), the requirements of energy in this process are 18% lower than that of SAGD. Similarly, Zhao et al. (2004a) reported that in their lab experiments and numerical simulations, the energy requirements were reduced by 47% when solvent was used alternately with steam.

A limited number of studies have been carried out to analyze the effect of temperature on solvent injection for heavy-oil/bitumen recovery. Results obtained from these studies and observations pointed out that there exists a critical temperature that yields a maximum recovery, and this value depends on the solvent type and pressure. These studies include a detailed analysis of phase behaviour, diffusion coefficient, viscosity reduction, permeability reduction due to asphaltene precipitation, and the dependence of the recovery factor on pressure and temperature for different solvent types. However, a very limited number of studies have dealt with the optimization of this process based on detailed lab (experimental) and field scale (numerical simulation) modeling studies. Efforts have been made for sands but applications in naturally fractured carbonate reservoirs require special attention.

This research focuses on the determination of the key parameters that control the solvent injection at different pressures and temperatures in sands and carbonate reservoirs. Numerical models, supported by experiments conducted at static conditions, were used to explore the feasibility of hot solvent injection into shallow sands reservoirs. Sensitivity studies were performed for permeability reduction by asphaltene. Finally, an optimization study was performed through a numerical model output linked to a genetic algorithm to identify the relative contributions of the effective parameters (pressure, temperature, solvent type, injection/production rate, and injection schedule) and to propose an optimal application scheme.

1.2 Literature review

The VAPEX process was introduced by Butler and Mokrys (1991) as an alternative to SAGD. VAPEX is a non-thermal technique in which a gaseous solvent is injected from an upper horizontal injection well into a heavy-oil reservoir. The production is enhanced by the reduction of the oil viscosity due to the diffusion of solvent into the heavy-oil. In contrast to SAGD, VAPEX is an attractive process for thin reservoirs where the potential excessive heat loss above and below the reservoir makes steam injection impractical. In the VAPEX process, solvent is injected in the vapour form but its pressure and temperature conditions are chosen close to the dew point at reservoir conditions. Then, because the process is carried out at reservoir temperature, there is no heat loss involved and much of the residual solvent can be recovered by the reservoir pressure blow-down. While providing in-situ upgrading of oil, asphaltene precipitation may occur due to the presence of light solvent.

The main issue in the solvent injection processes like VAPEX is the diffusion rate between the heavy-oil and solvent injected. Several researchers carried out studies to determine the diffusion coefficient of solvent into heavy-oil/bitumen but this was quite a challenge as both heat and mass transfer processes were involved. Oballa and Butler (1989) studied the diffusion in a bitumen-toluene system. They investigated how the concentration of solvent and permeability affect diffusivity using a vertical cell with closely flat windows. Guerrero-Aconcha et al. (2008, 2009) studied the diffusion of propane, n-hexane, n-heptane, and n-octane into heavy-oil. They found that the diffusion coefficient of heavy-oil is a function of concentration. Luo and Kantzas (2008)

studied the diffusion coefficient of heptane in an oil saturated sand pack and concluded that the heterogeneity of porous media is an important parameter to be considered in the diffusion of fluids when heterogeneity is not negligible. Luo et al. (2007) studied the effect of volume changes due to mixing on the diffusion coefficient.

In SAGD, the recovery is enhanced due to the viscosity reduction by the heat transfer from steam into the heavy-oil/bitumen, while in VAPEX the solvent vapours diffuse through the oil reducing its viscosity and flowing down to the producer well. In the hot solvent technique, the reduction of viscosity is the result of the combined heating effect of steam or hot water and the dilution effect of solvent to give even better heavy-oil/bitumen recovery than SAGD or VAPEX alone (Edmunds et al. 2009a-b).

When hot solvent is dissolved into heavy-oil the viscosity reduction of oil is not the only physical phenomena occurring; also, the permeability reduction of porous media due to asphaltene precipitation plays a significant role. Luo and Gu (2009) found that in an oil-propane system the asphaltene precipitation occurred when the saturation pressure of the system is close to the vapour pressure of propane at 20.8°C. Castellanos-Diaz et al. (2011) evaluated the phase behaviour of solvent mixtures including propane, n-heptane, and CO₂ using conventional oil characterization methods combined with the Peng-Robinson EOS to predict saturation pressures and asphaltene precipitation of n-heptane diluted bitumen. Pathak et al. (2010, 2011a-b) observed in their laboratory experiments with mixtures of propane and butane in heavy-oil that oil recovery decreases with the increase of temperature and pressure and that the peak recovery is reached when these parameters are near the saturation line of the solvent but in the region of the gaseous phase of the solvent used.

In-situ de-asphalting reduces oil viscosity yielding upgraded oil. However, the asphaltene can reduce the permeability of rock, which results in a reduction in oil production. Hence, one has to question whether in-situ de-asphalting is beneficial for the oil recovery process (Haghighat and Maini 2008). Moreno and Babadagli (2013) reported their experimental results of a deasphalting work of heavy oil samples mixed with n-alkane solvents using a pressure-volume-temperature cell. In addition, they performed gravity drainage recovery experiments on unconsolidated sands using the same n-alkane solvents. They concluded that asphaltene precipitation increases with

decreasing carbon number of the solvent and asphaltene deposition causes a reduction in permeability due to their flocculation and agglomeration.

Naturally fractured carbonate reservoirs are complex systems. They are formed by a structure that contains faults, fractures, micro fractures, vugs, matrix with low porosity, and unfavorable wettability. Exploitation of this kind of reservoirs is difficult and challenging when combined with high viscosity oil. Several researches carried out static and dynamic experiments on fractured core carbonates to understand the dynamic of heavy-oil recovery by solvent injection into naturally carbonate reservoirs. Earlier studies include single block and multiple block systems with the matrix surrounded by fracture networks. Rostami et al. (2005) carried out a simulation work using a dual porosity fracture system, considering different injection rates at a fixed solvent injection temperature. They concluded, among other things, that in the carbonate reservoir the solvent flows faster through fractures and forms solvent fingers. Also they observed that an optimization procedure is necessary to find the optimum solvent injection rate.

Rahnema et al. (2008) conducted experiments using laboratory cells made of sand packs for fractured and non-fractured cases. They stated that the presence of fractures can compensate the low matrix permeability and enhance the whole process. Al-Bahlani and Babadagli (2009, 2011) performed static and dynamic experiments using sandstones and carbonate samples to study alternate injection of steam/hot-water and solvent for heavy-oil recovery from matrix. Their numerical simulation results indicated that large block sizes required larger solvent volumes and thereby injection rates.

A number of studies focussing on experimental analysis of solvent injection in heterogeneous media have been done. Among them, Syed et al. (2012) studied permeability reduction due to the presence of hydrocarbon gas under reservoir conditions using packstone plugs. Rezaei and Mohammadzadeh (2010) reported investigations on the recovery of bitumen using VAPEX process on a vuggy porous media, creating the vugular media by embedding wood particles in glass beads. They concluded that the presence of vugs improves the production characteristics of VAPEX. Naderi et al. (2013) and Naderi and Babadagli (2014) focused on heavy-oil recovery from heterogeneous carbonates by solvent injection alternated by steam or hot-water.

1.3 Statement of the problem and objectives

It is well known that oil viscosity can be reduced dramatically if hot solvent is added to the system. The common perception is that increasing the temperature of the injected solvent as much as possible would be the way to improve oil recovery. However, recent experiments showed that there is a temperature limit at which the oil recovery starts to decline. Hence, the sole injection of steam or solvent may not be sufficient to make any heavy-oil/bitumen recovery process successful. The possible reasons for this behaviour need to be clarified and an effective way to recover the solvent injected should be implemented.

Bringing heavy-oil to the surface from a homogeneous reservoir is difficult due to its high viscosity; however, in the case of fractured and/or vuggy carbonate reservoirs, the problem becomes more challenging because low matrix permeability and high permeability fractures. If the reservoir has a strong water drive, the problem becomes even worse due to possible conning and channeling caused by small difference in fluid densities ($\Delta\rho_{o/w}$) and their high viscosity contrast (μ_o / μ_w). Other important issues to be considered are permeability reduction due to asphaltene precipitation, and the early gas breakthrough at the production wells.

The above literature survey indicates that limited efforts have been made as to understanding the physical phenomena involved in the oil recovery process during solvent injection under isothermal conditions (or at elevated temperatures). To our knowledge, no detailed studies on the temperature effect on solvent injection have been reported despite the consensus reached on the necessity of combining thermal and solvent techniques for efficient recovery of heavy-oil.

Temperature is of particular importance if the reservoir is deep (low temperature steam injection). In addition, application of solvent injection and the determination of critical temperature to optimize recovery require more attention in fractured reservoirs (efficient matrix diffusion requires proper injection scheme to prevent any channelling) with a strong water drive support (causing conning). Thus, the objective of this research is to determine the optimal operating conditions and ideal solvent type to exploit a heavy-oil reservoir to yield maximum economic benefit.

1.4 Solution methodology

As presented in **Figure 1-1**, the methodology applied to this study was divided into three main stages: (1) experimental work, (2) numerical model of experiments, and (3) field scale numerical model and optimization

Experiments are needed to determine the diffusion capability of solvent into oil-saturated rock matrix under different conditions, mainly temperature. Previously, static experiments were performed by Pathak et al. (2010, 2011a-b). These experiments revealed some information as to the recovery potential for different solvent at different temperatures for oilsands and carbonates containing heavy-oil and bitumen, respectively. However, for optimization problems, dynamic experiments would be much more beneficial as they relate the injected solvent to produced oil, which is not obtainable from static experiments. Static experiments would be useful for more complex and time-consuming dynamic experiments in terms of narrowing down the solvent type and temperature.

The next step was to determine the many parameters that are not directly obtainable from experiment through the numerical simulation of experiments (at the original scale). These include diffusion coefficient, asphaltene deposition, and permeability reduction parameters. A history matching of the experiment at higher and lower pressure and temperature conditions using the STARS numerical simulator were carried out by tuning these parameters. Later, the experimental model was scaled up to reservoir dimensions and a sensitivity analysis was done to identify the key parameters and how they impact the heavy-oil recovery by gas injection.

The key parameters obtained from the previous two stages (i.e. diffusion coefficients, asphaltene precipitation parameter, permeability change parameter due to asphaltene, etc.) were used together to conduct field scale applications for different solvent types (propane, heptane, and distilled oil). The process was optimized using the numeric model and applying a genetic algorithm. In this application, the findings on the experiments performed and the sensitivity analysis results as well as a numerical simulation model of a real heavy-oil naturally fractured vuggy reservoir were used all together with a genetic algorithm program for optimization, written in java language

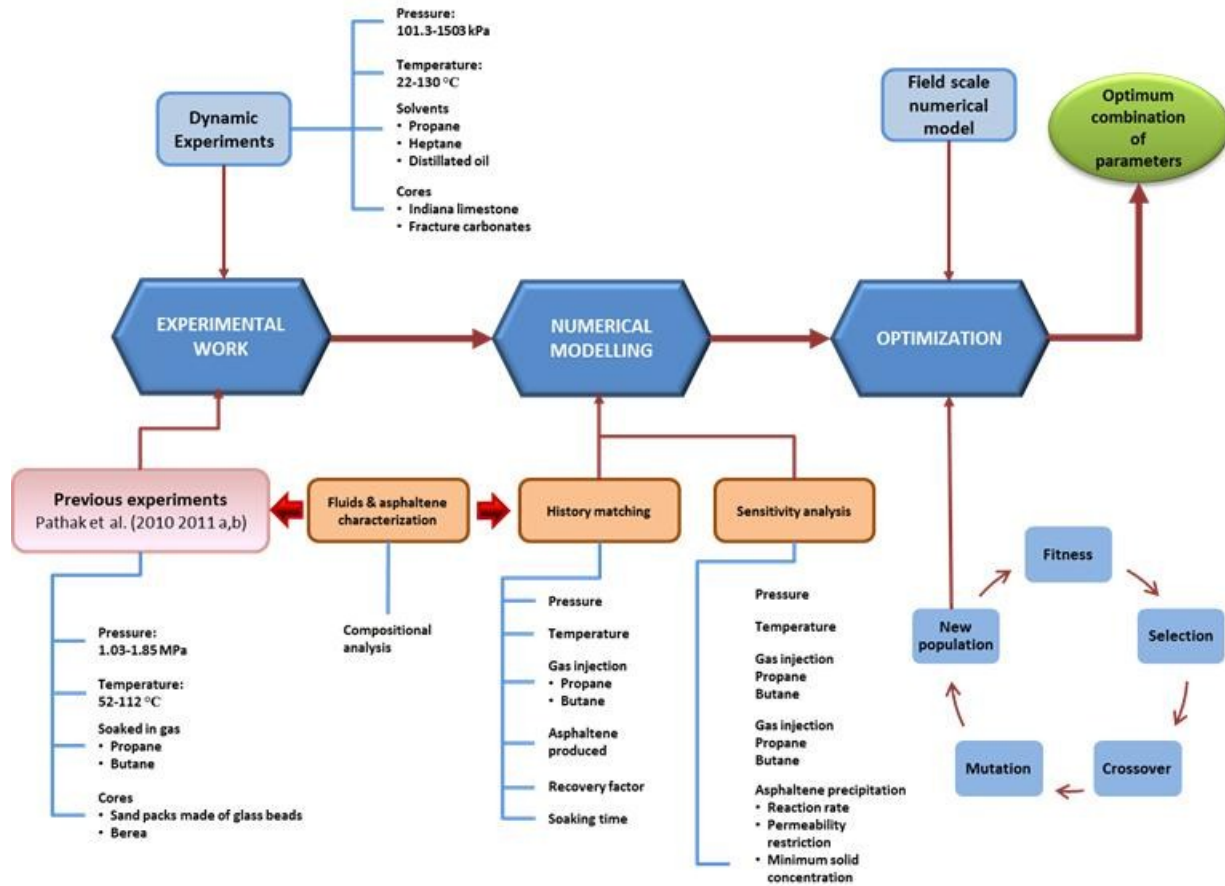


Figure 1-1. Methodology proposed for this study.

1.5 Outline

This paper-based thesis consists of four papers comprising four chapters. For each chapter, an abstract, introduction, conclusions, and references are included. An introductory chapter at the beginning (chapter 1) and a summary/contributions chapter at the end of the thesis (chapter 6) were also included.

In chapter 2, history matching to previously reported experimental results (at static conditions) are presented. As a result of this exercise, important parameters related to the asphaltene precipitation were identified (i.e. flow restriction factor, reaction rate, and minimum solid concentration). It was determined that higher recovery factor is obtained when the temperature of solvent is located close to the saturation temperature of the solvent, but in the liquid phase region.

In chapter 3, optimal operational conditions were determined for a hypothetical reservoir. In addition to temperature, parameters such as injection/production pressure, injection rate, and production scheme were involved in this reservoir scale simulation. These parameters, among others, were included in the numerical model, which in turn was linked to an optimization genetic algorithm.

Chapter 4 presents the results obtained from dynamic experiments. On these, heptane was injected through artificially fractured Berea sandstone cores for a wide range of temperatures. One more set of experiments was performed using oil-wet Berea sandstone cores.

Chapter 5 includes results from more experiments performed with propane, heptane, and distilled oil for a wide range of temperatures. For these experiments, artificially fracture Indiana limestone was used as well as naturally vuggy carbonate cores.

In chapter 6, the contributions of this dissertation to the literature and petroleum industry were outlined.

1.6 References

- Al-Bahlani A. M., Babadagli T. 2009. Steam-over-Solvent in Fracture Reservoirs (SOS-FR) for Heavy Oil Recovery: Experimental Analysis of the Mechanism. Paper SPE 123568 presented at the Asia Pacific Oil and Exhibition held in Jakarta, Indonesia, 4-6 August. [Doi:10.2118/124047-MS](https://doi.org/10.2118/124047-MS).
- Al-Bahlani A., Babadagli T. 2011. Steam-over-Solvent Injection in Fractured Reservoir (SOS-FR) Technique as a New Approach for Heavy-Oil and Bitumen Recovery: An Overview of the Method. *Energy and Fuels* **25**: 4528-4539. [Doi.10.1021/ef200809z](https://doi.org/10.1021/ef200809z).
- Butler, R.M., Mokrys, I.J. 1991. A New Process (VAPEX) for Recovering Heavy Oils using Hot Water and Hydrocarbon Vapour. *J. Can. Pet. Technol.* **30** (1): 97-110. <http://dx.doi.org/10.2118/91-01-09>.
- Butler, R.M., Mokrys, I.J. 1993. Recovery of Heavy Oils Using Vapourized Hydrocarbon Solvents: Further Development of the VAPEX Process. *J. Can. Pet. Technol.* **32** (6): 38-55. <http://dx.doi.org/10.2118/SS-92-7>.
- Castellanos Díaz, O., Modaresghazani, M.A., and Yarranton, H. W. 2011. Modelling the Phase Behaviour of Heavy Oil and Solvent Mixtures. *Fluid Phase Equilibria* **304**: 74-85. <http://dx.doi.org/10.1016/j.fluid.2011.02.011>.

- Edmunds, N., Barrett, K., Solanki, S., et al. 2009a. Prospects for Commercial Bitumen Recovery from the Grosmont Carbonate, Alberta. *J. Can. Pet. Technol.* 48 (9), 26-32. <http://dx.doi.org/10.2118/09-09-26>.
- Edmunds, N., Moini, B., Peterson, J. 2009b. Advanced Solvent-Additive Processes via Genetic Optimization. Paper PETSOC 2009-115 presented at the Canadian International Petroleum Conference (CIPC) 2009, Calgary, Alberta, Canada, 16-18 June. <http://dx.doi.org/10.2118/2009-115>.
- Government of Alberta, 2011. The Resource Recovering the Resource. Document available at www.oilsands.alberta.ca/FactSheets/About_Albertas_oil_sands.pdf-2011-07-13.
- Guerrero-Aconcha, U., Salama, D., and Kantzas, A. 2008. Diffusion Coefficient of n-alkanes in Heavy Oil. Paper SPE 115346 presented at the SPE annual Technical Conference and Exhibition, Denver, Colorado, 21-24 September. [Doi:10.2118/115346-MS](https://doi.org/10.2118/115346-MS).
- Guerrero-Aconcha, U., Kantzas, A. 2009. Diffusion of Hydrocarbon Gases in Heavy Oil and Bitumen. Paper SPE 122783 presented at the SPE Latin American and Caribbean Petroleum Engineering Conference, Cartagena, Colombia, 31 May-3 June. <http://dx.10.2118/122783-MS>.
- Haghithat P. and Maini B.B. 2008. Role of Asphaltene Precipitation in Vapex Process. Paper PETSOC 2008-087 presented at Canadian International Petroleum Conference (CIPC), Calgary, Alberta, Canada, 17-19 June. [Doi:10.2118/2008-087](https://doi.org/10.2118/2008-087).
- Li, W., Mamora and D.D. 2011. Light-and Heavy-Solvent Impacts on Solvent-Aided-SAGD Process: A Low-Pressure Experimental Study. Paper SPE 133277 presented at the Annual Technical Conference and Exhibition, Florence, Tuscany, 20-22 September. [Doi:10.2118/133277-MS](https://doi.org/10.2118/133277-MS).
- Luo, P. and Gu, Y. 2009. Characterization of a Heavy Oil-Propane System in the Presence or Absence of Asphaltene Precipitation. *Fluid Phase Equilibria* 277: 1-8. <http://dx.doi.org/10.1016/j.fluid.2008.10.019>.
- Luo, H., Salama, D., Sryuchkov, S., et al. 2007. The Effect of Volume Changes Due to Mixing on Diffusion Coefficient Determination in Heavy Oil and Hydrocarbon Solvent System. Paper SPE 110522 presented at the Annual Technical Conference and Exhibition, Anaheim, California, 11-14 November. [Doi:10.2118/110522-MS](https://doi.org/10.2118/110522-MS).
- Luo, H. and Kantzas, A. 2008. Investigation of Diffusion Coefficients of Heavy Oil and Hydrocarbon Solvent Systems in Porous Media. Paper SPE 113995 presented at the Improved Oil Recovery Symposium, Tulsa, Oklahoma, 19-23 April. [Doi:10.2118/113995-MS](https://doi.org/10.2118/113995-MS).
- Moreno, L. and Babadagli, T. 2013. Optimal Application Conditions of Solvent Injection into Oilsands to Minimize the Effect of Asphaltene Deposition: An Experimental Investigation. SPE 165531, 2013 SPE Heavy Oil Conf., Calgary, AB, Canada, 11-13 June. [Doi:10.2118/165531-MS](https://doi.org/10.2118/165531-MS).

- Naderi, K., Babadagli, T. and Coskuner, G. 2013. Bitumen Recovery by the SOS-FR (Steam-Over-Solvent Injection in Fractured Reservoirs) Method: An Experimental Study on Grosmont Carbonates. *Energy and Fuels* **27**: 6501–6517. DOI: 10.1021/ef401333u.
- Pathak, V. and Babadagli, T. 2010. Hot Solvent Injection for Heavy Oil/Bitumen Recovery: an Experimental Investigation. Paper SPE 137440 presented at the Canadian Unconventional Resources & International Petroleum Conference, Calgary, Alberta, 19-21 October. [Doi:10.2118/137440-MS](https://doi.org/10.2118/137440-MS).
- Pathak, V., Babadagli, T. and Edmunds, N.R. 2011a. Mechanics of Heavy Oil and Bitumen Recovery by Hot Solvent Injection. Paper SPE 144546 presented at the Western North American Regional Meeting, Anchorage, Alaska, 7-11 May. [Doi:10.2118/144546-PA](https://doi.org/10.2118/144546-PA).
- Pathak, V., Babadagli, T. and Edmunds, N.R. 2011b. Heavy Oil and Bitumen Recovery by Hot Solvent Injection. *J. Petr. Sci. and Eng.* **78**: 637-645. <http://dx.doi.org/10.1016/j.petrol.2011.08.002>.
- Oballa, V. and Butler, R.M. 1989. An Experimental Study of Diffusion in the Bitumen-Toluene System. *J. Can. Pet. Tech.* **28** (2): 63-69. <http://dx.doi.org/10.2118/89-02-03>.
- Rahnema, H., Kharrat, R. and Rostami, B. 2008. Experimental and Numerical Study of Vapour Extraction Process (VAPEX) in Heavy Oil Fractured Reservoir. Presented at the PETSOC-2008-116-P, Calgary, Alberta, Canada, 17-19 June. <http://dx.doi.org/10.2118/2008-116>.
- Rezaei, N. and Mohammadzadeh, O. 2010. Experimental Investigation of Vapor Extraction Process for the Recovery of Bitumen from Vuggy Porous Media. Presented at the Canadian Unconventional Resources & International Petroleum Conference, Calgary, Alberta, Canada, 19-21 October. [Doi:10.2118/2008-116](https://doi.org/10.2118/2008-116).
- Rostami, B., Azin, R. and Kharrat, R. 2005. Investigation of the Vapex Process in High-Pressure Fractured Heavy-Oil Reservoirs. Paper SPE 97766 presented at the 2005 SPE international Thermal Operations and Heavy Oil symposium, Calgary, Alberta, Canada, 1-3 November. [Doi:10.2118/97766-MS](https://doi.org/10.2118/97766-MS).
- Syed, F.I, Ghedan, S.G., Hage, A.R., et al. 2012. Formation Flow Impairment in Carbonate Reservoirs due to Asphaltene Precipitation and Deposition during Hydrocarbon Gas Flooding. Paper SPE 160253 presented at the Abu Dhabi International Petroleum Exhibition and Conference, Abu Dhabi, UAE, 11-14 November. [Doi:10.2118/160253-MS](https://doi.org/10.2118/160253-MS).
- Thomas, S. 2007. Enhanced Oil Recovery – An Overview. *Oil & Gas Science and Technology – Rev. IFP* **63** (1): 9-19. <http://dx.doi.org/10.2516/ogst:2007060>.
- Zhao, L. 2004. Steam Alternating Solvent Process. Paper SPE 86957 presented at International Thermal Operations and Heavy Oil and Western Regional Meeting, Bakersfield, California, 16-18 March. [Doi:10.2118/86957-MS](https://doi.org/10.2118/86957-MS).
- Zhao, L., Nasr, H., Huang, G., et al. 2004a. Steam Alternating Solvent Process: Lab Test and Simulation. Paper SPE 2004-044 presented at the Canadian International Petroleum Conference, Calgary, Alberta, Canada, 8-10 June. [Doi:0.2118/2004-044](https://doi.org/10.2118/2004-044).

Chapter 2: Numerical Simulation of Heavy-Oil/bitumen Recovery by Solvent Injection at Elevated Temperatures

A version of this chapter was published at the SPE Heavy Oil Conference and Exhibition, held in Kuwait City, Kuwait, 12-14 Dec. 2011 (paper SPE-150315-MS), and was also published in Journal of Petroleum Science and Engineering **110** (2013) 199-209.

2.1 Summary

Hydrocarbon solvent injection into preheated reservoirs has been suggested as an alternative to sole injection of steam or solvent for heavy-oil recovery. But, this is a highly pressure and temperature sensitive process. This paper investigates this process through a numerical modeling exercise and formulates the optimal pressure and temperature conditions for maximized recovery and minimized asphaltene precipitation.

We first report the results of numerical simulation of laboratory experiments, in which heavy-oil was exposed to solvent vapour at high temperatures. To achieve these results, a radial 3D numerical model of $15 \times 1 \times 48$ cells was constructed using a commercial numeric simulator. The injection of either propane or butane into sand packs or consolidated sandstones at elevated temperatures was simulated. A pressure-temperature sensitivity analysis was carried out for different core sizes to understand the dynamics of the gravity drainage process associated with asphaltene precipitation. Asphaltene pore plugging behaviour was modeled and diffusion of solvent into the heavy-oil was analyzed to determine both ideal solvent type and optimal operating conditions for propane or butane injection in a temperature range of 52°C to 112°C.

Our results and observations showed that the solvent should be in the gas phase and its sensitivity to temperature and sample height (for effective gravity drainage) is more critical than the pressure. There also exists a critical temperature that yields a maximum recovery and this value was determined for the rock/reservoir types and solvents considered in this study. Solvents considered, i.e., propane and butane, behaved differently in terms of asphaltene precipitation and its effects on ultimate recovery.

2.2 Introduction

Steam Assisted Gravity Drainage (SAGD) was introduced by Butler in the early 1980s and is currently used in many field projects in Canada to recover bitumen (Government of Alberta 2011). This process requires large volumes of water for steam generation, resulting in costly post production water treatment. Thomas (2007) reported that water consumption for steam generation ranged from 200 to 500 ton/m³ of bitumen. As a consequence of this, the emission of CO₂ from burning natural gas to heat the water becomes a critical factor in designing steam

injection processes. Due to these limitations and concerns, several alternative techniques to SAGD that involve solvent injection have been proposed. They include vapour extraction (VAPEX) (Butler and Mokrys 1991 and 1993b), expanding solvent SAGD (ES-SAGD) (Nasr et al. 2003), steam alternate solvent (SAS) (Zhao et al. 2004, 2004b), steam-over-solvent injection in fractured reservoirs (SOS-FR) (Al-Bahlani and Babadagli 2009, 2011a-b; Babadagli and Al-Bahlani 2008) or the injection of solvents at a higher temperature (Pathak et al. 2010, 2011a-b).

VAPEX is a non-thermal technique in which a gaseous solvent is injected from an upper horizontal injection well into a heavy-oil reservoir; then, the production is enhanced by the reduction of the oil viscosity due to the diffusion of solvent into the heavy-oil. In contrast, SAS is a process in which the steam and solvent are injected alternately (Zhao 2004). According to preliminary estimations by Li and Mamora (2011), the requirements of energy in this process are 18% lower than that of SAGD. Similarly, Zhao et al. (2005) reported that in their lab experiments and numerical simulations, the energy requirements were reduced by 47% when solvent was used alternately with steam.

In SAGD, the recovery is enhanced due to the viscosity reduction by the heat transfer from steam into the heavy-oil/bitumen, while in VAPEX the solvent vapours diffuse through the oil reducing its viscosity and flowing down to the producer well. In the hot solvent technique, the reduction of viscosity is the result of the combined heating effect of steam or hot water and the dilution effect of solvent to give even better heavy-oil/bitumen recovery than SAGD or VAPEX alone (Edmunds et al. 2009a-b).

Several researchers carried out studies to determine the diffusion coefficient of solvent into heavy-oil/bitumen but this was quite a challenge as both heat and mass transfer processes were involved in this process. Oballa and Butler (1989) studied the diffusion in a bitumen-toluene system. They investigated how the concentration of solvent and permeability affect the diffusivity using a vertical cell with closely flat windows. Guerrero-Aconcha and Kantzas (2008, 2009) studied the diffusion of propane, n-hexane, n-heptane, and n-octane into heavy-oil. They found that the diffusion coefficient of heavy-oil is a function of concentration. Luo and Kantzas (2008) studied the diffusion coefficient of heptane in an oil saturated sand pack and concluded that the heterogeneity of porous media is an important parameter to be considered in the

diffusion of fluids when heterogeneity is not negligible. Luo et al. (2007) studied the effect of volume changes due to mixing on the diffusion coefficient.

When hot solvent is dissolved into heavy-oil the viscosity reduction of oil is not the only physical phenomena occurring; the permeability reduction of porous media due to asphaltene precipitation also plays a significant role. Luo and Gu (2009) found that, in an oil-propane system, the asphaltene precipitation occurred when the saturation pressure of the system is close to the vapour pressure of propane at 20.8°C. Castellanos-Diaz et al. (2010) evaluated the phase behaviour of solvent mixtures including propane, n-heptane, and CO₂ using conventional oil characterization methods combined with the Peng-Robinson EOS to predict saturation pressures and asphaltene precipitation of n-heptane diluted bitumen. Pathak et al. (2010, 2011a-b), in their laboratory experiments with mixtures of propane and butane in heavy-oil observed that oil recovery decreases with the increase of temperature and pressure and that the peak recovery is reached when these parameters are near the saturation line of the solvent but in the region of the gaseous phase of the solvent used.

In the present work, we report the results of the numerical simulation of laboratory experiments reported in the literature, in which heavy-oil or bitumen was exposed to solvent vapour at high temperatures, ranging from 52 to 112°C. To achieve this, a radial 3D numerical model of 15×1×48 grids was constructed using a commercial numeric simulator and the exact system used in the experiments was modeled. The heavy-oil recovery under static conditions (soaking rather than continuous injection) from a volume element of oilsands by either propane or butane at elevated (and constant) temperatures mimicking solvent injection into a preheated reservoir was simulated. The difficulties and challenges in modeling and approaches used for successful history matching were outlined and discussed. Next, a pressure-temperature sensitivity analysis was carried out for different core sizes to understand the dynamics of the gravity drainage process associated with asphaltene precipitation of n-heptane diluted heavy-oil. Asphaltene pore plugging behaviour was modeled and diffusion of solvent into the heavy-oil was analyzed to determine both the ideal solvent type and the optimal operating conditions for solvent injection at high temperatures.

2.3 Statement of the problem

Sole injection of steam or solvent may not be sufficient to make any heavy-oil/bitumen recovery process successful. Their alternate injection resulting in hot solvent injection could be a solution to this problem. It is well known that the oil viscosity can be reduced dramatically if hot solvent is added to the system. The common perception is that increasing the temperature of the injected solvent as much as possible would be the way to improve the oil recovery. However, recent experiments showed that there is a temperature limit at which the oil recovery starts to decline. The possible reasons for this behaviour need to be clarified. The objective of this work is to simulate the oil recovery from sandpacks made of glass beads under the hot solvent injection process over a wide range of pressure and temperature conditions to determine what parameters control this process at different pressures and temperatures. Eventually, the optimal operating conditions and ideal solvent based on the matched experimental results are defined.

2.4 Description of the model

In the experiments performed by Pathak et al. (2010, 2011a-b), a sand pack porous system made of glass beads saturated with heavy-oil with no light components (C_6 and below) were placed inside a cylinder located in a constant temperature oven. Next, the cylinder was filled with solvent and pressure and temperature was maintained at a constant value for several hours to days depending on the size of the core sample, to expose the heavy-oil to vapours for a sufficiently long time for diffusion. The oil was collected from the lower part of the core using a collection system at the end of this period and the total oil and asphaltene recovered were reported. This represents heavy-oil recovery under static conditions (no continuous injection) driven by diffusion and gravity drainage.

In the present work, a radial 3D numerical model of $15 \times 1 \times 48$ cells was constructed to simulate this process, as shown in **Figure 2-1**. The first 10 inner cells were set at 0.25 cm wide and 0.5 cm wide for the remaining 5 outer cells. The heights of the layers 4 to 33 were changed in the same proportion to match the height of each core used in the experiments. Cells 1-3 and 34-48 were set to 1 cm height in all simulation cases. The model was divided into three regions: (1) The core saturated with 100% oil, (2) the collecting area located just below the core, and (3) the surrounding area to the core saturated with 100% propane or butane with a production well at the

top of the grid located to release the gas and pressure. The lower part with 8% porosity has the function of collecting the oil and asphaltene drained by gravity from the core. The model considers negligible capillary pressure. Linear relative permeability curves for oil and gas were adopted. The permeability of the glass bead packs was 100 D for all the cases; all other parameters reported by Pathak et al. (2010, 2011a-b) for their experimental system were used as input in the current numerical model (**Table 2-1**).

Gridding sensitivity analysis in numerical simulation is important due to the variations of certain parameters against the size of the cells. Grid size is also important from computing time point of view. As will be seen later, the volume of the oil recovered in the experiments is a function of, at least, three parameters, which have to be determined during the matching processes for every single experiment. Considering all these factors and for simplify the problem, an arbitrary but reasonable grid size was chosen and fixed during the history matching exercise.

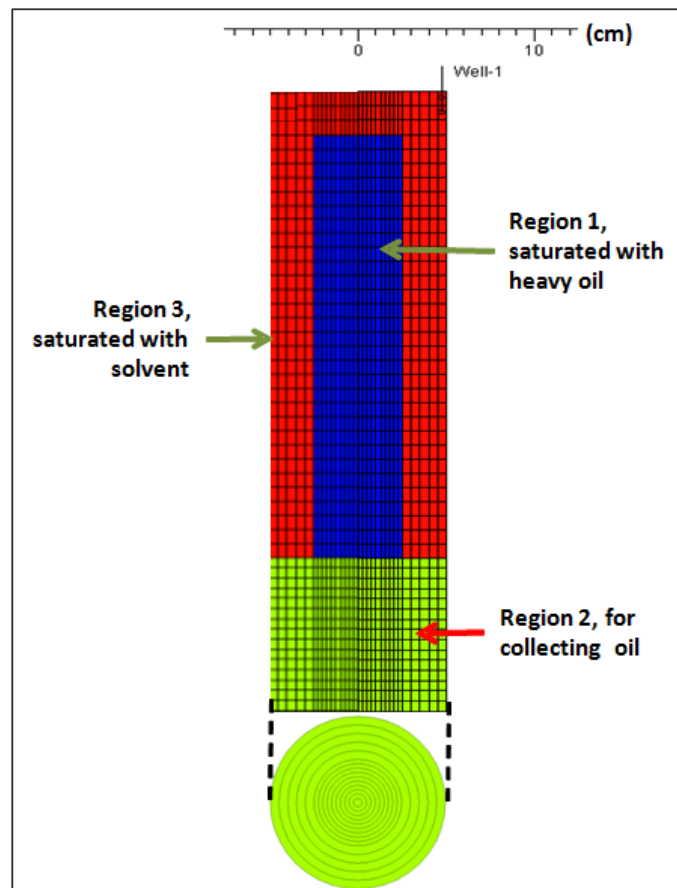


Figure 2-1. Grid model used for the simulation.

According to the findings of Guerrero-Aconcha and Kantzas (2009), the diffusion coefficient in a propane-heavy-oil system, similar to the one used by Pathak et al. (2010, 2011a-b) in their experiments, was around 7.0×10^{-6} cm²/s depending on the temperature among other parameters. Considering this value and the soaking time for the experiments (Table 2-1), the diffusion coefficient in the simulator was set to 4.60×10^{-4} and 3.492×10^{-5} cm²/s for propane and butane respectively.

Table 2-1. Summary of the experimental details reported by Pathak et al. (2010, 2011a-b).

No.	Solvent	Type*	Height (cm)	ϕ (%)	Temp (°C)	Pressure (KPa)	Recovery (%)	Approx. Soaking Time (hours)	Asphaltene recovered	
									From oil produced (weight %)	From the core (weight %)
1	Butane	GB 500 μ	29	40	70	1030	55.6	4	5.7	11.5
2	Butane	GB 500 μ	29	40	80	1030	52.6	4	6.5	11.2
3	Butane	GB 500 μ	18	30	98	1400	94.5	6	6.7	8.2
4	Butane	GB 500 μ	26	30	98	1500	72.1	12	11.3	6.4
5	Butane	GB 500 μ	10	30	98	1600	62.3	8	N/M	N/M
6	Butane	GB 500 μ	17	30	112	1500	45	7	11.3	N/M
7	Butane	GB 500 μ	17	30	108	1600	64.5	8	13.8	
8	Propane	GB 500 μ	29	40	90	1500	55.3	4	13.7	7.0
9	Propane	GB 500 μ	15	40	85	1500	53.7	4	11.4	8.5
10	Propane	GB 500 μ	17	40	67	1500	47.8	4	12.5	8.6
11	Propane	GB 500 μ	17	30	52	1500	83.8	4	10.1	6.15
12	Propane	GB 500 μ	17	30	54	1830	64.2	4	10.6	7.75
13	Propane	GB 500 μ	23	30	53	1500	75.5	10	12.3	5.35
14	Propane	GB 500 μ	27	30	53	1500	60.3	10	13.6	6.4
15	Propane	GB 500 μ	20	30	52	1500	65.5	6	N/M	N/M
16	Propane	GB 500 μ	17	30	54	1650	43.3	8	10.8	N/M
17	Propane	GB 500 μ	18	30	53	1450	74.6	8	12.7	N/M
18	Propane	GB 2400 μ	19	30	52	1450	59.9	8	N/M	N/M
19	Propane	GB 2400 μ	15	30	54	1650	40.4	7	N/M	N/M
20	Propane	Berea core	15	23	53	1500	27.5	48	N/M	N/M
21	Butane	Berea core	15	21	98	1350	44.4	28	N/M	N/M
22	Propane	Berea core	30	21	53	Started at 1600	41.12	360	14.1	N/M
23	Butane	Berea core	15	21	101	Started at 1470	63.6	240	N/M	N/M

The original oil composition used in the experiments was characterized from C₇ to C₃₁⁺ using the Peng Robinson EOS and Modified Pendersen Viscosity Model. Solvent was added to the original

composition and then was lumped into four components, following the criteria of similar molecular weights (**Table 2-2**). The heaviest component was split into a precipitating and non-precipitating components, C_{31A}^+ and C_{31B}^+ respectively, as described by Nghiem and Coombe (1997). Both components have identical properties and acentric factors but, they may have different binary interaction coefficients with light components (propane or butane in our cases). The proportion of the precipitating component (C_{31B}^+) was computed using the following relationship:

$$x_{Asph}MW_{Asph} = W_{Asph}MW_{Oil} \quad (2-1)$$

where $MW_{Asph} = 274.89$ g/mol, $MW_{Oil} = 404.0$ g/mol and x_{Asph} was obtained from the asphaltene precipitation reported in the Pathak et al. (2010, 2011a-b) experiments (Table 2-1). The amount of non-precipitating component (C_{31A}^+) was then calculated by subtracting the amount obtained above to the C_{31}^+ component. These quantities were used to simulate all the experiments reported in **Table 2-2**.

Table 2-2. Heavy oil composition.

Component	Fraction
C ₇ to C ₁₄	0.282972
C ₁₅ to C ₂₄	0.361564
C ₂₅ to C ₃₀	0.118188
C ₃₁ ⁺	0.237276

There were four experimental data points available for the viscosity of the oil produced from the experiments of Pathak et al. (2010, 2011a-b) for both propane and butane and the original oil composition. Using the WINPROP® option of the simulator, the oil-produced viscosity curves for both solvents used were modeled (**Figure 2-2**) and extrapolated to high temperatures in a wide range of pressures to be used in the STARS® option of the simulator.

2.4.1 History matching

To carry out the simulations, Regions 2 and 3 of the model were filled with solvent and the core region with heavy-oil, at the desired temperature and pressure at an initial time of t_0 (Figure 2-1).

The simulation ended when the respective soaking time (t_{soak}) was reached. Temperature was maintained at a constant value during the simulation time. Heavy-oil was accumulated in the collecting region as indicated by Region 3, located below the core. This is the exact model of the experiment given by Pathak et al. (2010). The recovery factor was calculated by dividing the accumulated oil in region 2 by the initial oil volume of region 1 and then expressed in a percentage. **Figure 2-3** shows the recovery from simulation before opening the valve to produce the collected oil. Both oil and asphaltene recovery values reported by Pathak et al. (2010) were the matching target in the experiments #1 to #21.

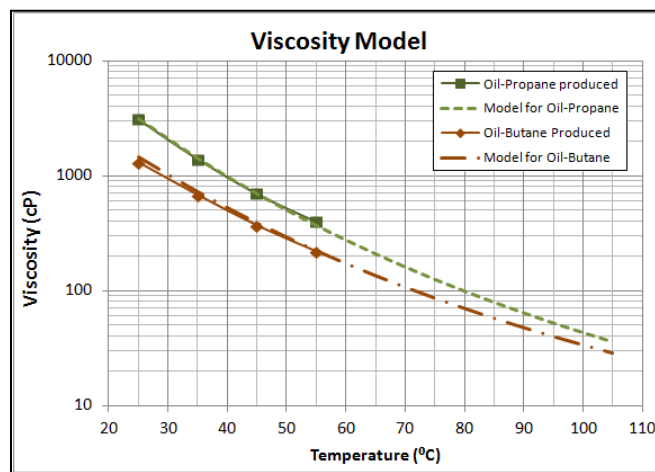


Figure 2-2. Viscosity model used to match the data of the oil produced in the previous experiments provided by Pathak et al. (2010).

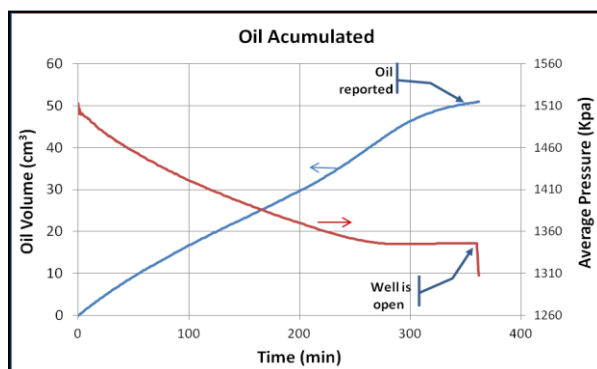


Figure 2-3. Oil accumulated in the collecting area and average pressure of the system for a particular case.

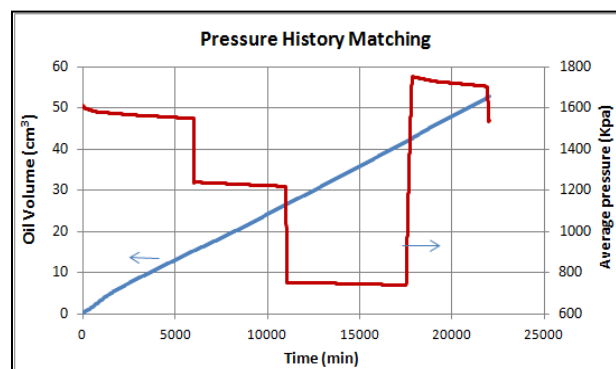


Figure 2-4. Oil recovered and pressure for experiments in which the drainage valve was opened.

The soaking times for experiments #22 and #23 were of days, and in this period of time, the drainage valve was opened to measure the amount of oil drainage from the core several times (Pathak et al., 2011a-b). These kinds of events were also included in simulations and the matching target for these two experiments were the pressure history, oil recovery and asphaltene reported by Pathak et al. (2001), **Figure 2-4**. As seen in **Figures 2-5** through **Figures 2-10**, experimental matches were reasonably accurate.

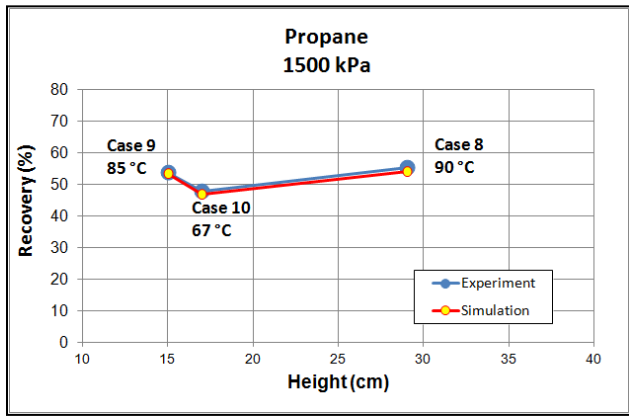


Figure 2-5. Match of the experiments given in Table 2-1 at 1500 kPa.

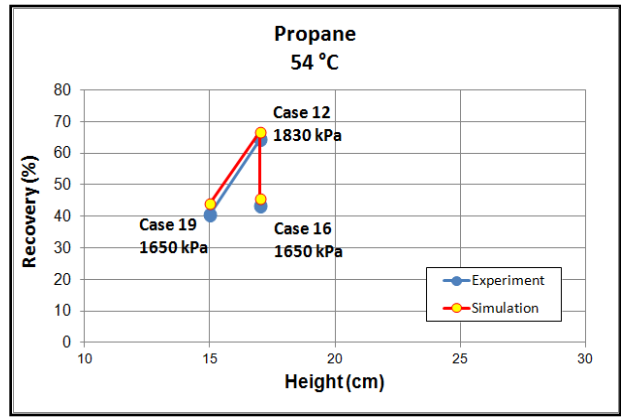


Figure 2-6. Match of the experiments given in Table 2-1 at 54°C.

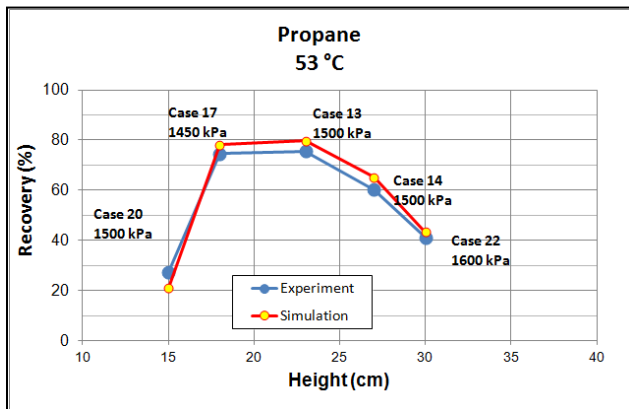


Figure 2-7. Match of the experiments given in Table 2-1 at 53°C.

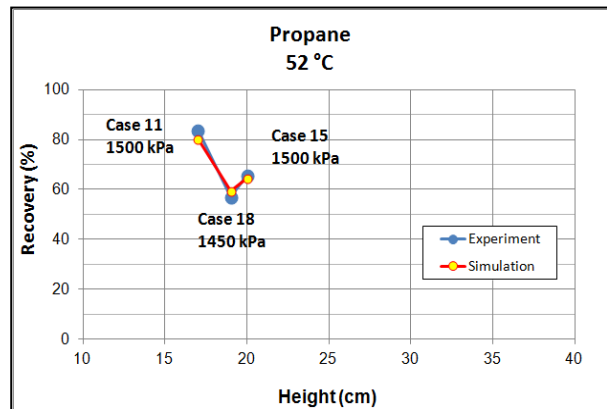


Figure 2-8. Match of the experiments given in Table 2-1 at 52°C.

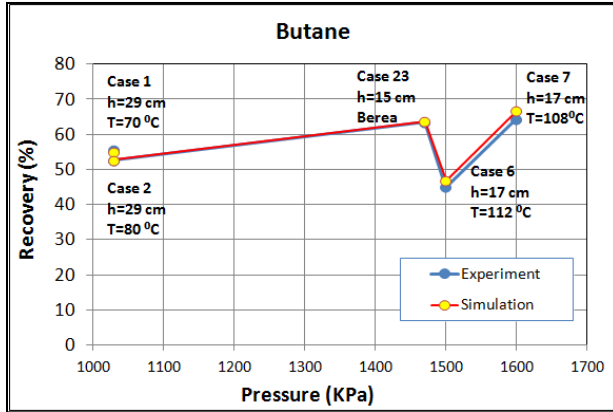


Figure 2-9. Match of the experiments given in Table 2-1 at different pressures.

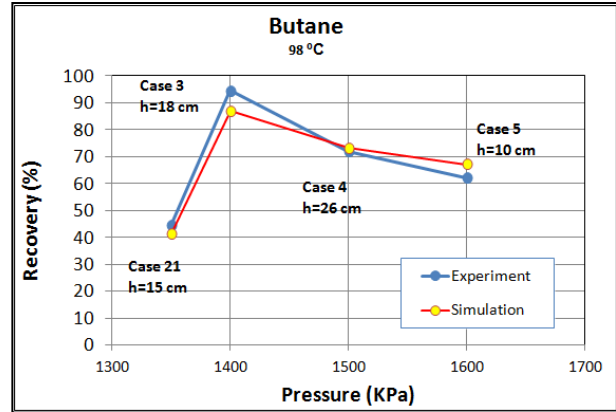


Figure 2-10. Match of the experiments given in Table 2-1 at 98 °C.

It was observed that the process is strictly sensitive to asphaltene precipitation and the pore plugging process which differs for different solvents. To match the simulation data to the experiments, the parameters reported by Pathak et al. (2001); i.e., height, porosity, temperature, pressure, type of solvent, and soaking time were used as input for each particular case. Asphaltene precipitation was taken into account by introducing into the model three parameters: The flow restriction factor (FRF) (Figures 2-11 and 2-12), Reaction Rate (RR) (Figures 2-13 and 2-14), and the Minimum Solid Concentration (MSC), which was needed in order to start the blockage. They were tuned to match the simulation data to the experimental results.

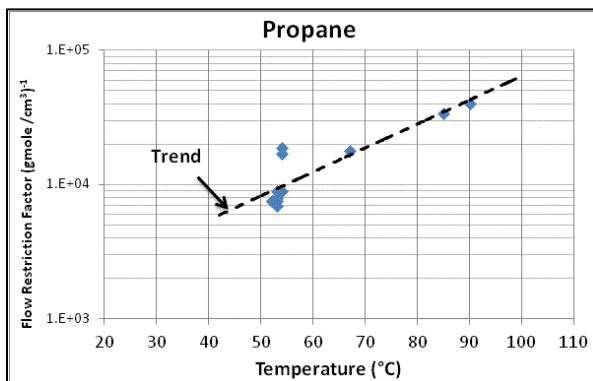


Figure 2-11. Flow restriction factor (FRF) and its trend, used to match the experiments with propane.

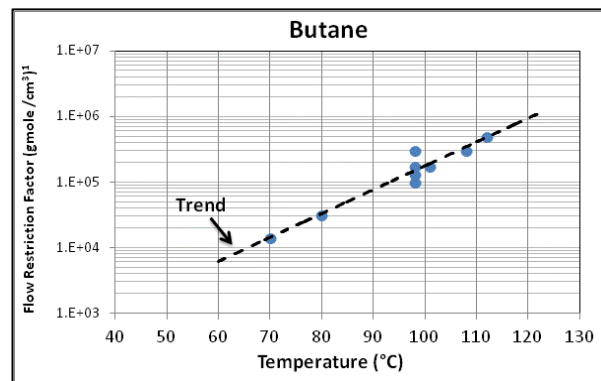


Figure 2-12. Flow restriction factor (FRF) and its trend, used to match the experiments with butane.

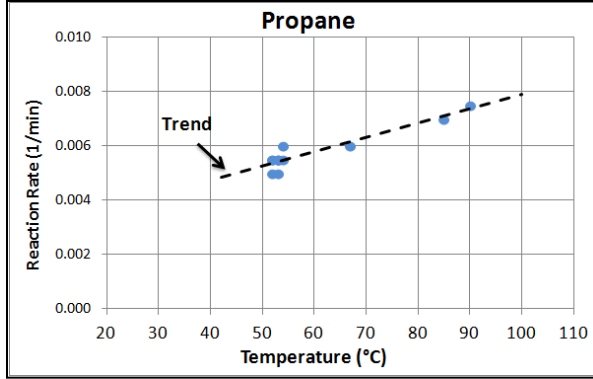


Figure 2- 13. Reaction rate factor (RR) and its trend, used to match the experiments with propane.

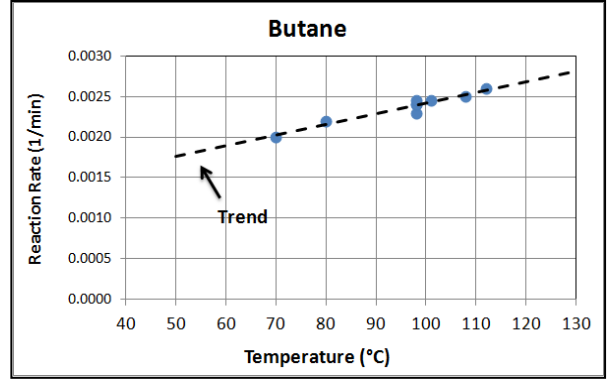


Figure 2-14. Reaction rate (RR) factor and its trend, used to match the experiments with butane.

The RR is the speed with which the reaction is proceeding; i.e. the velocity in which the precipitating component (reactant) reacts with the other hydrocarbon components to give the Volumetric Reaction Rate (VRR), defined as the speed at which asphaltene precipitates in the system:

$$V_{RR} = RR * \left[e^{-Ea/T * R} \right] \left[C_1^{enrr(1)} * \dots * C_{ncomp}^{enrr(ncomp)} \right] \quad (2-2)$$

According to the CMG-STARS manual, C_1 to C_{ncomp} in the above equation is the component concentration in a fluid phase, given in density units. For a non-reacting component, the order of reaction $enrr(i)$ is 0, for a reacting component, $enrr(i)$ is 1. In this study, there is only one reacting component (C_{31B}^+) and as a consequence of this, the above equation was simplified.

The FRF gives the restriction to effective permeability, applied to the oil liquid phase as the blockage of flow by the precipitation of solid components into the porous media. Assuming that the particle comes from the oil phase, oil phase effective permeability can be estimated using the following equation (STARS Manual 2011):

$$K_{oeff} = \frac{K_{abs} K_{ro}}{R_{fo}} \quad (2-3)$$

where

$$R_{fo} = \prod_j [1 + FRF_j * \max(0, C_{sj} - MSC)] \quad (2-4)$$

In Eq. 2-3, R_{fo} is the product of the resistance factor of each blocking component. For this particular case, $j=1$ because there is only one blocking component as a result of interaction of C_{31B}^+ with the light component, either propane or butane. The FRF is the flow restriction factor and C_s is the concentration of asphaltene in the system given by the asphaltene precipitation curves. Blockage will occur when C_s is greater than MSC.

These three factors were estimated for every single case and were the parameters to be determined in the match processes. The match was made on the reported quantity of asphaltene recovered from oil produced by Pathak et al. (2010). For all the other cases, the match was done only on the quantity of oil recovered following the trend of the FRF and RR parameters.

The values of FRF and RR factors, estimated for every single case and used to match the experiments, were plotted against temperature for propane and butane. Both parameters follow a trend (Figures 2-11 to 2-14). For those experiments, where the amount of asphaltene precipitation data was not available, the values for the FRF and RR parameters were obtained from the trends shown in Figures 2-11 to 2-14 to match the reported oil recovery. MSC factors used to match the experiments are given in **Tables 2-3** and **2-4**. It was observed that the final drained oil is highly sensitive to this parameter. Having a wide range of MSC parameter (from 0 to 5×10^{-4} g-mol/cm³) can be explained by the variations in permeability in the glass bead packs and Berea cores. Lower glass bead compaction causes high permeability on the packs and as a consequence, a faster oil drainage is obtained. To control the drainage rates, the MSC parameter had to be adjusted until a good match was obtained to the ultimate recovery. The MSC values obtained for the Berea sandstone cases were close to each other (Table 2-4) as their permeabilities were very similar. In the glass beads pack cases, however, the permeability values are expected to change due to the nature of manual packing process. This caused different drainage rates and as a result variations in the MSC values for those samples were observed (between 0 to 5×10^{-4} g-mol/cm³).

Table 2-3. Values of MSC for simulation using Propane.

Propane		
Material	Case	MSC/10 ⁻⁴ (g-mol/cm ³)
Glass Beads	9, 16, 18, 19	0
	10	0.5
	8, 14, 15	1.0
	12	1.2
	13, 17	2.0
Berea Core	11	5.0
	20	1.0
	22	3.5

Table 2-4. Values of MSC for simulation using Butane.

Butane		
Material	Case	MSC/10 ⁻⁴ (g-mol/cm ³)
Glass Beads	1 to 7	0.0
Berea Core	21	4.0
	23	3.1

Satisfactory matches on oil drained for propane and butane experiments were obtained. However, to obtain these results it was necessary to increase the value of RFR factor on experiments 5, 16 and 19 to avoid excessive oil drained. This behaviour can be attributed to the presence of solvent in the liquid phase during the soaking time because the conditions of pressure and temperature for these particular cases (54°C and 1650 kPa for propane and 98°C and 1600 kPa for butane) are close to the approximated values of pressure and temperature of the saturation curve of 54°C at 1879.6 kPa for propane and 98°C at 1474.9 kPa for butane.

2.4.2 Prediction of recovery factor

To predict the oil recovery using solvent at high temperature and pressure, the porosity of the simulation model was fixed at 30% porosity and $t_{soak} = 1600$ min (26.67 hours) for propane and 10300 min (171.67 hrs.) for butane. Note that the experiments were conducted for a fixed period of time and it was not clear when exactly the ultimate recovery was reached (Pathak et al. 2010, 2011a-b). Three different core heights were used: 10, 20 and 30 cm. The values of FRF and RR were obtained from Figures 2-11 to 2-14 for the given temperature and pressure and extrapolated in pressure and temperature for propane and butane. Results are shown in **Figures 2-15 to 2-26**. Note that the recovered oil includes the original heavy-oil in-place and solvent injected in Figures 2-15 and 2-16 at reservoir conditions. Asphaltene precipitation and produced with oil are shown in **Figures 2-27 and 2-28** for propane and butane, respectively.

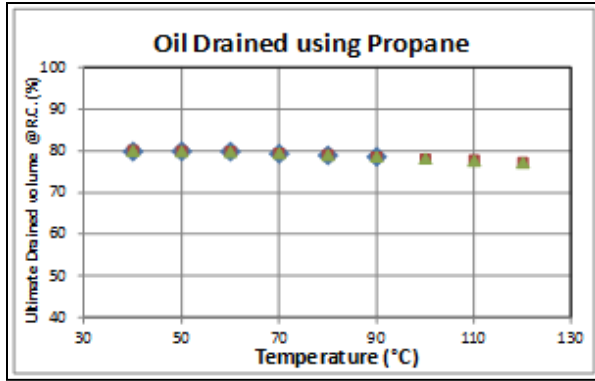


Figure 2-15. Final oil drained using propane at 500, 1650 and 1830 kPa.

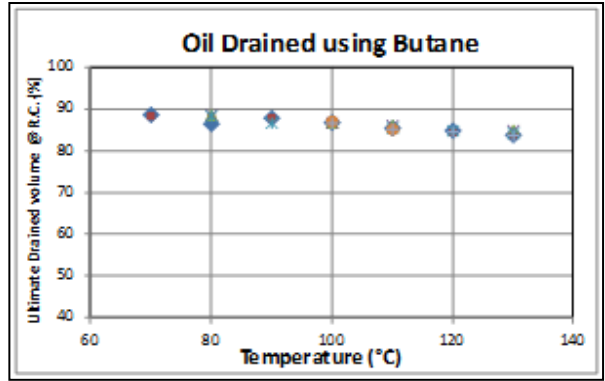


Figure 2-16. Final oil drained using Butane at 1500, 1650 and 1830 kPa.

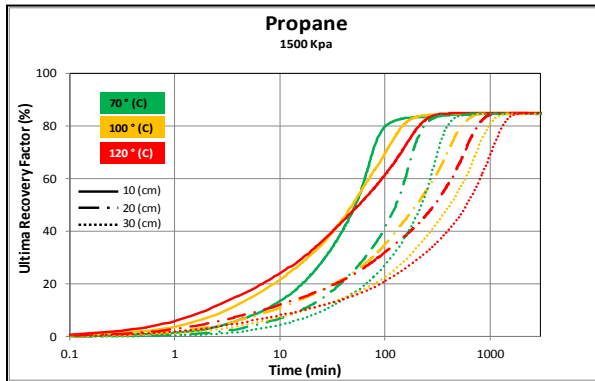


Figure 2-17. Final drained oil into region 2 using propane as a solvent, for 1500 kPa and three different core heights and temperatures.

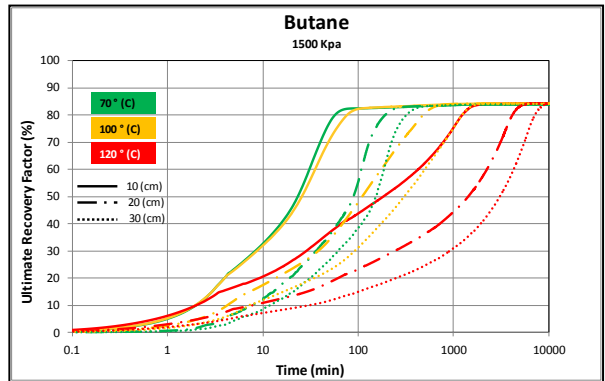


Figure 2-18. Final drained into region 2 oil using butane as a solvent, for 1500 kPa and three different core heights and temperatures.

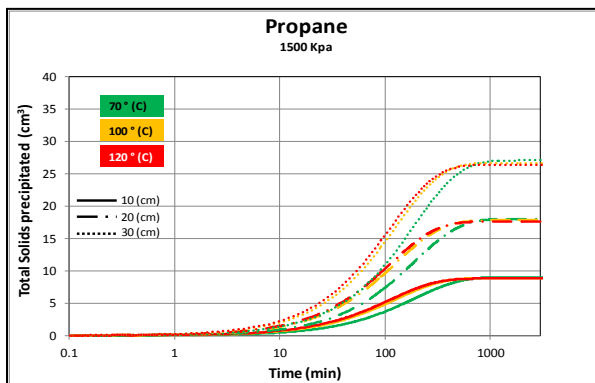


Figure 2-19. Total solids precipitated in the system vs. time. Propane at 1500 kPa at three different temperatures and heights.

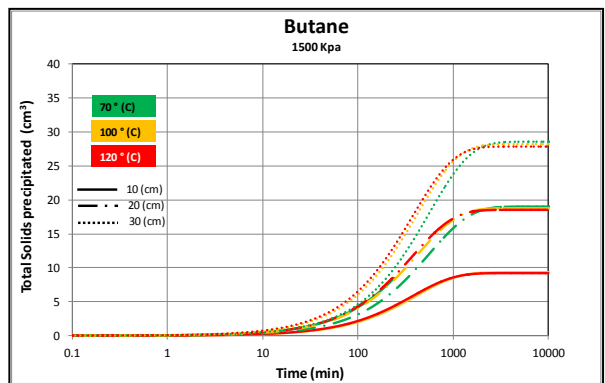


Figure 2-20. Total solids precipitated in the system vs. time using butane at 1500 kPa at three different temperatures and heights.

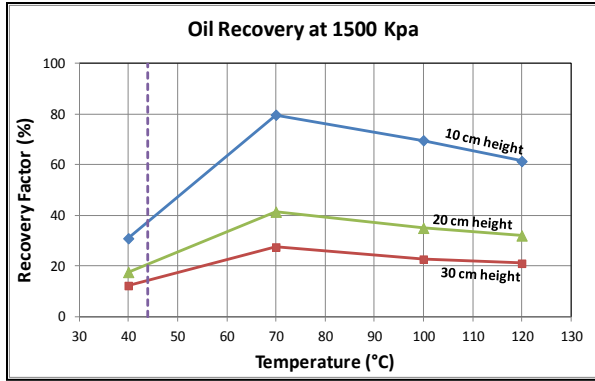


Figure 2-21. Total drained oil into region 2. Propane at 1500 kPa and its saturation temperature for three different core heights at 100 min.

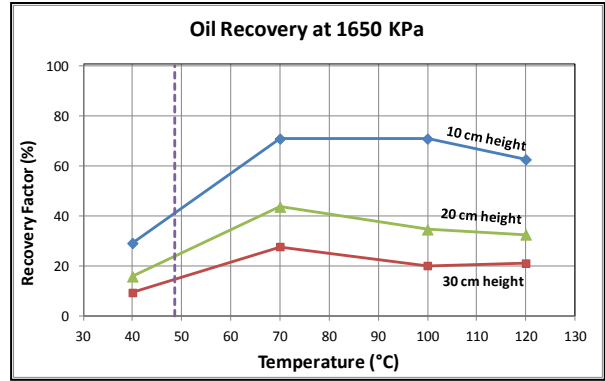


Figure 2-22. Total drained oil into region 2. Propane at 1650 kPa and its saturation temperature for three different core heights at 100 min.

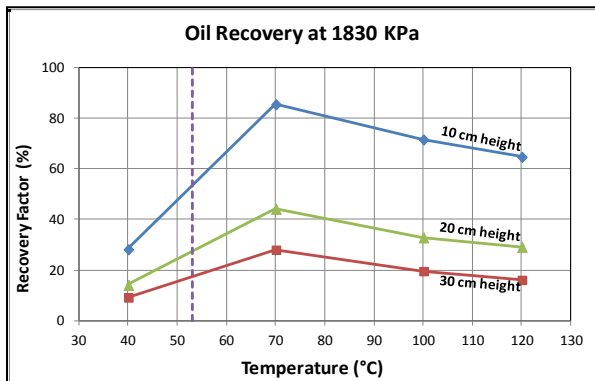


Figure 2-23. Total drained oil into region 2. Propane at 1830 kPa and its saturation temperature for three different core heights at 100 min.

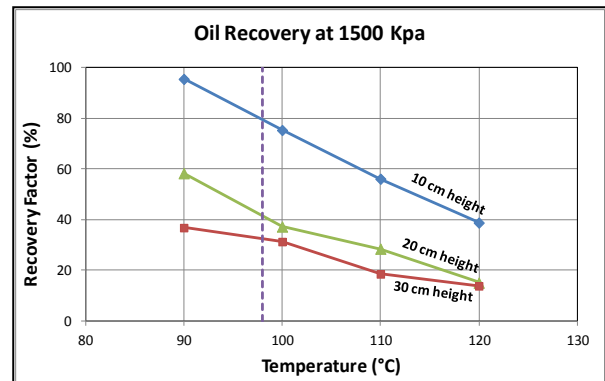


Figure 2-24. Total drained oil into region 2. Butane at 1500 kPa and its saturation temperature for three different core heights at 60 min.

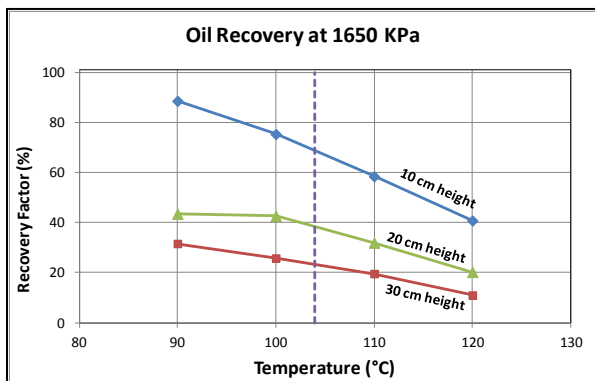


Figure 2-25. Total drained oil into region 2. Butane at 1650 kPa and its saturation temperature for three different core heights at 60 min.

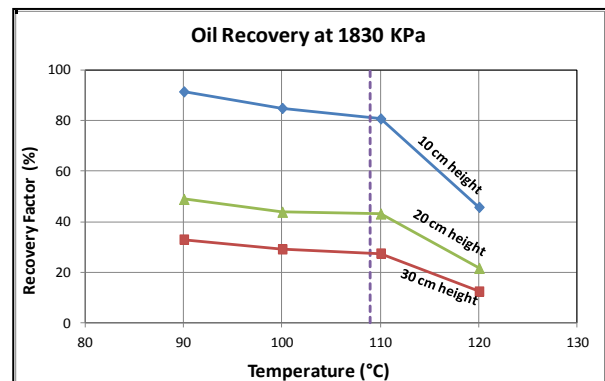


Figure 2-26. Total drained oil into region 2. Butane at 1830 kPa and its saturation temperature for three different core heights at 60 min.

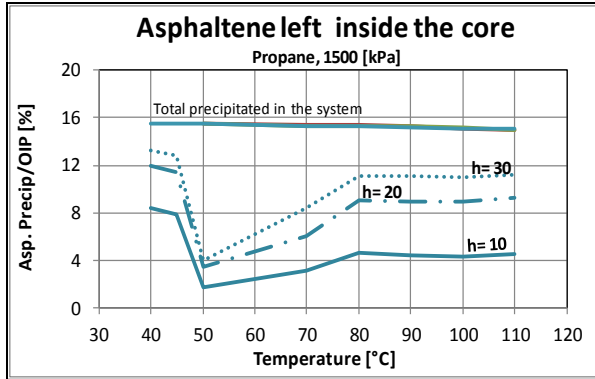


Figure 2-27. Total asphaltene precipitated and produced with drained oil. Propane as a solvent for 1500 kPa and three different core heights.

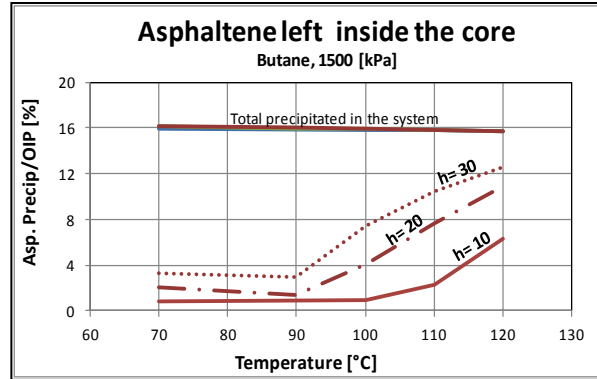


Figure 2-28. Total asphaltene precipitated and produced with drained oil. Butane as a solvent for 1500 kPa and three different core heights.

2.5 Analysis of the results

The above summarized results show that the recovery factor is a strict function of pressure and temperature. The highest recovery was reached in a minimum soaking time when the temperature and pressure are close to the saturation temperature and pressure in the vapor region of the solvent used.

Shown in Figures 2-17 and 2-18 it is observed that for short times with temperatures of 50, 70 and 100°C, more than 100% of oil is accumulated in region 2. In addition, a faster recovery was observed using propane than butane because the FRF of propane is lower than that of butane.

It was also observed that the time to reach the final oil recovery depends on the height of the core. For all the simulated cases, faster recovery was obtained from a 10 cm core. This is due to the fact that as the core length increases more asphaltene blockage and capillary entrapment occurs during the downward flow of oil inside the bottom of the core; in consequence, more time is needed for oil to travel from top to bottom.

Time to reach the final recovery is highly sensitive to temperature. As the temperature increased above the saturation temperature of solvent, more time is needed to reach the final recovery. This is attributed to higher amount of precipitated asphaltene that eventually delays the drainage of oil out of the core.

Shown in Figures 2-17 and 2-18, the total oil drained into region 2 after a long soaking time. Note that the amount of oil reported does not include the volume of solids precipitated and drained into this region. The corresponding solids precipitated versus time are shown in Figures 2-19 and 2-20. It can be observed that more time is needed to reach the final volume drained into region 2 when butane is used as a solvent. Also, precipitation of solids occurs faster as the temperature increases. A higher amount of solids delays the oil drain and therefore more time is needed to reach the same amount of oil as temperature increases.

Figures 2-21 to 2-26 show the oil drained into region 2 for 100 and 60 minutes of simulation with propane and butane respectively at different pressures (1500, 1650 and 1830 kPa). Note that only oil recovered is reported without solids at standard conditions. It can be observed that oil recovered decreases faster when the simulation temperature is higher than saturation temperature of solvent at the simulation pressure.

The amount of asphaltene precipitation when propane was used as solvent is lower around the saturation temperature and precipitation increases as temperature increases or decreases. The asphaltene precipitated when butane was used as a solvent showed a different behavior. In this case, asphaltene precipitation starts to increase after 90°C when temperature is below the saturation value. **Figures 2-27 and 2-28** show the total asphaltene precipitation in the system and the asphaltene in oil production. The difference between these two values is the asphaltene left inside the core. In the range of temperature and pressure shown in these figures, the precipitation quality lines are nearly flat and then the total asphaltene precipitated are almost constant. The amount of asphaltene produced with oil depends on the blockage in the core and, as a consequence of this, the longer the core, the lower the amount of oil produced, within the same period of time.

Propane and butane showed differences not only in oil recovery but also in asphaltene precipitation. This behaviour could be a consequence of the fact that asphaltenes are insoluble in paraffins of linear chain (Speight, 1973), which means that the number of carbons of the precipitating agent has a direct effect over the quantity of insoluble components of crude oil.

2.6 Up-scaling to field conditions

Obviously, a final attempt would be the application of this process at the field scale. This requires an upscaling analysis initially. Butler and Mokris (1991) suggested the way to scale up time and permeability of their results by using the following relations, where M and F refers to “model” and “field” respectively:

$$\left[\frac{\phi t}{H^2}\right]_M = \left[\frac{\phi t}{H^2}\right]_F \quad (2-5)$$

$$k_M = k_F \cdot \frac{H_F \phi_M^2 (\Delta S_o)_M}{H_M \phi_F^2 (\Delta S_o)_F} \quad (2-6)$$

where $(\Delta S_o)_M = S_{oi} - S_{or}$

Two different scaling exercises were performed using the above equations:

Scaling exercise 1:

The permeability of the simulation model was set to 100 and 0.8 Darcy for the glass bead packs and Berea cores, respectively. These are the parameters used in the matching process along with the others given in Table 1. Assuming $\phi_F = 0.3$, $k_F = 3$ Darcy for the field scale corresponding to the experiments 1 through 19 and $\phi_F = \phi_M$ and $k_F = k_M$ for the experiments 20 to 23 (Berea cores), the height and time reported by Pathak et al. (2010, 2011a-b) were scaled up to field conditions (**Table 2-5**, columns 8 and 9). In this exercise, $(\Delta S_o)_M$ values obtained from the experiments by Pathak et al. (2011-b), as given in column 5 of **Table 2-5**, were used. These values were also assumed to be the same in the field $(\Delta S_o)_F$. The H_F values were obtained from Eq. 2-6 and the time to reach the ultimate recovery in this equation was taken as the soaking time given in the 4th column of Table 2-5.

Table 2- 5. Scaling of soaking time and core height, reported by Pathak et al. (2010, 2011a-b), and from simulation.

No.	Height (cm)	ϕ (%)	Approx. Soaking Time (hours)	$(\Delta So)_M$	Temp. (°C)	Pressure (kPa)	SCALING EXERCISE 1 $(\Delta So)_M = (\Delta So)_F$		SCALING EXERCISE 2 $H_F=10$ (m)	
							H_F (m)	Time (years)	Time to reach ultimate recovery (min) SIMULATION	Time to reach ultimate recovery (years) FIELD
1	29	0.4	4	0.5560	70	1030	5.44	0.214	576	1.737
2	29	0.4	4	0.5260	80	1030	5.44	0.214	816	2.461
3	18	0.3	6	0.9450	98	1400	6.00	0.761	250	1.468
4	26	0.3	12	0.7210	98	1500	8.67	1.522	734	2.066
5	10	0.3	8	0.6230	98	1600	3.33	1.015	404	7.686
6	17	0.3	7	0.4500	112	1500	5.67	0.888	2332	15.352
7	17	0.3	8	0.6450	108	1600	5.67	1.015	1104	7.268
8	29	0.4	4	0.5530	90	1500	5.44	0.214	874	2.636
9	15	0.4	4	0.5370	85	1500	2.81	0.214	641	7.227
10	17	0.4	4	0.4780	67	1500	3.19	0.214	1656	14.536
11	17	0.3	4	0.8380	52	1500	5.67	0.507	246	1.620
12	17	0.3	4	0.6420	54	1830	5.67	0.507	388	2.554
13	23	0.3	10	0.7550	53	1500	7.67	1.268	516	1.856
14	27	0.3	10	0.6030	53	1500	9.00	1.268	1008	2.631
15	20	0.3	6	0.6550	52	1500	6.67	0.761	634	3.016
16	17	0.3	8	0.4330	54	1650	5.67	1.015	1734	11.416
17	18	0.3	8	0.7460	53	1450	6.00	1.015	338	1.985
18	19	0.3	8	0.5690	52	1450	6.33	1.015	898	4.733
19	15	0.3	7	0.4040	54	1650	5.00	0.888	1336	11.297
20*	15	0.23	48	0.2750	53	1500	10.0	24.353	13716	115.982
21*	15	0.21	28	0.4440	98	1350	10.0	14.206	4610	38.982
22*	30	0.21	360	0.4120	53	Started at 1600	10.0	45.662	43640	92.254
23*	15	0.21	240	0.6360	101	Started at 1470	10.0	121.766	35920	303.738

* For Berea cores, $H_F = 10$ (m) was used when $(\Delta So)_M = (\Delta So)_F$

Scaling exercise 2:

Note that the experiments given in Table 2-1 are static experiments and a time period was chosen as soaking time. The time (column 4 of Table 2-5) to reach this recovery given as $(\Delta So)_M$ (column 5 of Table 2-5), however, could be shorter. In other words, time-recovery plots were not available to obtain the time to reach the ultimate recovery. Hence, the numerical model results

given in Figures 2-17 through 2-20 were used to obtain this. Column 10 of Table 2-5 shows those values. Assuming a typical distance between two horizontal wells in steam/solvent applications in unconsolidated sands to be 10 m, the time to reach ultimate recovery at the field scale was calculated using Eq. 5 (column 11 of Table 2-5).

Inconsistencies between these two upscaled time values (column 9 and 11) exist as two different approaches and data sets were used. But, these values give an idea about upper and lower limits of the time required to reach the ultimate recovery at the field scale for further practices.

The next step is the field scale simulation of the process, using the data obtained through this work, especially asphaltene precipitation parameters (and permeability modification), and determine the optimal application conditions including injection rate, durations, pressure and temperature. This is an on-going part of the work and will be the subject of the next paper.

2.7 Conclusions and recommendations

1. Heavy-oil recovery by using solvent injection depends on pressure and temperature. Simulation results show recovery is more sensitive to temperature than to pressure, at least for the range of pressures analyzed. The oil recovery is greater when the temperature is located in the vapor region of the saturation curve of solvent used than in the liquid region. Simulation using butane shows that when the temperature is at the liquid region, an important amount of solvent will be produced with the oil.
2. Asphaltene precipitation also depends of the operating conditions; i.e., pressure, temperature and solvent type. Precipitation is greater when temperature is at the vapor region of the solvent used. There is a range of temperature in which a major quantity of solids is produced with the oil produced. Out of this range, a major quantity of solids remains inside the core; in a reservoir, it would cause a plugging of the pore throats.
3. From the simulations of varying height of the core, it can be concluded that more time is needed to obtain the same factor recovery than when using a short core. Similarly, more

time is needed to obtain the same recovery factor when temperature is above the saturation temperature of the solvent used.

4. The FRF, RR and MSC factors are found to be useful in simulating solvent injection at elevated temperatures. It is, however, necessary to carry out more experiments to define the trend of these factors for different solvents.

2.8 Nomenclature

C_i	Concentration factor contributed by reactant component i (gmole/cm ³)
E_a	Activation Energy (J/gmol)
$Enrr$	Order of reaction with respect to component i , 0 for non-reacting component and 1 for reacting
FRF	Flow restriction factor (g-mol/cm ³) ⁻¹
Kro	Oil relative permeability
$Koeff$	Effective permeability of oil phase (mD)
MW	Molecular weight (g/mol)
MSC	Minimum solid concentration to star the blockage of porous media (g-mol/cm ³)
R	Universal gas constant (J/mole-°K)
RR	Reaction Rate (1/min)
Csj	Concentration of captured oil droplets (gmole/cm ³)
V_{RR}	Volumetric reaction rate (gmole/cm ³ -min)
T	Temperature (°C), (°K in eq. 2)
t_{Soak}	Soaking time (min)
w	Weight fraction (% weight)
x	Mole fraction of the asphaltene component

2.9 References

Al-Bahlani A., Babadagli T. 2009. Steam-over-Solvent in Fracture Reservoirs (SOS-FR) for Heavy Oil Recovery: Experimental Analysis of the Mechanism. Paper SPE 123568 presented at the Asia Pacific Oil and Exhibition held in Jakarta, Indonesia, 4-6 August.

[Doi:10.2118/124047-MS](https://doi.org/10.2118/124047-MS)

- Al-Bahlani, A.M., Babadagli, T. 2011a. Field Scale Applicability and Efficiency Analysis of Steam-Over-Solvent Injection in Fractured Reservoirs (SOS-FR) Method for Heavy-Oil Recovery. *J. Petr. Sci. and Eng.* **78**: 338-346. <http://dx.doi.org/10.2523/13023-ABSTRACT>
- Al-Bahlani, A.M., Babadagli, T., 2011b. SOS-FR (Solvent-Over-Steam Injection in Fractured Reservoir) Technique as a New Approach for Heavy-Oil and Bitumen Recovery: An Overview of the Method. *Energy Fuels* **25** (10): 4528-4539. [Doi:10.1021/ef200809z](https://doi.org/10.1021/ef200809z).
- Babadagli, T., Al-Bahlani, A.M. 2008. Hydrocarbon Recovery Process for Fractured Reservoirs, Canadian Patent Application, Serial No: 2,639,997 filed on Oct. 6, 2008, International Patent Application Serial No. PCT/CA2009/001366, Oct. 5, 2009 (*US Patent Application*, Serial No: 13/121,682 filed on July 21, 2011).
- Butler, R.M., Mokrys, I.J. 1991. A New Process (VAPEX) for Recovering Heavy Oils using Hot Water and Hydrocarbon Vapour. *J. Can. Pet. Technol.* **30** (1): 97-110. <http://dx.doi.org/10.2118/91-01-09>.
- Butler, R.M., Mokrys, I.J. 1993. Recovery of Heavy Oils Using Vaporized Hydrocarbon Solvents: Further Development of the VAPEX Process. *J. Can. Pet. Technol.* **32** (6): 38-55. <http://dx.doi.org/10.2118/SS-92-7>.
- Castellanos Díaz, O., Modaresghazani, M.A., Satyro M.A., Yarranton, H.W. 2011. Modelling the Phase Behaviour of Heavy Oil and Solvent Mixtures. *Fluid Phase Equilibria* **304**: 74-85. <http://dx.doi.org/10.1016/j.fluid.2011.02.011>.
- Computer Modeling Group Ltd. "STARS User's Guide". 2011: 372-376.
- Edmunds, N., Barrett, K., Solanki, S., et al. 2009. Prospects for Commercial Bitumen Recovery from the Grosmont Carbonate, Alberta. *J. Can. Pet. Technol.* **48** (9): 26-32. <http://dx.doi.org/10.2118/09-09-26>.
- Edmunds, N., Moini, B., Peterson, J. 2009b. Advanced Solvent-Additive Processes via Genetic Optimization. Paper PETSOC 2009-115 presented at the Canadian International Petroleum Conference (CIPC) 2009, Calgary, Alberta, Canada, 16-18 June. <http://dx.doi.org/10.2118/2009-115>.
- Government of Alberta. 2011. *The Resource Recovering the Resource*. Document available at www.oilsands.alberta.ca/FactSheets/About_Albertas_oil_sands.pdf-2011-07-13.
- Guerrero-Aconcha, U., Salama, D., and Kantzas, A. 2008. Diffusion Coefficient of n-alkanes in Heavy Oil. Paper SPE 115346 presented at the SPE annual Technical Conference and Exhibition, Denver, Colorado, 21-24 September. [Doi:10.2118/115346-MS](https://doi.org/10.2118/115346-MS).
- Guerrero-Aconcha, U., Kantzas, A. 2009. Diffusion of Hydrocarbon Gases in Heavy Oil and Bitumen. Paper SPE 122783 presented at the SPE Latin American and Caribbean Petroleum Engineering Conference, Cartagena, Colombia, 31 May-3 June. [Doi:10.2118/122783-MS](https://doi.org/10.2118/122783-MS).
- Li, W., and Mamora, D.D. 2011. Light-and Heavy-Solvent Impacts on Solvent-Aided-SAGD Process: A Low-Pressure Experimental Study. Paper SPE 133277 presented at the Annual Technical Conference and Exhibition, Florence, Tuscany, 20-22 September. [Doi:10.2118/133277-MS](https://doi.org/10.2118/133277-MS).
- Luo, H., Kryuchkov, S., Kantzas A. 2007. The Effect of Volume Changes Due to Mixing on

- Diffusion Coefficient Determination in Heavy Oil and Hydrocarbon solvent System. Paper SPE 110522 presented at the Annual Technical Conference and Exhibition, Anaheim, California, 11-14 November. [Doi:10.2118/110522-MS](https://doi.org/10.2118/110522-MS).
- Luo, H. and Kantzas, A. 2008. Investigation of Diffusion Coefficients of Heavy Oil and Hydrocarbon Solvent Systems in Porous Media. Paper SPE 113995 presented at the Improved Oil Recovery Symposium, Tulsa, Oklahoma, 19-23 April. [Doi:10.2118/113995-MS](https://doi.org/10.2118/113995-MS).
- Luo, P. and Gu, Y. 2009. Characterization of a Heavy Oil-Propane System in the Presence or Absence of Asphaltene Precipitation. *Fluid Phase Equilibria* **277** (1): 1-8. Doi:10.1016/j.fluid.2008.10.019.
- Nasr, T.N., Beaulieu, G. Golbeck, H., et al. 2003. Novel Expanding Solvent-SAGD Process “ES-SAGD”. *J. Can. Pet. Technol. (Technical note)*. **42** (1): 13-16. <http://dx.doi.org/10.2118/03-01-TN>.
- Nghiem, L.X. and Coombe, D.A. 1996. Modeling Asphaltene Precipitation during Primary Depletion. SPE 36106 presented at the Fourt Latin American and Caribbean Petroleum Engineering Conference, Trinidad and Tobago, 23-26 April. [Doi:10.2118/36106-PA](https://doi.org/10.2118/36106-PA).
- Oballa, V. and Butler, R.M. 1989. An Experimental Study of Diffusion in the Bitumen-Toluene System. *J. Can. Pet. Tech.* **28** (2): 63-69. <http://dx.doi.org/10.2118/89-02-03>.
- Pathak, V. and Babadagli, T. 2010. Hot Solvent Injection for Heavy Oil/Bitumen Recovery: an Experimental Investigation. Paper SPE 137440 presented at the Canadian Unconventional Resources & International Petroleum Conference, Calgary, Alberta, 19-21 October. [Doi:10.2118/137440-MS](https://doi.org/10.2118/137440-MS).
- Pathak, V., Babadagli, T. and Edmunds, N.R. 2011a. Mechanics of Heavy Oil and Bitumen Recovery by Hot Solvent Injection. Paper SPE 144546 presented at the Western North American Regional Meeting, Anchorage, Alaska, 7-11 May. [Doi:10.2118/144546-PA](https://doi.org/10.2118/144546-PA).
- Pathak, V., Babadagli, T. and Edmunds, N.R. 2011b. Heavy Oil and Bitumen Recovery by Hot Solvent Injection. *J. Petr. Sci. and Eng.* **78**: 637-645. <http://dx.doi.org/10.1016/j.petrol.2011.08.002>.
- Speight, J.G. 1973. Some Observations on the Hydroprocessing of a Heavy Crude Oil. *Fuel* **52** (4): 300–301 [http://dx.doi.org/10.1016/0016-2361\(73\)90061-6](http://dx.doi.org/10.1016/0016-2361(73)90061-6).
- Thomas, S. 2007. Enhanced Oil Recovery – An Overview. *Oil & Gas Science and Technology – Rev. IFP* **63** (1): 9-19. <http://dx.doi.org/10.2516/ogst:2007060>.
- Zhao, L., Nasr, H., Huang, G. et al. 2004. Steam Alternating Solvent Process: Lab Test and Simulation. *J. Can. Pet. Technol.* **44** (9): 37-43. <http://dx.doi.org/10.2118/05-09-04>.
- Zhao, L. 2004. Steam Alternating Solvent Process. Paper SPE 86957 presented at International Thermal Operations and Heavy Oil and Western Regional Meeting, Bakersfield, California, 16-18 March. [Doi:10.2118/86957-MS](https://doi.org/10.2118/86957-MS).
- Zhao, L., Nasr, H., Huang, G. et al. 2004a. Steam Alternating Solvent Process: Lab Test and Simulation. Paper SPE 2004-044 presented at the Canadian International Petroleum Conference, Calgary, Alberta, Canada, 8-10 June. [Doi:0.2118/2004-044](https://doi.org/10.2118/2004-044).

Chapter 3: High -Temperature Solvent Injection for Heavy-Oil Recovery from Oil Sands: Determination of Optimal Application Conditions through Genetic Algorithm

A version of this chapter was included in the proceedings of the SPE LACPEC 2014, held in Maracaibo, Venezuela, 23-23 May (paper SPE-169342-MS). Also, it was accepted for publication in the SPE Reservoir Evaluation & Engineering (SPE-169342-PA).

3.1 Summary

Our recent experimental studies on superheated solvent injection for heavy-oil recovery showed that when a solvent is injected into the reservoir the process is highly sensitive to pressure and temperature. The effects of these parameters on the recovery factor are accentuated when the operating conditions are closer to the saturation curve of the solvent injected. This paper investigates this process and formulates the optimal field scale application conditions that yield the maximum profit as a continuation of the previous work. To achieve this, a hypothetical field scale numerical model was constructed and the key parameters identified through the aforementioned sensitivity analysis were incorporated. Then, injection process was simulated for a two-horizontal injection/production pattern. An optimization study was performed to identify the relative contributions of the effective parameters (pressure, temperature, and injection rate) and to propose an optimal application scheme using genetic algorithm. The critical pressure and temperature yielding maximum production and highest profit considering solvent retrieval were defined for different injection rates and application scenarios. Our results indicate that, at the end of the hot solvent injection process, an important volume of solvent is left in the reservoir and its volume depends on the injection-production scheme selected. Nevertheless, if the project is performed under appropriately selected operational parameters (obtained through the optimization processes) and followed by proper process to retrieve the solvent from the reservoir (low temperature steam or hot water applications) it can make the hot solvent injection process profitable.

3.2 Introduction

Combination of steam and solvent injection has been proposed as an alternative to steam assisted gravity drainage (SAGD) (Butler 1994, 2004) and vapour extraction (VAPEX) (Butler and Mokrys 1991, 1993). In an example of this kind of hybrid application, Pathak et al. (2010) and Pathak et al. (2011a-b) suggested the injection of vapour solvents at a temperature just above the saturation point of the solvent, which can be achieved by preheating the reservoir with steam to this temperature. In this case, the combined effects of solvent diffusion and heating on viscosity reduction will be maximized yielding better heavy-oil/bitumen recovery than the sole application

of SAGD or VAPEX (Edmunds et al. 2009). However, due to its high cost, this process should be optimized.

Temperature plays a critical role in this optimization process. A limited number of studies were carried out to analyze the effect of temperature on solvent injection for heavy oil/bitumen recovery (Moreno and Babadagli 2013, 2014; Haghghat and Maini 2013). Pathak and Babadagli (2010) and Pathak et al. (2011a-b) observed through a set of experimental study using propane and butane, that the peak of oil recovery is reached when pressure and temperature are near the saturation line of the solvent used, but in the region of the gaseous phase. Leyva and Babadagli (2011) reported on numerical simulation of these laboratory experiments and showed that a critical temperature exists that yields a maximum recovery, which depends of the solvent type, temperature, and pressure. These previous studies include a detailed analysis of phase behavior (Keshavarz et al. 2013), diffusion coefficient (Oballa and Butler 1989; Guerrero-Aconcha and Kantzas 2009; Luo and Kantzas 2008; Luo et al. 2007), viscosity reduction (Nasr et al. 2003; Li and Mamora 2011; Zhao et al. 2004; Zhao 2007), permeability reduction due to asphaltting precipitation (Moreno and Babadagli 2013, 2014), and the dependence of the recovery factor on pressure and temperature for different solvent types.

In the present work we worked at field scale using the aforementioned lab scale experimental (Pathak et al. 2010; Pathak 2011a-b) and numerical observations (Leyva and Babadagli 2011, 2013) and reported the results of numerical simulation of a hypothetical reservoir exploited by injecting solvent preheated at the surface and then injected into the reservoir. The objective is to propose an appropriate combination of controllable parameters, which result in the most economical option to exploit such a reservoir. A rectangular 2D grid model of $70 \times 1 \times 50$ cells was constructed to simulate the hot solvent injection into a homogeneous sand reservoir. The model considered the asphaltene precipitation and the operational cost to produce the heavy oil. Four different injection/production schemes were studied. The optimal values of injection parameters that maximize the profit were obtained by genetic algorithms.

3.3 Description of the problem and solution methodology

The optimum economical scheme to exploit a heavy oil/bitumen reservoir using solvents at elevated temperatures (or steam/solvent hybrid applications) is difficult to determine due to the

involvement of several operational parameters; e.g., type and concentration of solvent, injection pressure and temperature, injection schedule (rate and duration), cost of solvent, price of the heavy oil/bitumen, and reservoir preheat time, etc. If we consider two types of solvents, four different concentrations for each solvent, 20 different injection temperatures, five different injection pressures for each solvent, and seven for the flowing bottom hole pressure, we end up with 5,600 possible combinations at a single injection rate. If we consider a schedule of five different injection rates, the number of cases to run increases to 28,000. When the heterogeneity is included, the problem becomes even more complicated.

This problem cannot be solved practically by simulation alone and, hence, a well-designed optimization scheme needs to be applied to provide technically - and economically - viable solutions and optimal injection strategies for these complicated processes. For this purpose, clarification of the relevant effective parameters on the process using a sophisticated simulation model verified by experiments is needed. The next step is to use this data in a field scale model and apply an optimization algorithm using this model to define the optimal operating conditions and application strategies.

In an attempt to achieve this two-step exercise, we built a field scale dynamic (one injector/one producer) thermal/solvent injection model based on experimentally-validated laboratory scale static (core immersed into a solvent at different temperatures and pressures) simulation results. Next, the numerical model was coupled with genetic algorithm software and optimal operating conditions, which minimize the cost and maximizing the economical profit, were determined using four different initially proposed injection/production schemes.

3.4 Reservoir model

As shown in **Figure 3-1**, a homogeneous rectangular 2D numerical model of $70 \times 1 \times 50$ cells was constructed to simulate this process. Each single cell was of $1.0 \times 600.0 \times 0.5$ (m) size. Because it is a hypothetical model built with the aim to show the convenience of optimizes the operational parameters to obtain the highest economical profit, the grid block size was chosen arbitrarily and gridding sensitivity was not performed. The 2013 version of the Computer Modelling Group (CMG) simulator suite was used throughout the study (BUILDER, WINPROP, STARS for model construction, fluid modelling, and simulations, respectively). Because the well pattern is

symmetrical, only the half-well pattern was considered; however, injection and production rates reported refer to the whole reservoir. We assumed no pressure drop and flow resistance along the horizontal wells. The producer well is 1.5 m from the bottom of the reservoir and the space between injector and producer is 5 m. The reservoir thickness is 25 m. No flow boundaries were considered to limit the reservoir. Two wells were considered with a horizontal length of 600 m.

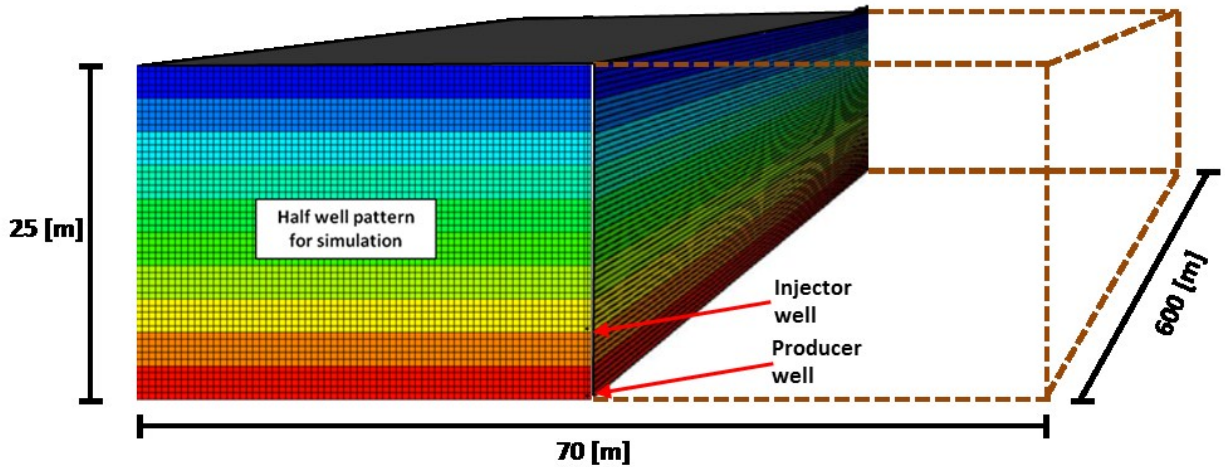


Figure 3-1. Entire well pattern and half well pattern used in the study showing the grid model of 70×1×50 cells and the two horizontal wells.

The reservoir properties used in the simulation model are listed in **Table 3-1**. Heavy oil composition and the viscosity model are the same and were used in the lab scale simulation model, which was introduced in our earlier study (Leyva and Babadagli 2011). Viscosity of the fluid produced in the numerical simulator was tuned to match those values reported by Pathak and Babadagli (2010).

To account for the asphaltene precipitation phenomena in our fluid model, the thermodynamic model proposed by Nghiem et al (1993) and the Winprop module of the software package were used. In their model, asphaltene is considered as a pure and dense phase and its precipitation is modelled by multiphase flash calculations. Previously, the heaviest component must be divided into a precipitating and non-precipitating component, with identical critical properties and acentric factors but different interaction coefficients between them. It was noted by these

researchers that as the interaction coefficients gets larger, a greater incompatibility between components exist favoring the formation of the asphaltene.

The solid precipitation was taken into account by considering the parameters corresponding to the flow restriction factor (FRF) and the frequency of solid precipitation (FSP) (**Figures 3-2 and 3-3**) as also suggested by Leyva and Babadagli (2011). In their work, they simulated the injection of propane and butane through either sandstone or sand pack samples saturated with heavy oil/bitumen using a 3D numerical model. The results were matched to the data from the experiments reported by Pathak et al. (2010), in which heavy oil saturated samples were exposed to solvent vapor at high temperatures. A pressure-temperature sensitivity analysis was carried out for different core sizes to understand the dynamics of gravity drainage process associated with asphaltene precipitation. Asphaltene pore plugging behavior was modeled by introducing and tuning the FRF and FSP. FRF gives the restriction to effective permeability while the FSP is the speed with which the reaction is proceeding; i.e. the speed at which asphaltene precipitates in the system. The values of FRF and FSP, estimated for every single case was used to match the experiments and then plotted against temperature for propane and butane.

These parameters were incorporated in the simulation model for every temperature used. For the range of pressures and temperatures of this study, oil and heptane can be mixed in different proportions and all mixtures remain as a single phase. Hence, there is no interface and the capillary pressure was considered negligible. Because of the high permeability of the medium, linear relative permeabilities were adapted.

Table 3-1. Main parameters used in the simulation model.

Reservoir key parameters		
Porosity	0.3	[-]
Permeability (i=j=k)	1000	[mD]
Rock compresibility	1.8×10^{-5}	[1/kPa]
Initial reservoir temperature	12	[°C]
Initial pressure	2000	[kPa]
Vol. heat capacity	1.5×10^{-6}	[J/m ³ · °C]
Thermal conductivity		
- Rock	1.5×10^{-5}	[J/m · day · °C]
- Oil	1.2×10^4	[J/m · day · °C]
- Water	5.4×10^4	[J/m · day · °C]
- Gas	1400	[J/m · day · °C]

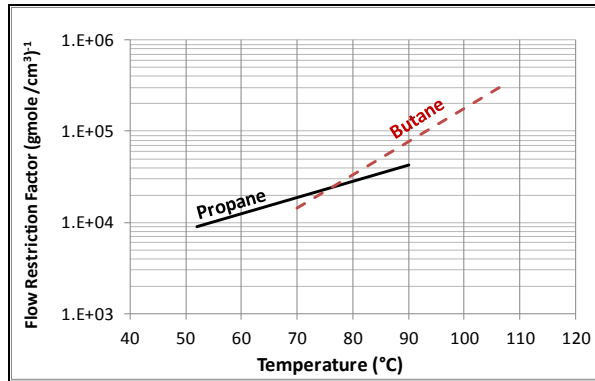


Figure 3-2. Restriction factor, adapted from Leyva and Babadagli (2011).

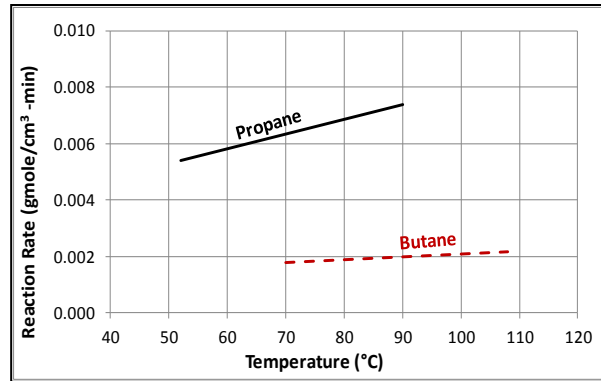


Figure 3-3. Frequency of solid precipitation, adapted from Leyva and Babadagli (2011).

Injection/production schemes. Four different injection/production schemes were considered. For each case, eight variables were allowed to change between a fixed lowest and a highest value (Table 3-2). This number of variables, for two types of solvents, results in more than $4,157 \times 10^6$ possible production/injection scenarios for a single injection/production scheme. If these four schemes are considered, the possible combinations of parameters increase to more than $16,628 \times 10^6$. It is evident that some of these possible combinations are not technically feasible and others could be discharged by a simple inspection or by applying basic reservoir engineering knowledge. Hence, the number of possible combinations can be reduced by choosing the appropriated range of values for each variable to be optimized. However, the quantity of possible combinations still remains so huge that the use of genetic algorithms is a necessary tool to obtain the optimal combination of parameters.

Table 3-2. Parameters to be optimized.

Parameter	Lowest value	Higher value	Step	Possible values
Injection rate (m ³ /day) @s.c.	3,000	9,000	500	13
Temperature (°C)				
-Propane	45	95	1	51
-Butane	70	112	1	43
Injection pressure (kPa)	2,000	4,000	100	21
Maximum production gas rate (m ³ /day) @ s.c.	3,000	5,000	500	5
Bottom hole pressure (kPa)	300	1,400	100	12
Time intervals Δt (days)	30	360	30	12
Maximum gas rate to recover solvent (m ³ /day)@s.c.	1,000	9,000	1,000	9
Time to shut-in injector well for solvent recovery (days)	1,800	9,000	360	25

For the four injection/production proposed schemes defined below, hydraulic communication between wells was enhanced using the heaters option of the numerical simulator. The preheating time was set to 2 months. Also, heat loss at the wellbore was considered negligible. It should be mentioned that once the value was selected for every parameter listed in Table 3-2, the value remains fixed throughout the simulation. In this exercise, solvent was allowed to be injected for a minimum of 5 years and a maximum of 25 years.

1. The first scheme is the continuous injection with continuous production case, as described in **Figure 3-4**. After the preheating period for the reservoir, solvent (either propane or butane in the gaseous form) was preheated at the surface. Then, the solvent was injected into the reservoir for a selected period of time. At the end of this time, the injection well was shut in and the reservoir started to be depressurized to recover and retrieve as much solvent as possible. The selected values of the parameters involved in this process (e.g. P_{inj} , Q_{inj} , Δt) were chosen stochastically from the ranges given in Table 3-2 for each parameter.
2. The second scheme corresponds to the intermittent injection with the simultaneous and continuous production case as described in **Figure 3-5**. Again, solvent was preheated at the surface at any temperature value given in Table 3-2. But, in this scheme, the production well remained opened to production during the entire life of the project.

Injector well was operational for a given time interval and then was shut in for the same period of time. This process was repeated several times and then the injection well was shut-in and the reservoir was depressurized to recover as much solvent as possible.

3. In the third scheme, injection and production were alternated (**Figure 3-6**). The simulation began with the injection of solvent after preheating the reservoir. After a while, the injection well was shut in and the production well was opened for the same time length as the previous injection period. This process was repeated several times and then the injection well was shut-in and the reservoir was depressurized to recover oil and retrieve as much solvent as possible.
4. The fourth scheme corresponds to injection-soaking-production type application (**Figure 3-7**). The process started with the injection of solvent after preheating the reservoir. Solvent injection continued for a period of time. Next, the injection well was shut in for a soaking period over the same time length. Subsequently, the production well was opened for the same time period as the previous injection and soaking time periods and the sequence was repeated several times. As in the previous schemes, the injection well was shut-in and the production well was opened to depressurize the reservoir and recover oil and as much solvent as possible.

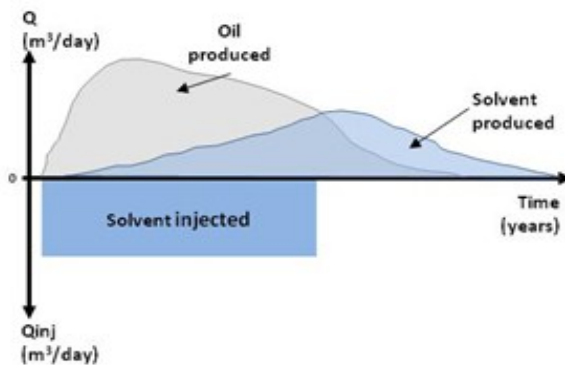


Figure 3-4. Continuous injection with simultaneous production scheme.

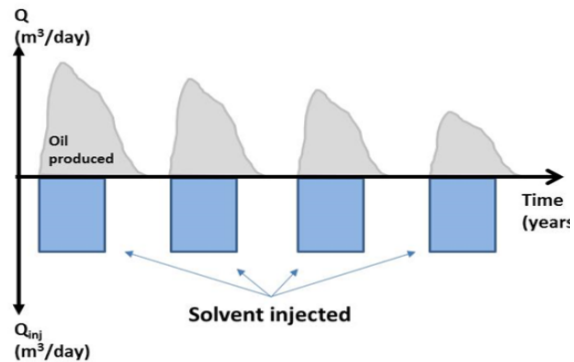


Figure 3-5. Intermittent injection scheme with simultaneous and continuous production.

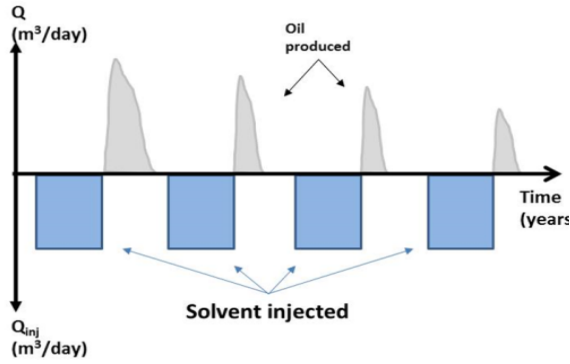


Figure 3-6. Alternated injection production scheme with simultaneous and continuous production.

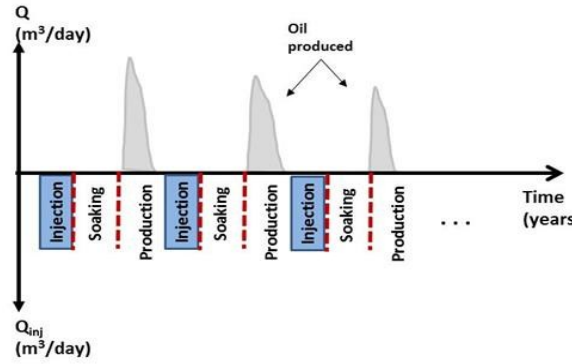


Figure 3-7. Injection-soaking-production scheme.

To obtain the optimal values of the parameters for each scheme, the genetic algorithm (GA) method was used. The advantage of the GA over other optimization techniques is that there are not mathematical restrictions on the properties of the fitness function (Sivanandam and Deepa 2008). Rojas (1996) stated that as the calculations on all points of a population are independent from each other, they can be performed in several processors. This, consequently, makes the GA appropriated for parallel implementation (De Felice et al. 2011).

GA technique has been used in the petroleum industry as an optimization technique including seismic velocity estimation (Jervis et al 1993 and Jin and Madariaga 1993), pipe line design (Goldberg and Kuo 1985), Water-Alternating-Gas (WAG) process (Chen et al. 2010), design of a CO₂-Miscible Flooding project, optimization of solvent-additive SAGD process (Edmunds et al. 2010), analysis of Steam-Over-Solvent injection in fracture reservoirs (Al-Bahlani and Babadagli 2012) and design of solvent assisted SAGD processes (Al-Gosayir et al. 2012).

The GA was invented to mimic the natural properties of organism in which stronger individuals are likely to be winners in a competing environment (Sumathi and Surekha 2010). Here, GA uses a direct analogy of such natural evolution. It presumes that the potential solution of a particular problem is an individual organism, represented by a set of parameters encoded into chromosomes. Each chromosome is represented by a binary string with only 0s and 1s. In this technique, chromosomes are analogous to individuals and genes to the variables. Hence, the solution to a particular problem in which several parameters are involved is similar to a

chromosome, composed of several genes. A set of chromosomes is called a *population*. A fitness score is assigned to each member of the population, representing the abilities of each individual to compete between them. Fitness is calculated through a specific function, selected for each specific problem, and it is called *objective function*. This should be chosen in such way that the closer chromosome near to the optimal solution has the highest fitness value. Through these *crossover* and *mutation* processes, possible solutions closer to the optimal solution of the problem are generated. The processes are repeated for a limited number of *evolutions* (if the algorithm does not converge to an optimum solution) *or* until desired tolerance is reached. Due to the crossover and mutation processes involved in each generation, GA is merely a stochastic, discrete event and a nonlinear process.

For this work the initial population was set using techniques such as Orthogonal Array and Nearly-Orthogonal Array to improve the quality of initial population (Al-Gosayir et al. 2011). The length of chromosomes was set to 8 genes, involving the combination of the variables shown previously in Table 3-2. The configuration of the Genetic Algorithm was set as shown in **Table 3-3**.

Table 3- 3. Genetic algorithm configuration.

Item	Value
Crossover rate	35 %
Mutation rate	3 %
Population	30
Evolutions	30

3.5 Objective function

We searched the highest profit by minimizing the costs associated with the solvent injected. Hence, the operational parameters involved in the revenues and costs were encoded into chromosomes. Next, several chromosomes representing the population were generated. To find the optimal combination of parameters that yields the maximum economic profit, we must evaluate the fitness of all those chromosomes in that population, until the one with the highest fitness is obtained.

The evaluation of all the individuals of the population was made through the fitness function called objective function. This is a mathematical expression that involves the parameters to be optimized. In our case, they are solvent temperature and quantity, heating cost, solvent handling, solvent recompression and the volume of oil produced. This expression is based on the money recovery factor (MRF) used previously by Al-Bahlani and Babadagli (2011).

MRF will be positive if revenues are greater than the costs associated. If the MRF is zero, then the revenues are equal to the expenses corresponding to the breakeven point. A negative value was obtained when the revenues are lower than the cost. It means that, for those values assigned to the parameters to be evaluated, the project is unprofitable. The negativity of the MRF will increase as the losses in the project increase.

$$MRF = \frac{Revenue - Cost}{STOOIP \times Oil\ Price} \times 100 \quad (3-1)$$

$$Revenue = \left[\begin{array}{l} \text{Cumulative} \\ \text{Oil Produced} \end{array} \times \begin{array}{l} \text{Oil} \\ \text{Price} \end{array} \right] + \left[\begin{array}{l} \text{Cumulative} \\ \text{Solvent Produced} \end{array} \times \begin{array}{l} \text{Solvent} \\ \text{Cost} \end{array} \right] \quad (3-2)$$

$$Cost = \left[\begin{array}{l} \text{Cumulative} \\ \text{Solvent Injected} \end{array} \times \begin{array}{l} \text{Cost of} \\ \text{Solvent} \end{array} \right] + \text{Heating} \text{ Solvent} + \text{Solvent} \text{ Handling} + \text{Solvent} \text{ Recompression} \quad (3-3)$$

where *STOOIP* = original oil in place @ std. conditions.

There are two main stages in each production/injection scheme. The first stage is when the injection well is active and the second stage is when this well is shut in permanently to recover the solvent from the reservoir. In the first stage, costs involved are of the solvent injected, heating solvent, solvent handling, and recompression of solvent produced. In the second stage, costs involved are those for solvent recompression only. Oil and gas produced were considered revenue. No administration cost was taken into account for the MRF. The prices and additional costs considered are shown in **Table 3-4**. Solvent recompression refers to the cost associated to increase the pressure of solvent produced in gas form from the injection well, to be incorporated to gas pipeline. Solvent handling includes all other cost associated as infrastructure maintenance

for solvent injection expressed in USD/day, along the project life. These two costs are those reported in literature (Frauenfeld et al. 2006). Propane cost is that reported by the Alberta Energy. Butane price was considered the same as propane. Solvent produced was considered revenue along with oil. The economic behaviour for each scheme along the life of the project, is described through *gross profit*, which is equal to the total sales of the company minus the cost of goods sold, the oil recovery factor (*RF*) and the *MRF*, above described. It is well know that time money value is important for a proper project evaluation. However, for sake of simplicity, the time value was neglected in this study (the aim of this work was just to show the necessity of optimization of the operating conditions for expensive solvent injection and how it can be achieved through the genetic algorithm method).

Table 3-4. Costs considered in the objective function.

Item	Value
Solvent recompression	0.017 [USD/m ³ @ s.c.]
Solvent handling	54.7946 [USD/day]
Heat content of propane	24.003795 [MMBTU/m ³ @ c.s.]
Propane cost (Alberta energy)	4.3 [USD/MMBTU]
Oil price	251.572 [USD/m ³]

3.6 Results and discussion

The optimization software linked up to the numerical simulator was launched for each one of the four schemes and solvent type according to the following sequence: the optimization software generates an initial population in which each individual is composed of a set of parameters represented by a set of chromosomes as described above. Then, the numerical simulator is run for each member of the population and MRF (objective function) and gross profit are calculated for all the individuals.

Next, the most fitness individuals are selected and then a new population is generated starting from this selection. The process is repeated until the maximum number of evolutions is reached. It was observed that an inappropriate selection of the operational variables (genes) values used to generate the first population could increase the number of evolutions needed to reach the optimal

solution. Hence, it is recommended to run an experimental design prior to optimization process in order to reduce the possibility of bias as the number of evolutions progress.

The changes of the main parameters (MRF, RF and gross profit) against the evolution number during the optimization processes for the four schemes with propane or butane are shown in **Figures 3-8 through 3-15**. One may observe through these figures that the best combination of parameters for the very original population gave a negative profit and MRF. This means that with those particular combinations of parameters, the total cost is greater than the total revenue in the proportion indicated by the MRF; in other words, it is not profitable. As will be shown later, these negative values are associated with the volume of solvent left in the reservoir. In some cases, as shown in Figures 3-9 through 3-14, the optimum combination of parameters from the second generation did not yield a higher profit. However, as the evolutions went forward, the optimization process eventually found a combination of parameters yielding less negative than the previous one.

The process continued until we reached 30 evolutions. The exception was the case of scheme # 2 with butane, in which 120 evolutions were used instead of 30 (Figure 3-13). Because no more changes in the main parameters were observed in the last evolutions of the 8 production/injection schemes, the values for profit, RF and MRF were taken as final for the exercise. A less negative profit was the result of a reduction in the operative costs or a higher solvent recovery or a combination of both. As seen in Figures 3-9 to 3-14, the highest recovery factor did not necessarily mean less negative profit. The final results for the 8 cases are shown in **Tables 3-5 and 3-6**. In these tables, the head “*Time to shut-inj*” refers to the number of days corresponding to shutting time of the injection well. It also corresponds to the time when the solvent begins to be recovered from the reservoir. As mentioned previously, each cycle (production, shut-off or soaking) time has the same time length. Then, the number of total cycles for each scheme can be obtained by dividing the Δt_n by “*Time to shutting well*”. These parameters are indicated in Tables 3-5 and 3-6.

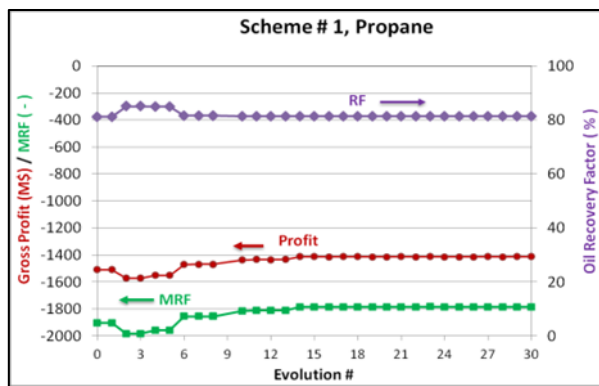


Figure 3-8. Progress of the main parameters during the optimization processes of scheme No. 1, injecting propane.

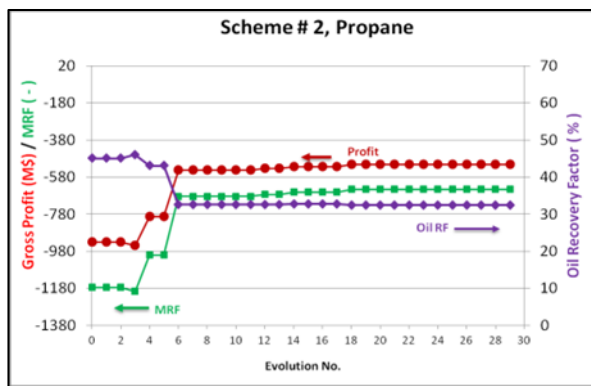


Figure 3-9. Progress of the main parameters during the optimization processes of scheme No. 2, injecting propane.

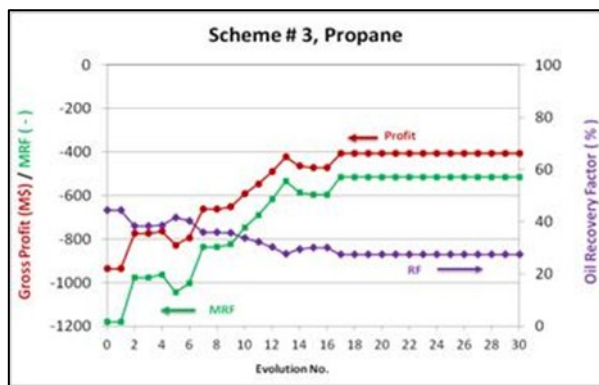


Figure 3-10. Progress of the main parameters during the optimization processes of scheme No. 3, injecting propane.

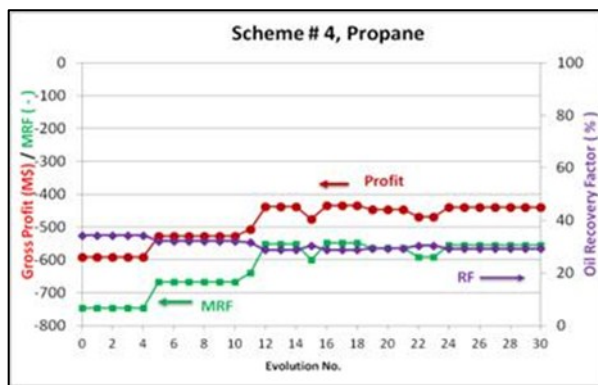


Figure 3-11. Progress of the main parameters during the optimization processes of scheme No. 4, injecting propane.

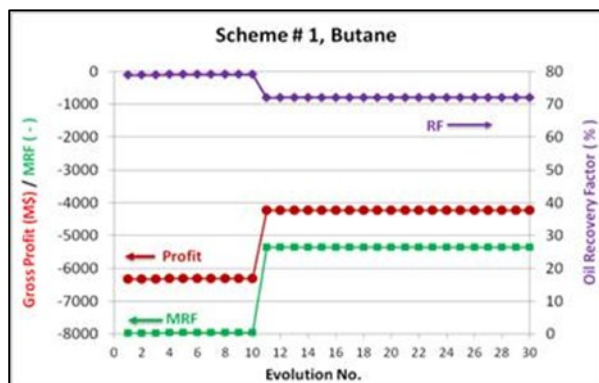


Figure 3-12. Progress of the main parameters during the optimization processes of scheme No. 4, injecting propane.

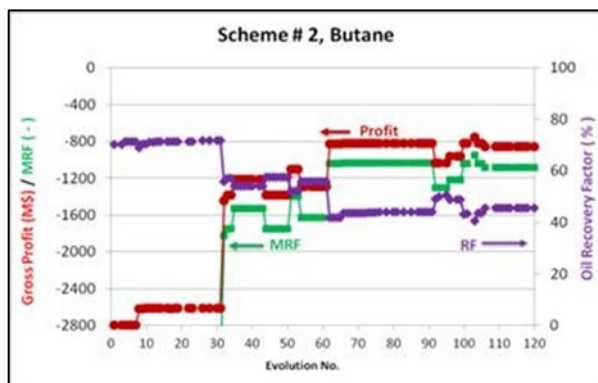


Figure 3-13. Progress of the main parameters during the optimization processes of scheme No. 2, injecting butane.

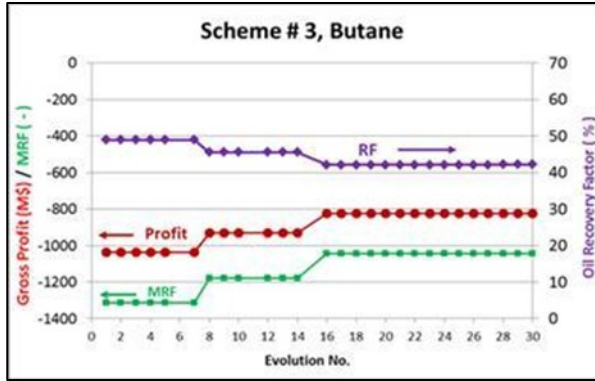


Figure 3-14. Progress of the main parameters during the optimization processes of scheme No. 3, injecting butane.

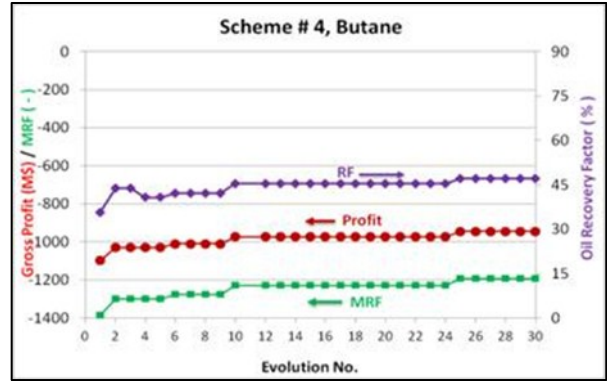


Figure 3-15. Progress of the main parameters during the optimization processes of scheme No. 4, injecting butane.

Table 3-5. Best combination of parameters yielding maximum economic benefit injecting propane.

Scheme No.	Q_{inj} [m ³ /day]	P_{wf} [kPa]	P_{inj} [kPa]	T_{inj} [°C]	T_{sat} @ P_{inj} [°C]	Δt_n [days]	Time to shut-in inj. Well [days]	Cum. solvent MM [m ³]		Q_{gmax} [m ³ /day]	
								Injected	Produced	before shut-in	After shut-in
1	9,000	600	3,000	83	77.6	---	3,650	32.301	30.825	---	---
2	3,000	1400	3,600	58	87.5	30	9,000	2.673	2.136	4,500	9,000
3	3,500	1400	2,000	78	57.2	360	9,000	1.741	1.312	3,000	9,000
4	3,000	1400	3,000	83	77.6	30	9,000	1.773	1.311	3,500	8,500

Table 3-6. Best combination of parameters yielding maximum economic benefit injecting butane.

Scheme No.	Q_{inj} [m ³ /day]	P_{wf} [kPa]	P_{inj} [kPa]	T_{inj} [°C]	T_{sat} @ P_{inj} [°C]	Δt_n [days]	Time to shut-in inj. Well [days]	Cum. solvent MM [m ³]	
								Injected	Produced
1	400	400	2,200	72	119.7	---	6,480	1.288	0.0
2	600	400	4,000	80	---	150	2,880	0.895	0.0
3	600	400	2,400	74	124.6	360	2,880	0.859	0.0
4	1,000	300	2,800	75	133.6	330	2,880	0.981	0.0

Only in injection/production scheme #2 with propane (Table 3-5), the optimal temperature of solvent injected was lower than the saturation temperature of the solvent at the injection

pressure. This means that the solvent was in liquid phase while being injected into the reservoir. As a consequence, oil viscosity was lower than that of schemes #3 and #4, in which the solvent was introduced into the reservoir in gas phase. In scheme #1, the solvent injected in gas form acted like a gas lift system, raising the diluted and less viscous oil to the surface. In schemes #3 and #4, heat was dissipated through the reservoir giving the solvent more time to segregate. Hence, unlike scheme #2, less diluted and more viscous oil was produced. However, temperature cannot be raised beyond a certain value due to the cost to heat the solvent and owing to decreasing gas solubility with increasing temperature at fixed pressure.

For schemes #2 through #4, the injection well remained operating for almost entire life of the project, while for scheme #1 the injection well was closed before reaching the half-life of the project. In scheme #1 the highest allowed injection rate was reached. It means that a higher injection rate likely improved the gas lift effect and thereby, a less negative profit was obtained. Similarly, in scheme #3, the higher allowed time was reached. Thus, more time to allow to gas diffuse into the oil was provided and it improved the profit.

Figure 3-16 shows the values of Gross Profit, RF and MRF for each one of the four schemes analyzed for propane. All cases showed negative MRF and profit, which were not necessarily proportional to the recovery factor.

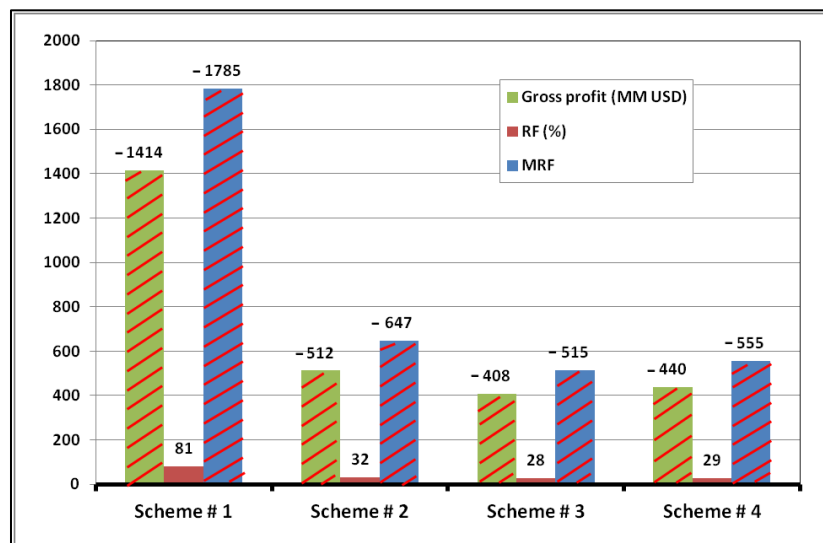


Figure 3-16. Economic benefit and RF injecting for propane. Note that MRF and Gross profit are negative.

In the butane case, the temperature of injection was lower than the saturation temperature at injection pressure for all cases (Table 3-6), with the exception of scheme #2, in which the solvent was injected at a value higher than the critical pressure (3796 kPa). The MRF in the butane cases was lower than the propane cases (**Fig. 3-17**) because solvent was not produced during the injection or after shut-in the injection well (Table 3-6). The optimization exercise showed the butane cases require a longer life project to begin to recover the solvent. The worst case was the continuous injection and production scheme, where the most negative MRF was obtained (scheme #1). In this case, the solvent was injected in the liquid form but the volume of solvent was not sufficient to create the gas lift system effect. The higher negative MRF obtained with butane was attributed to the combined effect of several factors highlighted below.

In the butane case, no gas was produced. By comparing Tables 3-5 and 3-6, one may observe that the volume of the gas injected into the reservoir is lower than in the propane case. For scheme 1 of the butane case, the injection rate was of 400 [m³/day] with 1.228 [MM m³] of solvent injected. In contrast, for the propane case, the injection rate was 9000 [m³/day] with a total of 32.301 [MM m³] injected. This case resulted in a considerable amount of solvent to be produced. For schemes 2 through 3, the solvent injected for the propane and butane cases are closer but in this case the Δt_n for butane cases is much longer than the Δt_n for the propane case. It gave more time to the butane to be diffused in to the oil than in the propane case.

None of the cases studied gave a positive MRF for given oil prices. However, certain cases resulted in significantly lower economical loss (e.g., No. 3, for both cases propane and butane). Hence, this case was chosen as the optimal and to be considered in the development plans and further optimization studies to make it “profitable”. Operational conditions for this are summarized in Tables 3-5 and 3-6. For this most optimal scheme, the volume of oil produced by 1 [m³] of solvent injected is 0.049 [m³] and 0.016 [m³] for propane and butane, respectively.

Regarding to the viscosity of oil produced, the production begins with 160 [cP] in the first production cycle and decrease to 20 [cP] in third production cycle for the propane case. Then, viscosity slowly decreases in each cycle to reach 12 [cP] at the end of the project life. In contrast, for the butane case, the viscosity remains around 122 [cP] along the project life. Viscosity value, for these two cases, does not require any addition of diluents to transport the oil produced indicating in-situ upgrading.

Higher flow restriction factor. Regardless the lower values of "frequency of solid precipitation" (Figure 3), "restriction factor" was higher for butane (Figure 3-2). This means that as the temperature increases, the permeability blockage becomes higher than in the propane case resulting in less oil drainage to the production well.

Cost of the solvent. A huge amount of solvent should be injected into the reservoir to produce the oil. After shutting the injection well, the producer was opened to release the solvent and recover it at the surface. As in the propane cases, a very important volume of solvent remained in the reservoir yielding a negative MRF. In all cases, the minimum bottom hole pressure constraint was set to 300 (kPa) (Table 3-2). With a lower constraint value, a higher gas volume could be released, improving the MRF. However, it is important to consider that a lower gas pressure means higher recompression cost. In this exercise, the price for propane was set to \$1,000 USD/m³ for the range of pressures of 2 through 4 MPa at 15°C.

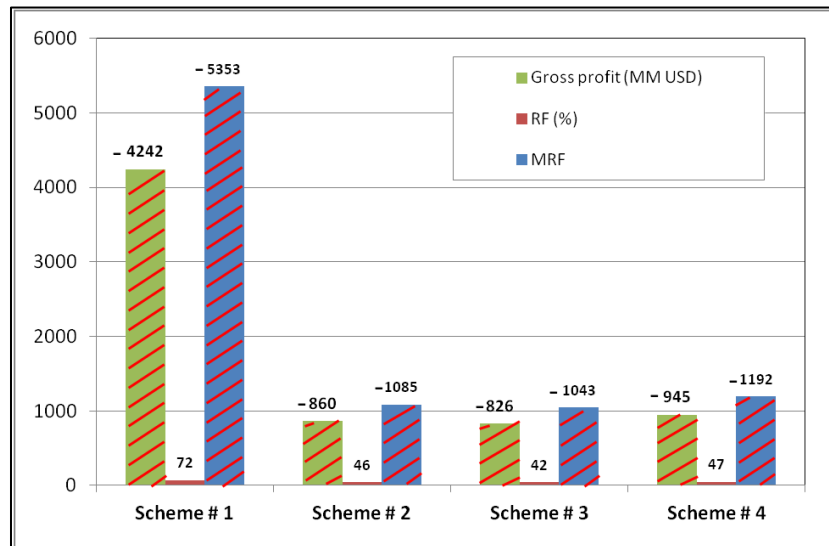


Figure 3-17. Economic benefit and RF injecting butane. Note that MRF and Gross profit are negative.

Heavy oil recovery by hot solvent injection is highly sensitive to the solvent and heavy oil prices. Defining R_p and R_b as the ratio *solvent price/oil price*, for propane and butane respectively, it is possible to determine what the volume of retrieved solvent should be in order to reach the

breakeven point (the point at which the gross profit or MRF is zero). Breakeven point for different values of R_p and R_b was obtained as follows:

1. By considering a fixed price of oil and different values of R_p and R_b , ranging from 1 to 10, the corresponding solvent cost was calculated (Table 3-7).

Table 3-7. Solvent cost

Oil price (USD/m ³)	Rp or Rb	Solvent cost (USD/m ³)
251.572	1	251.572
	1.1	276.729
	1.2	301.886
	.	.
	.	.
	10	2,515.720

2. Oil price and solvent cost from the above table as well as the cumulative oil produced and solvent injected from Tables 3-5 and 3-6 were substituted into Eqs. 1 through 3. The rest of the parameters were obtained from Table 3-4.
3. Eqs. 1 through 3 were solved simultaneously to find the amount of cumulative solvent produced that makes $MRF = 0$ (breakeven point).
4. Then, cumulative solvent produced was plotted against the ratio of solvent price/oil price.
5. This procedure was repeated for each production scheme and the type of solvent (**Figures 3-18 and 3-19**).

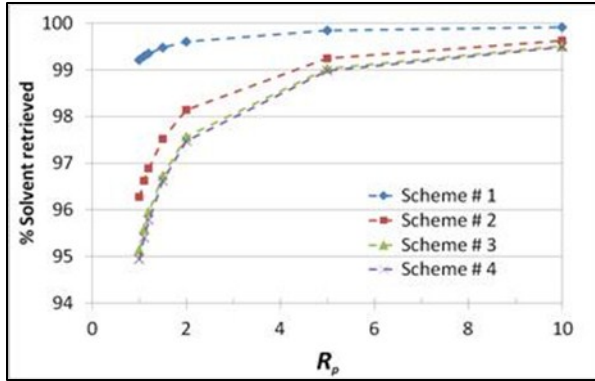


Figure 3-18 Breakeven point for propane

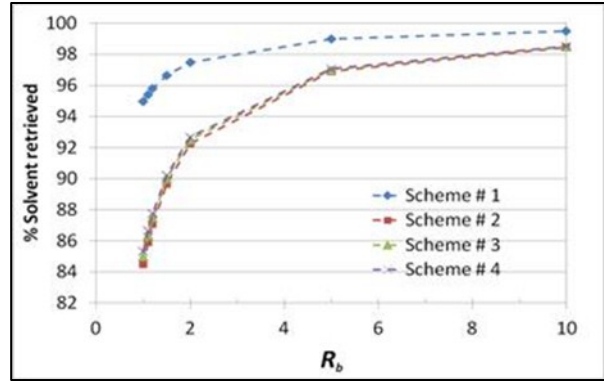


Figure 3-19 Breakeven point for butane.

One may observe through Figures 3-18 and 3-19 that as the ratio of R_p and R_b increases, almost all the solvent should be recovered to reach the breakeven point. For these cases in particular, if the solvent recovery increases above this critical value of solvent retrieval, the MRF will increase until it reaches a maximum value, shown in Figure 3-20.

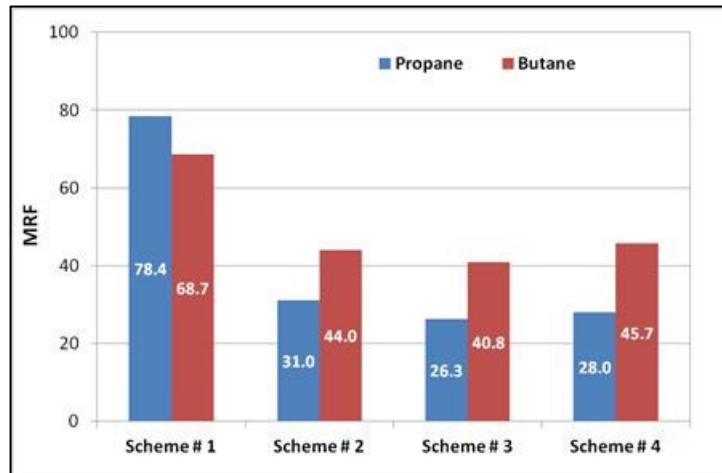


Figure 3- 20. Maximum economic benefit with 100% solvent retrieved.

Heat up the solvent. In this exercise, the cost to heat up the solvent represents less of 1% of the total revenue. Fuel used to heat up the solvent (either butane or propane) was propane. The cost was calculated as follows:

By assuming that solvent was delivered at the required injection pressure at the well head, its ρ , h_l and v_l were obtained at 15°C (T_l). Density was calculated for each injection pressure (Table 3-2) and then mass m was obtained from $\rho = m/V$. Hence, considering $V = 1$ (m^3), it was

possible to obtain m for the whole range of injection pressures. Next, h_2 and v_2 were obtained for the whole range of temperatures to be analyzed for the same pressures.

Thermal energy to raise the temperature of m to T_2 was calculated using the following equation, considering a constant pressure processes:

$$Q_{req} = m(h_2 - h_1) \quad (3-4)$$

Cost of propane for heating solvent was calculated based on its caloric content (Table 3-4), being 4.3 [USD/MM kJ]. This price corresponds to the average price during the first third of year 2014 (Alberta Energy). Thus, the cost of energy to heat up 1 m³ of solvent from T_1 to T_2 , at injecting pressure can be calculated as:

$$E_{cost} = \frac{Q_{req}}{\varepsilon} \times 4.3 \quad (3-5)$$

where ε is the efficiency of the process and equal to 0.9 in this study.

Due to the raise of temperature, the volume increases. So, the new volume, greater than 1, was calculated using equation 6.

$$V = m(v_2 - v_1) \quad (3-6)$$

The cost to raise 1 m³ of solvent was updated as follows:

$$E_{cost-new} = \frac{E_{cost-old}}{V} \quad (3-7)$$

Diffusivity of solvent. The diffusivity coefficients for propane and butane used were 7.83×10^{-11} and 5.82×10^{-11} [m²/s], respectively (Yanze and Clemens 2011). Thus, more time is needed for butane to diffuse in the same proportion as propane.

To make the heavy oil recovery by hot solvent injection process economically feasible, it is necessary to recover a great portion of the solvent injected into the reservoir. If all the injected solvent could be recovered by depressurizing the reservoir, then the MRF would be positive with the values shown in Figure 3-20. However, depressurizing the reservoir may not be sufficient to energize the solvent for retrieval and as a result, is necessary to apply a complementary recovery processes purely focusing on the retrieval of solvent.

Al-Bahlani and Babadagli (2009, 2012) introduced the technique called "steam-over-solvent injection in fractured reservoirs" (SOS-FR). This technique consists of alternated injection of steam and solvent, to improve the heavy oil recovery. The main stages of this technique are:

1. Thermal phase (hot water or steam injection),
2. Solvent phase (solvent injection cycles),
3. Final thermal phase (hot water or stem injection to heat the solvanted area to the boiling temperature of solvent) for solvent retrieval.

Naderi and Babadagli (2011, 2012, 2014) performed experiments applying this technique to different types of core samples at different pressures and temperatures. They found that the immersion of the samples into hot water at a temperature near to the boiling point of the solvent (stage 3 of the SOS-FR process) yields a recovery of 62 to 82% of the solvent diffused into the matrix. Similar results were obtained by Leyva-Gomez and Babadagli (2014). In their experiments, they injected liquid solvent into artificially fractured cores, for heavy oil recovery. They retrieved most of the solvent retained in the rock matrix, by injecting water at a temperature near to the saturation temperature of the solvent.

3.7 Conclusions

1. Heavy oil/bitumen recovery through hot solvent injection process is expensive and highly sensitive to the price of solvent, which entails robust optimization models. In this study, we selected the genetic algorithm to optimize the operational parameters during the exploitation of a reservoir. Because the stochastic optimization technique involved in the processes, the selection of the initial population is critical and is based on the knowledge of the problem to be solved. Our results showed that the wrong selection of the values of the operational parameters not only increase the number of evolutions needed to reach the optimal solution but also could yield a negative profit.
2. Another critical issue in this type of optimization scheme is the time involved in simulation runs. We reduced the computer time by using parallel processing and dynamic gridding.

3. We considered four schemes of solvent injection and oil production. For only a pair of injection/production well system considered in this study and the most negative economic benefit was obtained from the first scheme for propane, which is based on continuous injection with simultaneous and continuous production. Such benefit can only be achieved in the term of 10 years. For the schemes #2, #3 and #4 with propane, a less negative profit was obtained but it requires almost the entire life of the project. However, in these cases, the injection/production schemes applied leaves a considerable amount of oil and solvent in the reservoir. Hence, other production processes should be considered after hot solvent injection process to recover the remaining hydrocarbons to increase the profit. By contrast, the continuous injection scheme (Scheme 1) with butane gave a negative profit and the schemes #2 through #4 gave a lower profit than those with propane, but the time required to reach the breakeven point was shorter.
4. This paper dealt with complex problem and expensive process. Taking the laboratory scale experimental and simulations as the data base to a field scale optimization scheme, we showed that the inevitable solvent-heat injection combination (especially for extra heavy oil and bitumen cases) may result in a profitable project. The optimal application conditions were identified and critically analyzed to guide the practitioners for their field applications.

3.8 Nomenclature

E_{cost}	Energy cost [USD]
h	Enthalpy [kJ/kg]
m	Mass [kg]
P	Pressure (kPa)
Q_{inj}	Injection rate [m ³ /day]
Q_{req}	Energy required [kJ]
R	Ratio of <i>solvent price / oil price</i> [-]
RF	Recovery factor [%]
<i>s.c.</i>	Standard conditions
T	Temperature [°C]
t	Time [days]
V	Volume [m ³]

Greek

ε	Efficiency
Δ	Increment
ρ	Density [kg/m ³]
v	Specific volume [m ³ /kg]

3.9 References

- Al-Bahlani A.M. and Babadagli, T. 2009. Steam-Over-Solvent Injection in Fractured Reservoirs (SOS-FR) for Heavy-Oil Recovery: Experimental Analysis of the Mechanism. SPE 123568, presented at the 2009 SPE Asia Pacific Oil and Gas Conference & Exhibition, Jakarta, Indonesia, 4-6 Aug. [Doi:10.2118/124047-MS](https://doi.org/10.2118/124047-MS).
- Al-Bahlani, A.M. and Babadagli, T. 2011a. Field Scale Applicability and Efficiency Analysis of Steam-Over-Solvent Injection in Fractured Reservoirs (SOS-FR) Method for Heavy-Oil Recovery. *J. Petr. Sci. and Eng.* **78**: 338-346. <http://dx.doi.org/10.1016/j.petrol.2011.07.001>.
- Al-Bahlani, A.M. and Babadagli, T. 2011b. Steam-over-Solvent Injection in Fractured Reservoirs (SOS-FR) Technique as a New Approach for Heavy-Oil and Bitumen Recovery: An Overview of the Method. *Energy Fuels* **25** (10): 4528–4539. Doi:10.1021/ef200809z.l-
- Gosayir et al. 2012. Design of Solvent-Assisted SAGD Processes in Heterogeneous Reservoirs Using Hybrid Optimization Techniques. *J. of Canadian Petr. Tech.* **51** (6): 437-448.
- Babadagli, T. and Al-Bahlani, A.M. 2008. Hydrocarbon Recovery Process for Fractured Reservoirs, Canadian Patent Application, Serial No: 2,639,997 filed on Oct. 6, 2008, International Patent Application Serial No. PCT/CA2009/001366, Oct. 5, 2009 (US Patent Application, Serial No: 13/121,682 filed on July 21, 2011).
- Butler, R.M. and Mokrys, I.J. 1991. A New Process (VAPEX) for Recovering Heavy Oils Using Hot Water and Hydrocarbon Vapour. *J. Can. Pet. Technol.* **30** (1): 97-110. <http://dx.doi.org/10.2118/91-01-09>.
- Butler, R.M. and Mokrys, I.J. 1993b. Recovery of Heavy Oils Using Vaporized Hydrocarbon Solvents: Further Development of the VAPEX Process. *J. Can. Pet. Technol.* **32** (6): 38-55. Doi:10.2118/93-06-06.
- Castellanos Díaz, O., Modaresghazani, M.A., and Yarranton, H.W. 2011. Modelling the Phase Behaviour of Heavy Oil and Solvent Mixtures. *Fluid Phase Equilibria* **304**: 74-85. <http://dx.doi.org/10.1016/j.fluid.2011.02.011>.
- Computer Modeling Group Ltd. *STARS User's Guide*. 2011: 372-376.
- Edmunds, N., Barrett, K., Solanki, S., et al. 2009. Prospects for Commercial Bitumen Recovery from the Grosmont Carbonate, Alberta. *J. Can. Pet. Technol.* **48** (9): 26-32. Doi:10.2118/09-09-26.
- Edmunds, N., Moini, B., and Peterson, J. 2009. Advanced Solvent-Additive Processes via Genetic Optimization. Paper PETSOC 2009-115 presented at Canadian International

- Petroleum Conference (CIPC) 2009, Calgary, Alberta, Canada, 16-18 June. <http://dx.doi.org/10.2118/2009-115>.
- Government of Alberta. 2011. *The Resource Recovering the Resource*. Document available at www.oilsands.alberta.ca/FactSheets/About_Albertas_oil_sands.pdf-2011-07-13.
- Guerrero-Aconcha, U., Salama, D., and Kantzas, A. 2008. Diffusion Coefficient of n-alkanes in Heavy Oil. Paper SPE 115346 presented at the SPE annual Technical Conference and Exhibition, Denver, Colorado, 21-24 September. Doi:10.2118/115346-MS.
- Guerrero-Aconcha, U. and Kantzas, A. 2009. Diffusion of Hydrocarbon Gases in Heavy Oil and Bitumen. Paper SPE 122783 presented at the SPE Latin American and Caribbean Petroleum Engineering Conference, Cartagena, Colombia, 31 May-3 June. Doi:10.2118/122783-MS.
- Li, W., and Mamora, D.D. 2011. Light-and Heavy-Solvent Impacts on Solvent-Aided-SAGD Process: A Low-Pressure Experimental Study. Paper SPE 133277 presented at the Annual Technical Conference and Exhibition, Florence, Tuscany, 20-22 September. Doi:10.2118/133277-PA.
- Luo, H., Salama, D., Sryuchkov, S. et al. 2007. The Effect of Volume Changes Due to Mixing on Diffusion Coefficient Determination in Heavy Oil and Hydrocarbon solvent System. Paper SPE 110522 presented at the Annual Technical Conference and Exhibition, Anaheim, California, 11-14 November. Doi:10.2118/110522-MS.
- Luo, H. and Kantzas, A. 2008. Investigation of Diffusion Coefficients of Heavy Oil and Hydrocarbon Solvent Systems in Porous Media. Paper SPE 113995 presented at the Improved Oil Recovery Symposium, Tulsa, Oklahoma, 19-23 April. Doi:10.2118/113995-MS.
- Luo, P. and Gu, Y. 2009. Characterization of a Heavy Oil-Propane System in the Presence or Absence of Asphaltene Precipitation. *Fluid Phase Equilibria* **277**: 1-8. <http://dx.doi.org/10.1016/j.fluid.2008.10.019>.
- Nasr, T.N., Beaulieu, G., Golbeck, H. et al. 2003. Novel Expanding Solvent-SAGD Process “ES-SAGD”. *J. Can. Pet. Technol. (Technical note)* **42** (1): 13-16. Doi:10.2118/03-01-TN.
- Nghiem, L.X. and Coombe, D.A. 1996. Modeling Asphaltene Precipitation during Primary Depletion. SPE 36106 presented at the 4th Latin American and Caribbean Petroleum Engineering Conference, Trinidad and Tobago, 23-26 April. Doi:10.2118/36106-PA.
- Oballa, V. and Butler, R.M. 1989. An Experimental Study of Diffusion in the Bitumen-Toluene System. *J. Can. Pet. Tech.* **28** (2): 63-69. Doi:10.2118/89-02-03.
- Pathak, V. and Babadagli, T. 2010. Hot Solvent Injection for Heavy Oil/Bitumen Recovery: an Experimental Investigation. Paper SPE 137440 presented at the Canadian Unconventional Resources & International Petroleum Conference, Calgary, Alberta, 19-21 October. Doi:10.2118/137440-MS.
- Pathak, V., Babadagli, T., and Edmunds, N.R. 2011a. Mechanics of Heavy Oil and Bitumen Recovery by Hot Solvent Injection. Paper SPE 144546 presented at the Western North American Regional Meeting, Anchorage, Alaska, 7-11 May. Doi:10.2118/144546-PA.

- Pathak, V., Babadagli, T., and Edmunds, N.R. 2011b. Heavy Oil and Bitumen Recovery by Hot Solvent Injection. *J. Petr. Sci. and Eng.* **78**: 637-645. <http://dx.doi.org/10.1016/j.petrol.2011.08.002>.
- Speight J.G. 1973. Some Observations on the Hydroprocessing of a Heavy Crude Oil. *Fuel* **52** (4): 300–301. [http://dx.doi.org/10.1016/0016-2361\(73\)90061-6](http://dx.doi.org/10.1016/0016-2361(73)90061-6).
- Thomas, S. 2007. Enhanced Oil Recovery – An Overview. *Oil & Gas Science and Technology – Rev. IFP.* **63** (1): 9-19. <http://dx.doi.org/10.2516/ogst:2007060>.
- Zhao, L., Nasr, H., Huang, G. et al. 2004. Steam Alternating Solvent Process: Lab Test and Simulation. *J. Can. Pet. Technol.* **44** (9): 37-43. <http://dx.doi.org/10.2118/05-09-04>.
- Zhao, L. 2004. Steam Alternating Solvent Process. Paper SPE 86957 presented at International Thermal Operations and Heavy Oil and Western Regional Meeting, Bakersfield, California, 16-18 March. [Doi:10.2118/86957-MS](https://doi.org/10.2118/86957-MS).
- Zhao, L., Nasr, T. N., and Huang, H. et al. 2004b. Steam Alternating Solvent Process: Lab Test and Simulation. Paper SPE 2004-044 presented at the Canadian International Petroleum Conference, Calgary, Alberta, 8-10 June. [Doi:0.2118/2004-044](https://doi.org/10.2118/2004-044).

Chapter 4: Hot Solvent Injection for Heavy Oil/Bitumen Recovery from Fractured Reservoirs: An Experimental Approach to Determine Optimal Application Conditions

A version of this chapter was presented at the SPE Heavy Oil Conference and Exhibition held in Mangaf, Kuwait, 8-10 December 2014 (paper SPE-172901-MS), and also published in *Energy & Fuels*, 2016, 30 (4): 2780–2790.

4.1 Summary

We conducted a series of dynamic experiments in which liquid solvent (heptane) was injected into heavy oil saturated artificially fractured Berea sandstone samples with and without pre-thermal injection. To account for the effect of wettability on the process, experiments were repeated on the samples exposed to wettability alteration (more oil-wet) process. Cores were saturated with heavy crude oil and placed inside a rubber sleeve. Next, the system was placed into an oven and maintained at constant temperature conditions. Then, either hot solvent (superheated to be in vapour phase) or cold solvent was introduced into the system through the fracture at a constant rate. Pressure and temperature was continuously monitored at the inlet and center of the core. Properties of oil and liquid condensate from the gas produced were measured and analyzed. This scheme was repeated for a wide range of temperature conditions. The retrieval of the solvent during solvent injection phase and post-thermal method (steam or hot-water) injection performed for a wide range of temperature was monitored.

Our results and observations indicate that the first requirement for a successful application is an effective solvent diffusion into matrix before it breaks through and improves gravity drainage of oil by dilution. The second requirement is solvent retrieval.

4.2 Introduction

Steam injection for heavy-oil recovery demands a large volume of water and natural gas (Thomas 2007) to heat the reservoir and mobilize the oil. The use of solvent has been proposed to improve the efficiency of the steam processes by reducing the amount of steam injected and increasing the oil recovery. For example, vapour extraction (VAPEX) (Butler and Mokrys 1991, 1993), expanding solvent SAGD (ES-SAGD), steam alternate solvent (SAS) (Zhao 2007; Al-Bahlani and Babadagli 2009), steam-over-solvent injection in fractured reservoirs (SOS-FR) (Al-Bahlani and Babadagli 2008, 2011, 2014; Pathak and Babadagli 2010), or the injection of solvents at a higher temperature (Pathak and Babadagli 2011; Pathak et al. 2011; Leyva-Gomez and Babadagli 2013) were proposed and tested at the laboratory and field scale as alternative solutions. However, limited studies have been carried out to analyze the effect of temperature on solvent injection for heavy oil/bitumen recovery. Results from these experiments show that

heavy oil recovery is highly sensitive to temperature and model height (Pathak and Babadagli 2010, 2011; Pathak et al. 2011; Leyva-Gomez and Babadagli 2013).

In the case of carbonate and fracture systems, recovery of heavy oil/bitumen is more difficult due to low matrix recovery caused by unfavorable oil wetness and low permeability. A limited number of studies have been performed to explore and understand the physical phenomena involved in this process. Earlier studies on heavy oil recovery from carbonate systems include single and multiple block systems with the matrix surrounded by fracture networks. Rostami et al. (2007) performed a simulation study using a dual porosity system considering different injection rates at a fixed solvent injection temperature. They concluded, among other things, that solvent flows faster through fractures and forms solvent fingers. They also observed that an optimization procedure is necessary to find the optimum solvent injection rate.

Using laboratory cells made of sand packs for fractured and non-fractured cases, Rahnema et al. (2008) stated that the presence of fractures can compensate the low matrix permeability and enhance the whole process. Al-Bahlani and Babadagli performed static (2008) and dynamic (2011) experiments using sandstones and carbonate samples to study the alternate injection of steam/hot-water and solvent for heavy oil recovery from matrix. Their findings show there is a rate dependency in the process. Syed et al. (2012) studied permeability reduction due to the presence of hydrocarbon gas under reservoir conditions using packstone plugs. Rezaei and Mohammadzadeh (2010) reported on the recovery of bitumen using VAPEX process on a vuggy porous media, creating the vugular media by embedding wood particles in glass beads. The presence of vugs was found to improve the production characteristics of VAPEX. Naderi and Babadagli (2014) and Naderi et al. (2013) focused on heavy oil recovery from heterogeneous carbonates by solvent injection alternated by steam or hot-water. This technique yielded recoveries between 40% and 90% of the original oil in-place (OOIP) and recoveries of 62% to 82 % of the solvent diffused into the core during solvent exposure.

4.3 Description of the problem and solution methodology

Naturally fractured carbonate reservoirs are complex systems. They are formed by a structure containing faults, fractures, micro fractures, vugs, tight matrix with low porosity, and unfavorable wettability. This heterogeneous structure makes recovery a great challenge when

combined with high viscosity oil and excessive depth. Steam injection is typically inefficient due to its very heterogeneous structure. To overcome this problem, solvent involvement is needed. In SAGD processes, heat transfer occurs from steam or hot water into the heavy oil/bitumen. As a consequence, the viscosity of reservoir fluids decreases enhancing heavy oil/bitumen recovery. In contrast, in the hot solvent injection technique, the viscosity reduction is the result of heat transfer and dilution effect of the solvent yielding better results than SAGD or solvent injection alone (Edmunds et al. 2009a-b). This combined effect of heat transfer and dilution is expected to compensate the negative impact of the reservoir heterogeneity to some extent.

A very limited number of studies have dealt with heavy-oil recovery from this kind of reservoir using steam and solvent injection based on laboratory (experimental) and field scale (numerical simulation) modeling. Almost all laboratory scale studies used static models (just immersing the matrix element into a reactor filled with steam or solvent). This experimentation provides limited data as to the efficiency of the process and dynamic experiments (injection of steam or solvent to the model, continuously) are needed to provide information on the produced oil and solvent per steam and/or solvent injected. Most of the previous efforts on dynamic injection models were made for homogeneous sands. Experimentation of this kind requires special attention of the naturally fractured carbonate systems. The main objective of this work is to determine the optimal application conditions of hot-solvent injection for heavy oil recovery from fractured reservoirs applying dynamic tests. This will lead us to define the optimal rate and temperature when hot solvent is injected followed by hot water for solvent retrieval.

4.4 Experimental setup and procedures

Experiments were performed using Berea sandstone cores plugged out from the same block. They were artificially fractured by cutting along their longitudinal and transversal axes (**Figure 4-1**). All matrix pieces of every single core were saturated with oil under vacuum at 74°C, after placing them into a desiccator at a temperature of 140°C for 7 days. On the basis of the weight of the cores before and after saturation, the original oil in place (OOIP) was calculated using the density of the heavy oil used. Next, the core sections were joined using an epoxy. The final size of vertical fracture was 2 x 6 inches while the horizontal fracture had a radius of 1 inch. Thickness for both fractures was approximately 1 mm. The fracture space was filled with the

remaining oil used to saturate the rock matrix. The heavy oil used to saturate the cores was obtained from a Gulf of Mexico reservoir. Rock and oil properties are listed in **Table 4-1**.

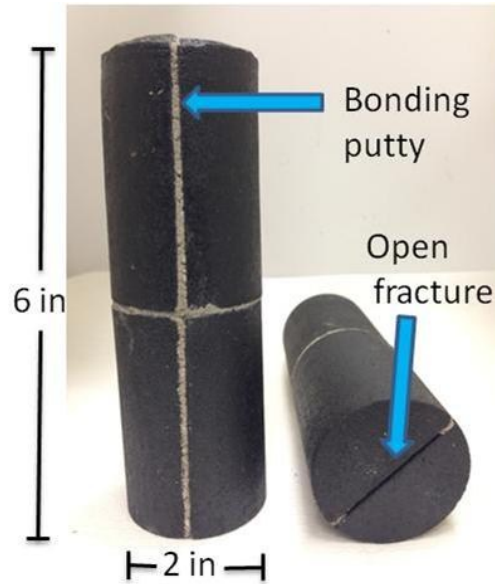


Figure 4-1. Artificial fractures in sandstone cores, used in the experiments.

It is known that sandstone is water wet while carbonates are preferentially oil wet. Therefore, to have a reference point of what would occur if the sandstone were oil wet, the wettability of a set of Berea sandstone cores was changed from water-wet to more oil-wet using Surfasil™ following the process described by Al-Bahlani and Babadagli (2008). After placing the cores into a desiccator at 140°C for 7 days to dry, the rock matrix pieces were submerged into a mixture of 10% Surfasil™ and 90% toluene for 24 hrs. Next, the cores were saturated three times with toluene to displace the excessive Surfasil™ creating a toluene monolayer covering the surface of the grains. Finally, the cores were saturated with methanol to preserve continuous oil wetness. After drying the cores for 24 hrs, the wetting angles were measured and found to be 134°. Then, oil saturation process was implemented as described above.

Table 4-1. Oil and core properties.

Parameter	Value	Units
Oil density	1.0003 @ 25°C 0.9903 @ 40°C 0.9772 @ 60°C	(g/cm ³)
Oil viscosity	136,000 @ 25°C 15,369 @ 40°C 2,097 @ 60°C	(cP)
Oil refractive index	1.57622 @ 25°C	(-)
Porosity	21	(%)
Permeability	286	(mD)
Core height	6	(in)
Core diameter	2	(in)
Fracture thickness for sandstone cores	1.0	(mm)
SARA analysis		
Saturates	12.4	
Aromatic	30.7	(%)
Resin	21.4	
Asphaltene	35.5	

Individual cores were placed inside a rubber sleeve (**Figure 4-2**) and pressure sensors were positioned at its inlet and outlet. Also, one temperature sensor was positioned at the inlet of the sleeve and one more in the center of the core, inside the fracture space. At the beginning of the experiments, pore and overburden pressures were at atmospheric pressure. While the second was maintained constant during each experiment, the pore pressure showed fluctuations along the experiments, as described later. The setup was designed to place the sleeve in a horizontal or vertical position. For the latter, the inlet was located at the top of the sample. Heptane was injected using a high precision syringe pump. Produced oil diluted with injected solvent was

collected using a graduated glass tube. At the inlet, the tubing was covered by heating tape connected to a high precision temperature controller. The entire system, excluding the graduated glass tube for vapour condensation, was placed inside an oven. Vapours produced were taken out the oven and collected in two graduated glass cylinders submerged into ice to cool the vapour solvent (heptane) by condensation.

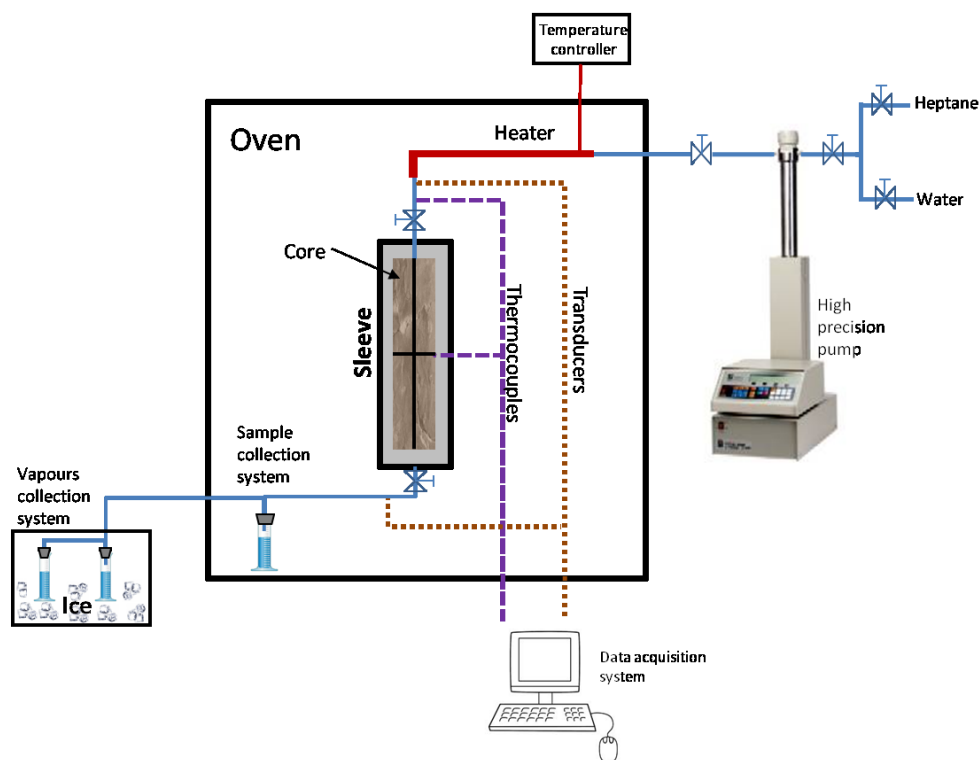


Figure 4-2. Experimental setup.

Density and refractive index (RI) measurements were performed for the diluted produced oil. Because the RI can be used as an indicator of the solvent concentration in the diluted oil (Moreno and Babadagli 2014), it was used to calculate the amount of oil-liquid produced. To achieve this, liquid heptane (**Table 4-2**) from *Fisher Scientific* supplier was mixed with the heavy oil used at several concentrations of wt% for each single concentration at 25°C. The average value of RI and density were obtained and wt% was converted to volume using $\rho_{oil} = m_{oil} / V_{oil}$. Then, the volume of heptane can be obtained by $V_{Hep} = 1 - V_{oil}$. Finally, the RI values were plotted against V_{Hep} and a trend line was created using a polynomial equation (**Figure 4-3**). By measuring the RI from the produced diluted oil, it was possible to correlate the amount of heptane and oil in the mixture.

Table 4-2. Heptane composition.

Component	Weight (%)
n-Heptane	>99
Methylcyclohexane	0 - 0.2
Isoctane	0 – 0.1
Dimethylcyclopentane	0 - 0.1

The experiments began by preheating the oven for several hours until the desired temperature inside the core was reached. Then, preheated heptane at the same temperature was injected through the core at a constant rate. Pressure and temperature at the inlet were recorded as well as the temperature at the center of the core and pressure at the outlet. During each experiment, produced fluid was collected and density measurements and RI were performed periodically. Volume of oil diluted and liquid condensate from vapours were registered. When the injection of the desired pore volume was completed, water injection was started. In most of the cases, temperature of water was increased several times until the heptane left inside the core was recovered by boiling. For all cases, initial temperature was that of the solvent injected.

To clarify the effect of injection rate on recovery from matrix through the diffusion of solvent, liquid heptane was injected through the core at a constant rate. One set of experiments was performed at 21°C (room temperature) using four injection rates: 0.1, 1.0, and 2.0 mL/min (**Figure 4-4**). In a second set of experiments, two different temperatures were applied: 45°C and 90°C for the core and heptane, respectively, to mimic hot solvent injection into a reservoir at its original temperature. In a field scale hot solvent injection project, the temperature of the reservoir is expected to be lower than the temperature of the solvent injected. At the atmospheric pressure, the saturation temperature of heptane is approximately 98.4°C. Hence, a temperature close to this value (90°C) was selected as the temperature of the experiment. Temperature of heavy oil reservoirs are presented in nature in a wide range of temperatures. Then, an “average” (or typical) value (45°C) was selected as temperature of the core. In these experiments, three

rates were applied: 0.5, 1.0, and 1.5 mL/min (Figure 4-5). In both sets of experiments, the core fracture plane along the longitudinal core axis was kept in horizontal position. These two sets of experiments were performed without oil in the core fracture space to avoid high displacement pressures due to the high oil viscosity.

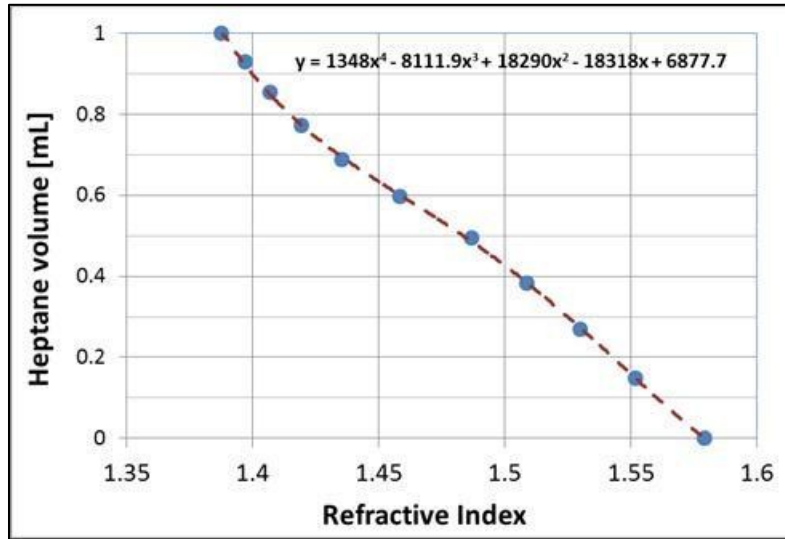


Figure 4-3. Comparison of recovery factor for experiments performed at 21°C.

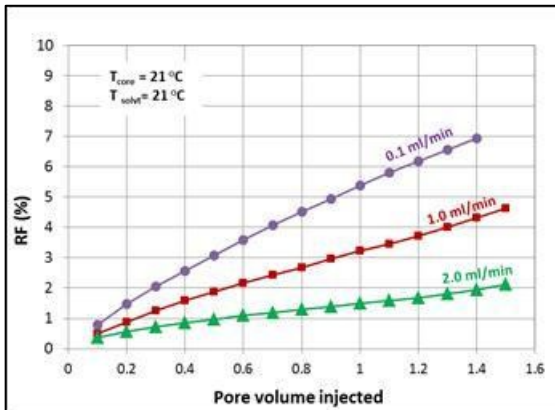


Figure 4-4. Comparison of recovery factor for experiments performed at 21°C.

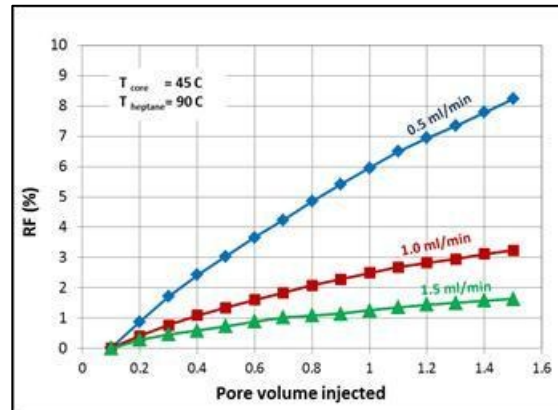


Figure 4-5. Comparison of recovery factor for experiments performed at 45 and 90°C for core and heptane, respectively

After these initial trials using horizontally positioned cores, a more realistic injection scheme for solvent injection was adapted and four more experiments were performed with the core vertical position. In these cases, the fracture was filled with heavy oil before the experiments, as these experiments were applied at higher temperatures causing much lower oil viscosity. Only one

injection rate (0.1 [mL/min]) was adapted based on the observations from the horizontal experiments by allowing sufficient contact time for the diffusion process between heavy oil and solvent. In all cases, solvent injection continued until 1 pore volume (PV) was reached. The main purpose of this was to obtain optimal temperature for this process as temperature critically controls the efficiency of the process (Pathak and Babadagli 2010, 2011; Leyva-Gomez and Babadagli 2013). Therefore, a wide range of temperatures was selected between 45°C and 130°C. As in the previous cases, pressure and temperature were recorded during solvent and heated water injection. All cores were preheated with both inlet and outlet valves closed. When the desired temperature was reached, the lower valve was opened and oil was allowed to be drained until no more oil was obtained after 30 min and the pressure in the system decreased to atmospheric pressure. An initial set of four experiments with the core in the vertical position was performed using Berea sandstone rock matrix. Another additional set of four experiments were carried out using the oil-wet cores. Note that the temperature of the core was the same as the injected solvent, mimicking injection of solvent to pre-heated reservoir as suggested in previous literature (Al-Bahlani and Babadagli 2008, 2009; Babadagli and Al-Bahlani 2009, 2014). In the SOS-FR method, injected steam (or hot-water) was proposed in the initial stage to heat up the matrix and recover the oil by thermal expansion. At the following stage, solvent was injected to recover oil from the matrix by diffusion-gravity drainage mechanism (Al-Bahlani and Babadagli 2008, 2009; Babadagli and Al-Bahlani 2009, 2014).

4.5 Results

Oil recovery was considerably low for the horizontal cases at ambient conditions (Figure 4-4). A slight increase in the system temperature (to 45°C) and injecting hot solvent (90°C) did not contribute remarkably to the recovery (Figure 4-5). Rate dependency was quite obvious in both trials. As we decreased the injection rate, more oil was recovered because, at low injection rates, heptane had more time to contact with matrix for effective diffusion. Consequently, more oil was taken out of the matrix. Although this method is favorable from oil recovered per solvent injected, the time required to recover the same amount of oil for low rate cases is much longer. Note that in the cases given in Figure 4-4, the recovery begins at 0.1 PV injected because the fracture space was empty and had to be filled with solvent before producing any fluid.

During the injection process for all cases, fluctuations were observed in the pressure reaching a peak point of 34.5 kPa (5 psi). This was attributed to the obstruction of the tubing at the outlet caused by the asphaltene precipitation. The temperature effect (Figure 4-5) is quite obvious on the recovery and enhanced not only thermal expansion process but also reduced viscosity. However, due to lack of gravity in the horizontally positioned samples, the gravity drainage mechanism on recovery can be assumed to be minimal. Enhancement of diffusion by increasing temperature within this range can also be assumed relatively small, due to the solvent channeling along the fracture, compared to the major contribution from thermal expansion.

One experiment was performed in horizontal position at 100°C and an injection rate of 0.1 mL/min. In this case, the last oil drop was obtained at 0.65 PV injected (**Figure 4-6**). Heptane injection was continued, however, until it reached 0.85 PV, but no oil production was observed. To retrieve the heptane diffused into matrix, water at 100°C was injected at an injection rate of 0.5 mL/min. Because the experiment was performed at atmospheric pressure, liquid water turned into saturated steam. Solvent vapour and steam were condensed and the heptane recovered was quantified after condensing it by cooling. When the sleeve was opened to remove the core, it was found that a considerable amount of oil accumulated around the outlet part of the core (**Figure 4-7**) between the sample and the end cap with the diffuser.

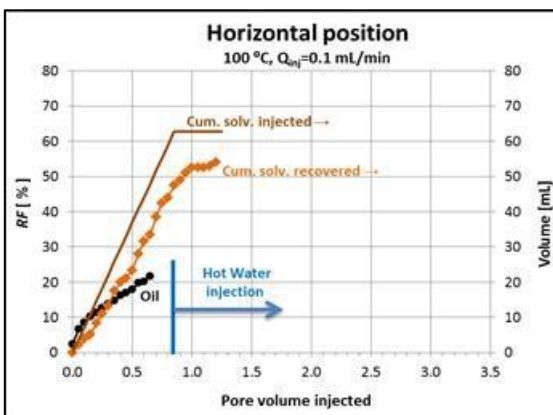


Figure 4-6. Oil recovery factor at 100°C from a core in horizontal position.

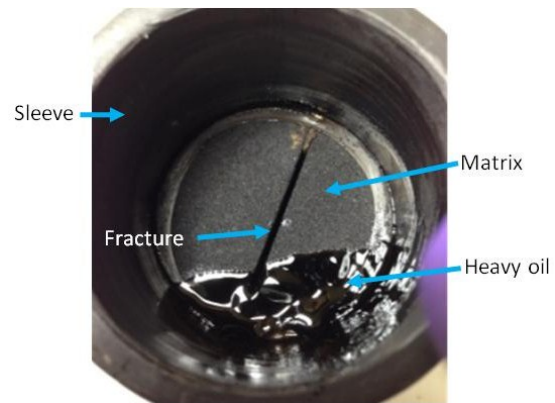


Figure 4-7. Oil accumulation at the bottom of the core, inside the sleeve at the outlet of the sleeve.

After these initial trials using horizontally positioned cores, a more realistic injection scheme for

light solvent injection was adapted and eight more experiments were performed with the core in vertical position. Of these, four experiments were performed on water-wet matrix (**Figures 4-8 through 4-15**) and the remaining with oil-wet matrix (**Figures 4-16 through 4-23**). The main purpose of these experiments was to obtain the optimal temperature as temperature critically controls the efficiency of the process (Pathak and Babadagli 2010, 2011; Leyva-Gomez and Babadagli 2011, 2013). Therefore, a wide range of temperatures were selected (45, 70, 100, and 130°C).

All cores were preheated with both inlet and outlet valves closed. When the desired temperature was reached, the lower valve was opened and oil was allowed to be drained until no more oil was obtained after 30 min and the pressure in the system decreased to atmospheric pressure. Only one injection rate (0.1 [mL/min]) for the solvent was adapted based on the observations from the horizontal experiments. In all cases, solvent injection continued until the amount reached 1 PV. Note that the temperature of the core was the same as the injected solvent mimicking the injection of solvent to a pre-heated reservoir as suggested earlier in literature (Al-Bahlani 2009; Babadagli and Al-Bahlani 2009, 2014). As in the previous cases, pressure and temperature were recorded during solvent and heated water injection.

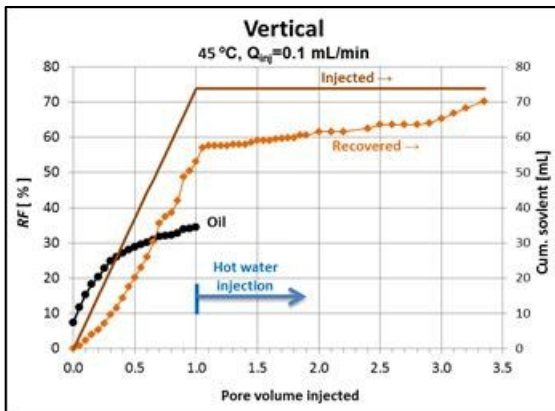


Figure 4-8. Oil diluted produced from experiment performed at 45°C. Water-wet rock matrix.

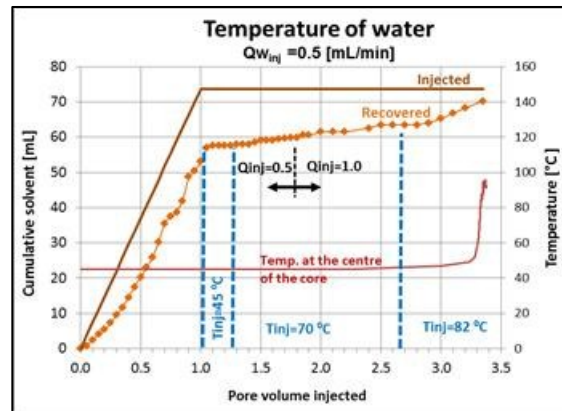


Figure 4-9. Solvent retrieval for experiment performed at 45°C. Water-wet rock matrix.

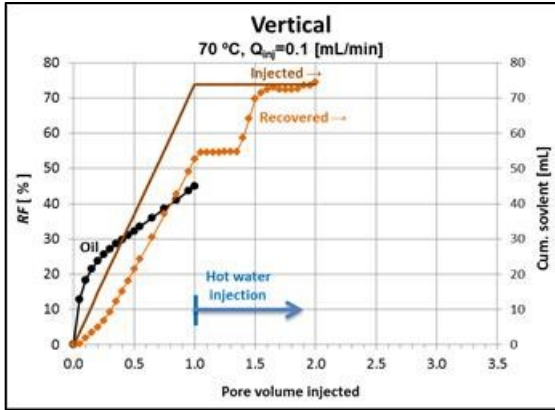


Figure 4-10. Oil diluted produced from experiment at 70°C. Water-wet rock matrix.

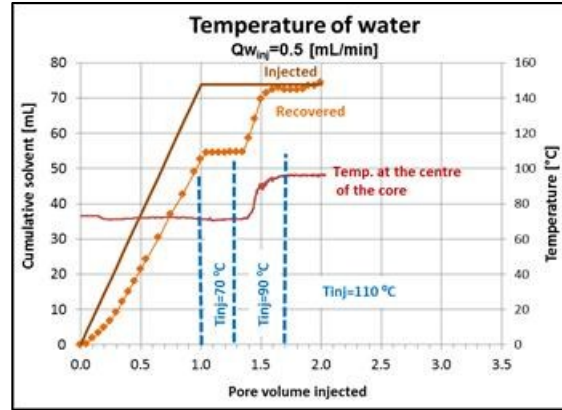


Figure 4-11. Solvent retrieval for experiment at 70°C. Water-wet rock matrix.

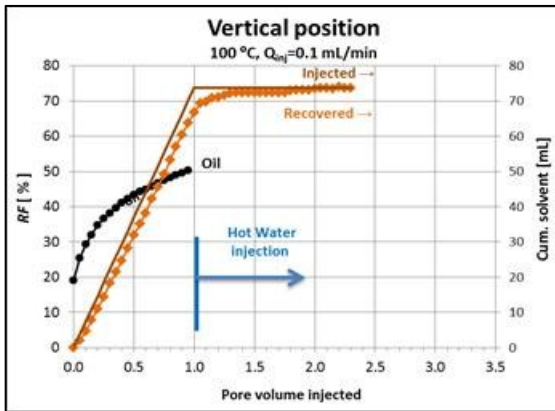


Figure 4-12. Oil diluted produced from experiment at 100°C. Water-wet rock matrix.

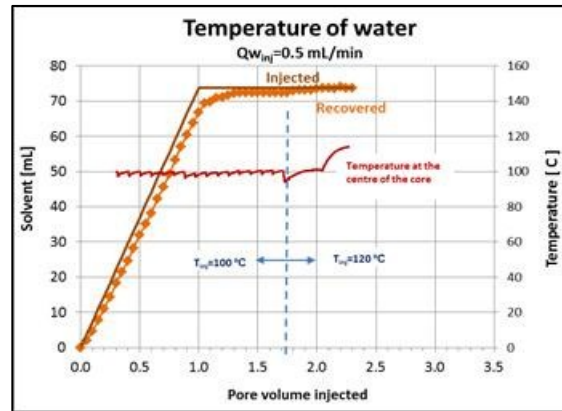


Figure 4-13. Solvent retrieval for experiment at 100°C. Water-wet rock matrix.

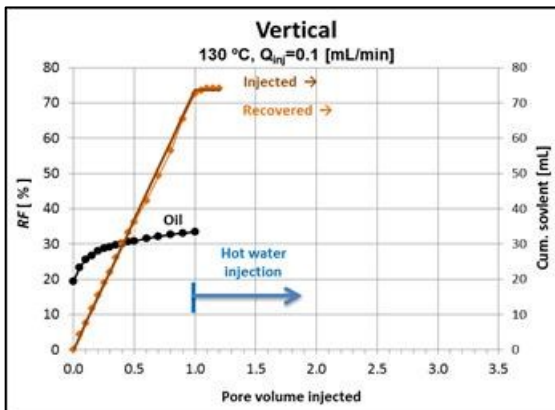


Figure 4-14. Oil diluted produced from experiment at 130°C. Water-wet rock matrix.

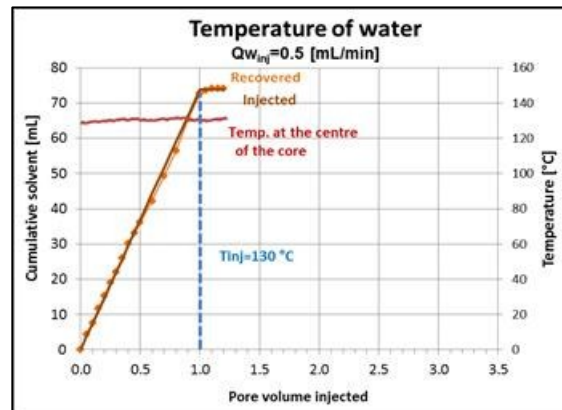


Figure 4-15. Solvent retrieval for experiment at 130°C. Water-wet rock matrix.

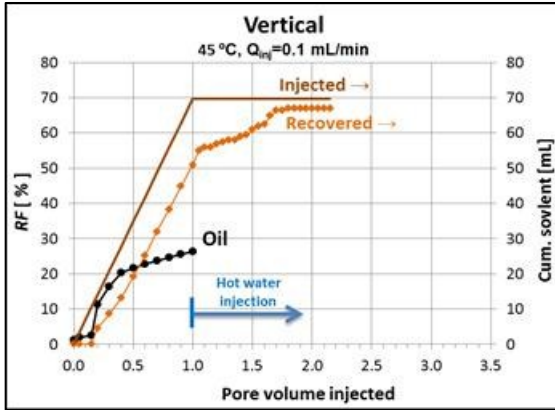


Figure 4-16. Oil diluted produced from experiment at 45°C using oil-wet rock matrix.

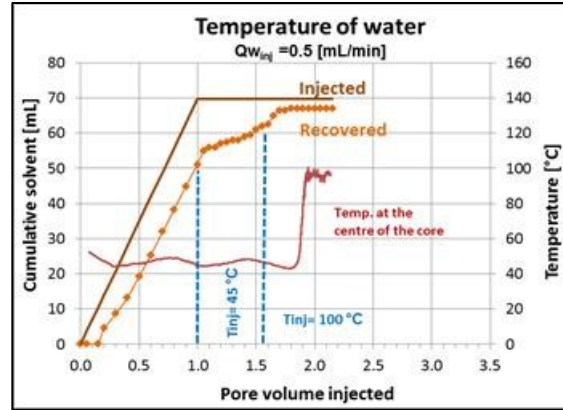


Figure 4-17. Solvent retrieval for experiment at 45°C using oil-wet rock matrix.

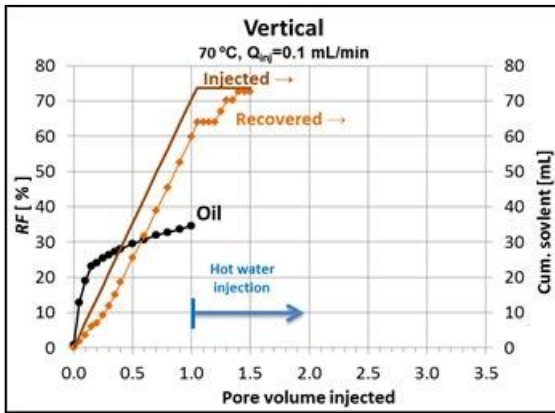


Figure 4-18. Oil diluted produced from experiment at 70°C using oil-wet rock matrix.

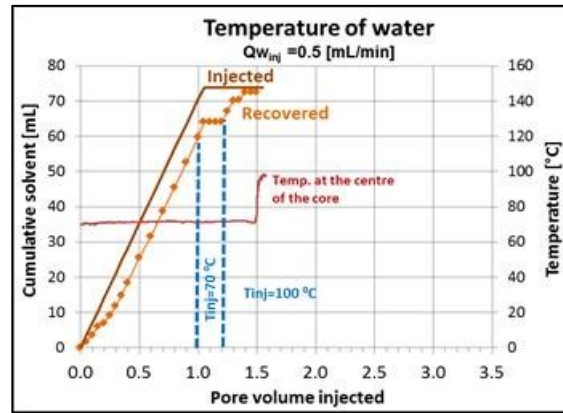


Figure 4-19. Solvent retrieval for experiment at 70°C using oil-wet rock matrix.

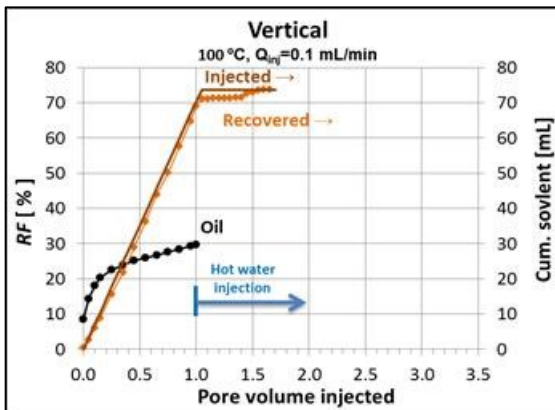


Figure 4-20. Oil diluted produced from experiment at 100°C using oil-wet rock matrix.

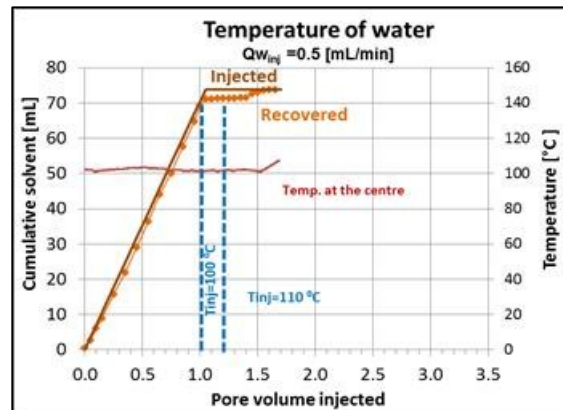


Figure 4-21. Solvent retrieval for experiment at 100°C using oil-wet rock matrix.

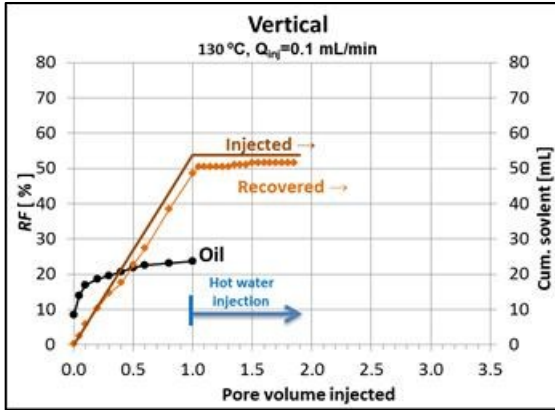


Figure 4-22. Oil diluted produced from experiment at 130°C using oil-wet rock matrix.

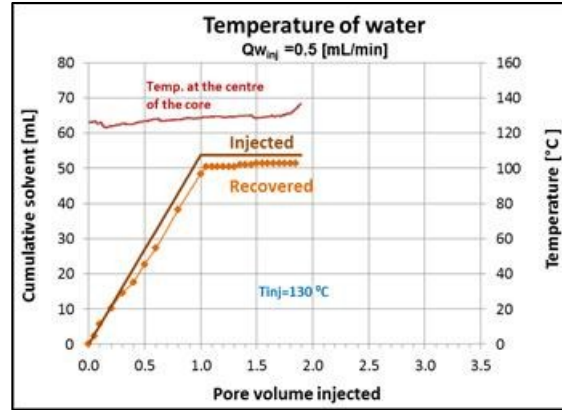


Figure 4-23. Solvent retrieval for experiment at 130°C using oil-wet rock matrix.

In Figure 4-8, the cumulative solvent injected was indicated by a brown solid line. Since the diluted oil produced is a mixture of solvent and heavy oil, individual volumes were calculated using refractive index measurements. The black dots correspond to the heavy oil produced while the orange dots were used for the solvent fraction obtained from the diluted oil plus the condensed solvent. After 1PV, solvent injection was stopped and hot water injection was started. For sake of simplicity and clarity, Figure 4-8 included only the recoveries of oil and injected solvent. In the next plot (Figure 4-9), temperature (measured at center of the core) profile was added to clarify its effect on the recovery with additional information including the temperature of the solvent injected and water injection rate. The same representation was followed in the further graph pairs (even number graphs include temperature profile and data) given in Figures 4-10 through 4-23.

Initially, the oil volume in the system was drained opening the outlet valve before injection of solvent was started. This is indicated by a “non-zero” recovery factor at “time zero” as the initial point on the oil curves given in Figures 4-8, 4-10, 4-112, 4-114, 4-16, 4-18, 4-20, and 4-22. This oil comes from the matrix and fracture mainly by gravity drainage (fracture) favored by high temperature and thermal expansion (matrix and fracture). The exception is the recovery obtained at 70°C for water-wet rock matrix (Figure 4-10) as well as 45°C and 70°C of oil-wet rock matrix where no oil was obtained after the outlet valve was opened. This could be due to the obstruction of the tubing; however, this amount was recovered right after solvent injection was started

through a quick jump (additional ~12% recovery) in both cases at 70°C. For the case at 45°C, it took more time to have this jump. The obstruction was inferred due to a pressure increase observed at the inlet of the core before the jump and the corresponding to a pressure release after the jump.

The efficiency of high temperature solvent injection truly depends on the retrieval of the solvent. Thus, it should also be optimized for an efficient process. The volume of solvent recovered during the solvent injection phase of the eight experiments and through the succeeding hot-water (or steam) injection process are given in Figures 4-8, 4-10, 4-12, 4-14, 4-16, 4-18, 4-20, and 4-22. The solvent was injected at a constant rate until 1.0 PV (solid brown line) was reached. The lines with diamond symbols correspond to the solvent recovered including solvent coming with oil (typically before hot water injection starts) and condensate (produced from the vapour phase during hot-water/steam injection after the solvent phase). The volume of solvent retained in the rock matrix is equal to the difference between these two lines. At 1.0 PV the solvent injection was stopped and hot-water (or steam) injection was started at the same temperature of the running experiment. When no more solvent was recovered the temperature of the injected water was increased until the solvent retrieval reached 100%.

Figure 4-24 presents ultimate recoveries of all eight experiments with respect to temperature. **Figure 4-25** shows the same data as Figure 4-23, but in this case the oil volume from the fracture was subtracted (only matrix recovery was included). The trend is similar to the case presented in Figure 4-24 (matrix and fracture together). The experimental results indicate that when temperature is below the boiling point of solvent (solvent is in liquid phase), the oil recovery increases with increasing temperature (Figure 4-24). In contrast, when the temperature of the solvent injected is above the saturation point of the solvent (solvent is in vapour phase), the recovery decreases with increasing temperature. This behaviour is in line with the experimental results obtained by Pathak et al. (2010, 2011) and numerical observations by Leyva-Gomez and Babadagli (2011) for propane and butane. Hence, liquid solvents (at ambient conditions such as pentane and above) also have an optimal temperature for maximal oil recovery by hot solvent, which is located near to the saturation temperature of the solvent injected.

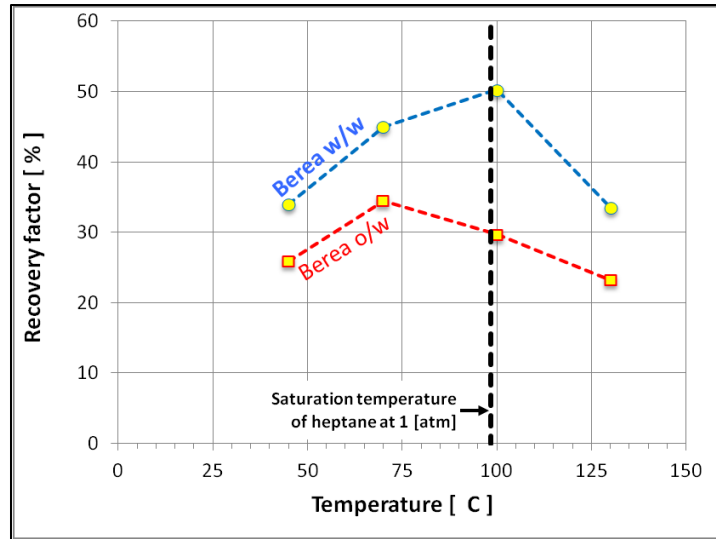


Figure 4-24. Oil recovery from all experiments, expressed as % of OOIP for different temperatures.

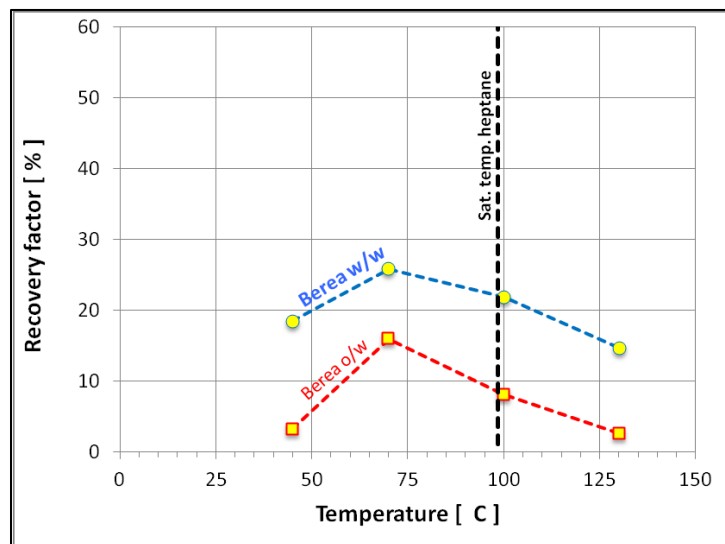


Figure 4-25. Oil recovery from rock matrix from all experiments. Note that oil from fracture space is not included.

The behaviour described above could be attributed to several reasons. Firstly, asphaltene precipitation becomes more severe with increasing temperature, which affects the diffusion rate and mixing quality. Temperature effect on asphaltene precipitation for mixtures of heavy oil and solvent was reported elsewhere. Nielsen et al. (1994) examined the effect of temperature and pressure on asphaltene precipitation and deposition from oil-sands/bitumen using n-pentene as diluent. He reported that larger amounts of asphaltene precipitation were obtained when either the temperature or the diluents-to-oil ratio increased. In contrast, Andersen (1994, 1995 and

1998) observed that asphaltene precipitation decreases as temperature increases. He performed dissolution experiments using solid Boscan asphaltenes and oil in toluene/n-heptane mixtures. He observed that, at higher temperatures, the asphaltene molecule dissociation decreases in the precipitated material as the temperature increased. Espinat (2004) investigated the effect of temperature on asphaltene aggregation at different temperatures. He reported that, at high temperatures, a reversible aggregation of asphaltenes leads to stable small entities. The apparent contradiction on these findings was explained by Andersen (1998) as the result of two different processes. One of them refers to the static precipitation at low pressure and the other to the continuous deasphalting with low n-alkane at high temperature and pressure. On other hand, Speight (1999) emphasized that one of the relevant parameters for asphaltene separation is the ratio of the volume of precipitation/volume of feedstock and asphaltene yield increases as this ratio increases.

These observations can be used to explain the increasing amount of asphaltene at higher temperature and why the volume of asphaltene decreased above the saturation temperature of the solvent in our experiments. The dynamic nature of our experiments are more similar to the continuous deasphalting processes mentioned above, and the continuous injection of solvent ensure a constant source of precipitant, which in turn cause a higher volume of asphaltene precipitated as temperature increase and solvent diffuse into the rock matrix. Beyond the boiling point, regardless the increased temperature, the volume of precipitant is lower (gas phase) and in consequence the volume of asphaltene precipitated decreases.

Secondly, asphaltene precipitation may also yield pore plugging not only in the tighter matrix but also in fractures. Hamadou et al. (2008) investigated the permeability reduction on core samples extracted from Rhourd-Nouss (RN) due to the asphaltenes and resins deposition. They reported permeability reductions ranging from 72.4% to 98.3% and as a result of this, irreversible retention of these components in the cores was observed. Syed et al. (2012) presented the results of formation damage due to asphaltene deposition as a result of hydrocarbon gas injection using representative core samples and reservoir fluids at real operating conditions. They found that permeability reduction depends of the rock type, pressure and length of the core sample. Thirdly, as can be inferred from **Figures 4-26 and 4-27**, however, the same oil recovery can be obtained

eventually but much more solvent needs to be injected, which in turn negatively affects the efficiency of the process.

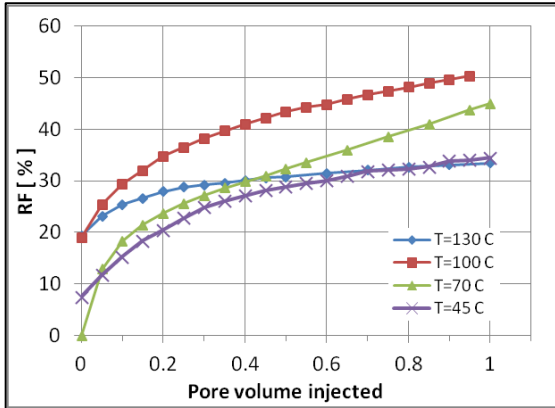


Figure 4-26. Oil diluted produced from experiments using Berea sandstone (water-wet).

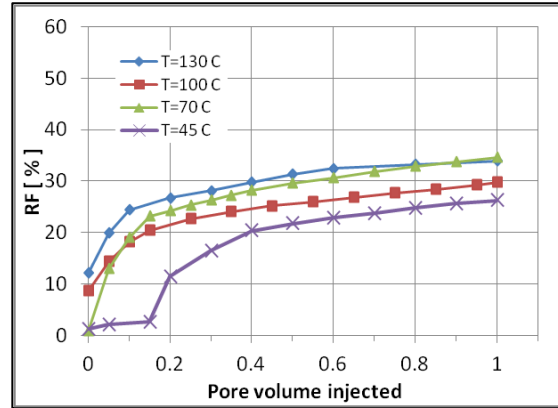


Figure 4-27. Solvent retrieval for experiments using Berea sandstone (oil-wet) treated chemically.

Density measurements for the diluted (produced) oil at 25°C are shown in **Figures 4-28 and 4-29**. Note that these values do not include the oil recovered from fracture, which has the same density as the original oil. As the pore volume of solvent injected increases, its density approaches to that of the density of the solvent used (in our case heptane density was 0.679 g/cm³). This density is related to the reduction of oil produced from the rock matrix, and not to the oil density itself. As commented previously, the refractive index was used to correlate the density of oil diluted to the volume of oil in the mixture. A lower density means that less oil is being produced from the core. Measurements of density of oil produced for the 130°C and 120°C experiments were not performed due to the small amount of volume recovered at each time and waiting for the accumulation of a sufficient amount caused evaporation of heptane out of the produced mixture. The humps observed at a 100°C shown in Figure 4-28 and those in Figure 4-29 at 45°C and 100°C were caused by the obstruction of the tubing due to asphaltene precipitation. When this occurred, the amount of oil recovered was small, causing a greater accumulation of solvent in the core. The restricted flow allowed more time for the solvent to be in contact with rock matrix and therefore more heavy oil was dissolved by diffusion. Consequently, when the tubing was unblocked, the oil produced had a greater density. On the

other hand, it can be seen that density decreased rapidly with hot solvent injection and stabilized beyond 0.3 PV injected.

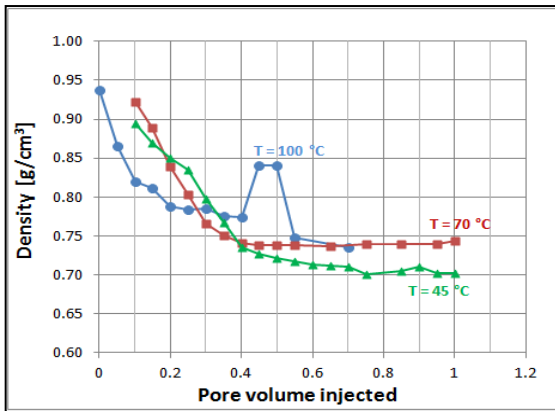


Figure 4-28. Density at 25°C of oil produced from Berea sandstone cores in vertical position.

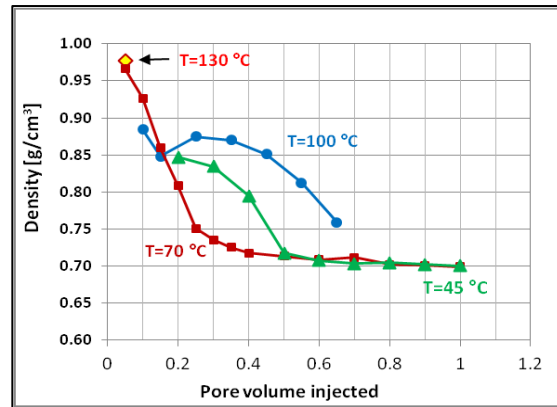


Figure 4-29. Density at 25°C of oil produced from oil-wet Berea sandstone cores in vertical position.

For the 45°C case with water-wet rock matrix (Figure 4-8), hot water injection began after 1 PV of solvent was injected. A great amount of solvent was retrieved during the solvent injection case (53 mL out of 74 mL) but solvent retrieval at this low water temperature (45°C) was negligibly small. Then, the temperature of water was increased to 70°C when 1.25 cumulative PV were injected. Having only a limited amount of solvent retrieval at this rate, the injection rate was increased from 0.5 to 1.0 mL/min at 1.75 cumulative PV injected. The total solvent retrieval was only 8 mL during this period. Finally, temperature was increased to 82°C at 2.6 cumulative PV injected and a sudden increase in the solvent retrieval was observed. This is mainly due to the temperature getting closer to the solvent boiling point. Note that increasing injection rate did not show any critical change in the solvent retrieval unless the temperature is increased.

The effect of temperature was much clearer for the next cases given in Figures 4-11, 4-13, 4-15, 4-17, 4-19, 4-21, and 4-23. First of all, the amount of solvent retrieved during the solvent injection phase of 70°C was quite similar to the case of 45°C. When the hot water injection was continued at the same temperature, no solvent was retrieved (Figure 4-10 and 4-18). However, when the temperature of water was increased to 90°C and 100°C for water-wet and oil-wet rock matrix respectively, almost all of the remaining solvent in the matrix was retrieved.

For the experiments at 100°C for water-wet and oil-wet (Figures 4-13 and 4-21), around 98 and 97% of the solvent injected was retrieved mainly due to solvent being about that of the boiling point (vapour phase). The remaining ~2-3% of the solvent was recovered by hot water injection at 120°C and 110°C, respectively. For the higher temperature (130°C) case, all of the solvent was retrieved during the solvent injection phase for both water- and oil-wet rock matrices.

Figure 4-30 summarizes all observations in a single plot. It shows the cumulative solvent retrieved during solvent injection and following hot-water injection against temperature for each experiment. Solvent retrieved from the oil-wet cores was indicated by circle symbols; while the solvent from water-wet cores was marked by diamond ones. Colors correspond to the temperature of the solvent when it was injected (45, 70, 100, or 130°C). For example, the first diamond symbol, from left to the right, corresponds to the solvent recovered from the experiment performed at 45°C using a water-wet core. Its position in the plot indicates that when water was injected at 45°C, the amount of solvent recovered was nearly 72%. When temperature was increased to 70°C, solvent retrieval reached 86%. Note that values shown include solvent produced with oil diluted (solvent in injection phase) and condensate solvent (produced from the vapour phase during hot-water/steam injection after the solvent phase).

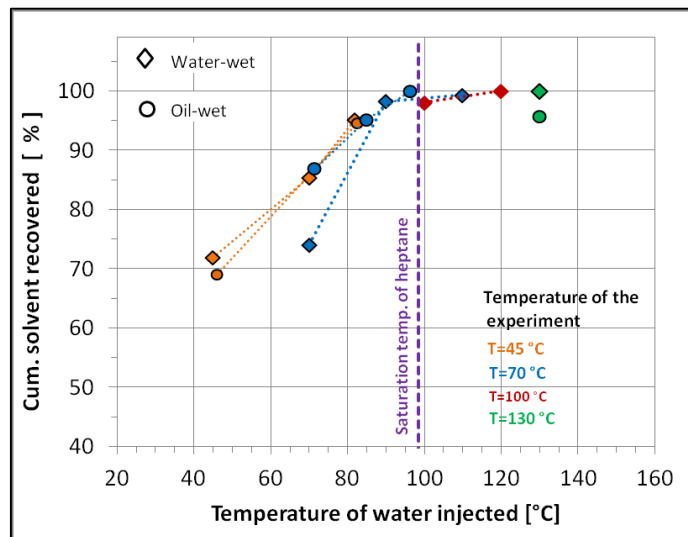


Figure 4-30. Percentage of solvent retrieval vs. temperature. Cumulative values shown include both solvent from the oil diluted and condensate from the solvent vapour.

4.6 Conclusions

1. A critical temperature that yields the maximum oil recovery exists in hot solvent application, which is located around the saturation temperature of the solvent. This verifies the observations from the previous studies that used propane and butane as solvent.
2. Heavy oil recovery is highly dependent on the solvent injection rate. Due to the low diffusion coefficient of solvent, longer times are needed to diffuse the solvent into the matrix. For this reason, the highest amount of production was obtained at the lower injection rate. Consequently, for a successful application of the recovery by hot solvent injection (or to improve the gravity drainage of matrix effectively), the rate should be adjusted based on the solvent diffusion capability into the matrix oil as well as temperature.
3. From an economic point of view, when the density of the oil diluted tends to stabilize, a different injection/production scheme should be considered to increase the amount of heavy oil recovered.
4. Most of the oil recovered at temperatures beyond the saturation temperature of the solvent was produced by gravity drainage, accelerated by a reduction of viscosity due to elevated temperatures. Solvent retrieval by hot water injection depends on temperature. A more efficient solvent retrieval process was observed when the temperature of the water was close and beyond the saturation temperature of the solvent.
5. Almost all the injected solvent was retrieved during the solvent injection phase (as dissolved in the oil produced or in the form of vapour) in the temperature cases of 100°C and 130°C. Hence, no further hot-water injection was needed for solvent retrieval. No asphaltene precipitation was found in the cores for the cases of 120°C and 130°C.
6. Experiments below the saturation temperature yielded some solvent recovery during the solvent phase (around ~70%) and further hot-water injection at the temperature around the boiling point of the solvent was needed to totally recover the rest of the solvent.
7. From an experimentation point of view, the refractive index was useful to estimate the fractions of oil and solvent due to the small volume of sample required for the analysis.

4.7 Nomenclature

A	Arrhenius constant (also known as frequency factor or pre-exponential factor)
C_m	instantaneous concentration of fuel
C_3	Propane
CMG	Computer Modelling Group
CO	Carbon monoxide
CO ₂	Carbon dioxide
DSC	Differential Scanning Calorimetry
E	Activation energy
EOS	Equation of state
HPDSC	High Pressure Differential Scanning Calorimetry
k	Rate constant
L	Matrix block side length
LTAI	Low-temperature air injection
LTASI	Low-temperature air-solvent injection
LTO	Low Temperature Oxidation
m, n	reaction orders
N ₂	Nitrogen
NFR	Naturally fractured reservoir
O ₂	Oxygen
$p_{O_2}^m$	partial pressure of oxygen
PVT	Pressure-Volume-Temperature
R	Universal gas constant
RF	Recovery factor
SARA	Saturates- Aromatics-Resins-Asphaltenes
T	Temperature
TGA	= Thermogravimetric Analysis

4.8 References

- Al-Bahlani, A.M. and Babadagli, T. 2009. Laboratory and Field Scale Analysis of Steam Over Solvent Injection in Fractured Reservoirs (SOS-FR) for Heavy Oil Recovery. Annual Technical Conference and Exhibition, New Orleans, LA, 4–7 October. <http://dx.doi.org/10.2118/124047-MS>.
- Al-Bahlani, A.M. and Babadagli, T. 2011. Field Scale Applicability and Efficiency Analysis of Steam-Over-Solvent Injection in Fractured Reservoirs (SOS-FR) Method for Heavy-Oil Recovery. *J. Petr. Sci. and Eng.* **78**: 338–346. <http://dx.doi.org/10.1016/j.petrol.2011.07.001>.
- Al-Bahlani, A.M. and Babadagli, T. 2008. Heavy-Oil Recovery in Naturally Fractured Reservoirs with Varying Wettability by Steam Solvent Co-Injection. International Thermal

- Operations and Heavy Oil Symposium, Calgary, AB, 20–23 October. DOI: 10.2118/117626-MS.
- Andersen, S.I. 1994. Dissolution of Solid Boscan Asphaltenes in Mixed Solvents. *Fuel Sci. Tech. Int.* **12**: 1551–1577. DOI:10.1080/08843759408916249.
- Andersen, S.I. 1995. Effect of Precipitation Temperature on the Composition of n-Heptane Asphaltenes: Part 2. *Fuel Sci. Tech. Int.* **13**: 579–604. DOI:10.1080/08843759508947696.
- Andersen, S.I. 1998. Investigation of Asphaltene Precipitation at Elevated Temperature. *Fuel Sci. Tech. Int.* **6**: 323–334. DOI:10.1080/10916469808949786.
- Babadagli, T. and Al Bahlani, A. M. 2009. Applicability of SOS-FR (Steam-Over-Solvent Injection in Fractured Reservoirs) Method for Heavy-Oil Recovery from Deep Fractured Carbonates. International Petroleum Technology Conference, Doha, Qatar, 7–9 December. <http://dx.doi.org/10.2523/13023-ABSTRACT>.
- Babadagli, T. and Al-Bahlani, A.M. 2014. Hydrocarbon Recovery Process for Fractured Reservoirs. U.S. Patent (U.S. Patent No. 8,813,846).
- Butler, R.M. and Mokrys, I.J. 1991. A New Process (VAPEX) for Recovering Heavy Oils Using Hot Water and Hydrocarbon Vapour. *J. Cdn. Pet. Tech.* **30**: 97–110. <http://dx.doi.org/10.2118/91-01-09>.
- Butler, R.M. and Mokrys, I.J. 1993. Recovery of Heavy Oils Using Vapourized Hydrocarbon Solvents: Further Development of the VAPEX Process. *J. Cdn. Pet. Tech.* **32**: 38–55. <http://dx.doi.org/10.2118/SS-92-7>.
- Edmunds, N., Barrett, K., Solanki, S., et al. 2009a. Prospects for Commercial Bitumen Recovery from the Grosmont Carbonate, Alberta. *JCPT* **48**: 26–32. <http://dx.doi.org/10.2118/09-09-26>.
- Edmunds, N., Moini, B. and Peterson, J. 2009b. Advanced Solvent-Additive Processes via Genetic Optimization. Canadian International Petroleum Conference (CIPC), Calgary, AB, 16–18. doi:10.2118/2009-115.
- Espinat, D., Fenistein, L. Barré, D. et al. 2004. Effects of Temperature and Pressure on Asphaltenes Agglomeration in Toluene. A Light, X-ray, and Neutron Scattering Investigation. *Energy and Fuels* **18**: 1243. DOI: 10.1021/ef030190.
- Hamadou, R., Khodja, M., Kartout, M. et al. 2008. Permeability Reduction by Asphaltenes and Resins Deposition in Porous Media. *Fuel* **87**: 2178–2185. <http://dx.doi.org/10.1016/j.fuel.2007.12.009>.
- Leyva-Gomez, H. and Babadagli, T. 2011. Optimal Application Conditions for Heavy-Oil/Bitumen Recovery by Solvent Injection at Elevated Temperatures. SPE Heavy Oil Conference and Exhibition, Kuwait City, Kuwait, 12–14 December. <http://dx.doi.org/10.2118/150315-MS>.
- Leyva-Gomez, H. and Babadagli, T. 2013. Numerical Simulation of Heavy-Oil/Bitumen Recovery by Solvent Injection at Elevated Temperatures. *J. Petr. Sci. and Eng.* **110**: 199–209. <http://dx.doi.org/10.1016/j.petrol.2013.08.015>.

- Moreno, L. and Babadagli, T. 2014. Asphaltene Precipitation, Flocculation and Deposition During Solvent Injection at Elevated Temperatures for Heavy Oil Recovery. *Fuel* **124**: 202–211. <http://dx.doi.org/10.1016/j.fuel.2014.02.003>.
- Naderi, K. and Babadagli, T. 2014. Use of Carbon Dioxide and Hydrocarbon Solvents During the Method of Steam-Over-Solvent Injection in Fractured Reservoirs for Heavy-Oil Recovery From Sandstones and Carbonates. *SPE Res. Eval and Eng.* **17**: 286–301. <http://dx.doi.org/10.2118/169815-PA>.
- Naderi, K., Babadagli, T. and Coskuner, G. 2013. Bitumen Recovery by the SOS-FR (Steam-Over-Solvent Injection in Fractured Reservoirs) Method: An Experimental Study on Grosmont Carbonates. *Energy and Fuels* **27**: 6501–6517. DOI: 10.1021/ef401333u.
- Nasr, T.N., Beaulieu, G. Golbeck, H. et al. 2003. Novel Expanding Solvent-SAGD Process “ES-SAGD”. *J. Cdn. Pet. Tech. (technical note)*. **42**: 13–16. <http://dx.doi.org/10.2118/03-01-TN>.
- Nielsen, B.B., Svrcek, W.Y., and Mehrotra, A.K. 1994. Effects of Temperature and Pressure on Asphaltene Particle Size Distributions in Crude Oils Diluted with n-Pentane. *Ind. Eng. Chem. Res.*: 1324–1330. DOI: 10.1021/ie00029a031.
- Pathak, V and Babadagli, T. 2010. Hot Solvent Injection for Heavy Oil/Bitumen Recovery: An Experimental Investigation. Paper SPE 137440 presented at the Canadian Unconventional Resources & International Petroleum Conference, Calgary, AB, October 19–21. <http://dx.doi.org/10.2118/137440-MS>.
- Pathak, V., Babadagli, T., and Edmunds, N.R. 2011. Mechanics of Heavy Oil and Bitumen Recovery by Hot Solvent Injection. Western North American Regional Meeting, Anchorage, Alaska, 7–11 May. <http://dx.doi.org/10.2118/144546-PA>.
- Pathak, V., Babadagli, T., and Edmunds, N.R. 2011. Heavy Oil and Bitumen Recovery by Hot Solvent Injection. *J. Petr. Sci. and Eng.* **78**: 637–645. <http://dx.doi.org/10.1016/j.petrol.2011.08.002>.
- Rahnema, H., Kharrat, R., and Rostami, B. 2008. Experimental and Numerical Study of Vapor Extraction Process (VAPEX) in Heavy Oil Fractured Reservoir. Proceedings of the Canadian International Petroleum Conference/SPE Gas Technology Symposium 2008. <http://dx.doi.org/10.2118/2008-116>.
- Rezaei, N. and Mohammadzadeh, O. 2010. Pore-Level Investigation of Heavy Oil and Bitumen Recovery Using Hybrid SAGD. SPE Improved Oil Recovery Symposium, Tulsa, Oklahoma, 24–28 April. <http://dx.doi.org/10.2118/130011-MS>.
- Rostami, B., Azin, R., and Kharrat, R. 2007. Investigation of the Vapex Process in High Pressure Fractured Heavy Oil Reservoirs. International Thermal Operations and Heavy Oil Symposium, Calgary, AB, 1-3 November. <http://dx.doi.org/10.2118/97766-MS>.
- Syed, F.I., Ghedan, S.G., Al-Hage, A. et al. 2012. Formation Flow Impairment in Carbonate Reservoirs Due to Asphaltene Precipitation and Deposition during Hydrocarbon Gas Flooding. Abu Dhabi International Petroleum Conference and Exhibition, Abu Dhabi, UAE, 11–14 November. <http://dx.doi.org/10.2118/160253-MS>.

- Speight J.G. 1999. *The Chemistry and Technology of Petroleum*. 3rd edition, New York: Marcel Dekker.
- Zhao, L., Nasr, T.N., Huang, H. et al. 2004. Steam Alternating Solvent Process: Lab Test and Simulation. Canadian International Petroleum Conference, Calgary, AB, 8-10 June. <http://dx.doi.org/10.2118/05-09-04>.
- Thomas, S. 2007. Enhanced Oil Recovery – An Overview. *Oil & Gas Science and Technology – Rev., IFP*. **63**: 9–19. DOI: 10.2516/ogst:2007060.
- Zhao, L. Steam Alternating Solvent Process. 2007. International Thermal Operations and Heavy Oil and Western Regional Meeting, Bakersfield, CA, 16–18 March. <http://dx.doi.org/10.2118/86957-PA>.

Chapter 5: Heavy Oil/Bitumen Recovery from Fracture Carbonates by Hot-Solvent Injection: An Experimental Approach to Determine Optimal Application Conditions

A version of this chapter was presented at the SPE International Heavy Oil Conference and Exhibition, held in Mangaf, Kuwait, 6-8 December 2016 (SPE-184095-MS). Also, it was submitted to SPE Journal for publication.

5.1 Summary

This paper presents an extensive analysis solvent injection at elevated temperatures to recover heavy-oil/bitumen from fractured carbonates. Three different solvents (propane, heptane and distillate oil -naphtha) were injected at different temperatures representing a wide range of carbon number. Indiana limestone (outcrop) and vuggy naturally fractured carbonate samples (outcrop core samples from a producing formation in Mexico) were selected as core samples. Hot solvent was injected continuously through artificially fractured cores followed by hot water (or steam injection) phase. The optimal temperatures for heavy oil recovery and solvent retrieval, in the subsequent hot water injection, for each kind of rock sample and type of solvent were determined. The results revealed that heavy oil recovery increase with the solvent carbon number used. Also, it was observed that when the temperature is higher than the saturation value for the given pressure curve, the recovery decreases and the lightest component of the heavy oil are dragged by the gas stream.

5.2 Introduction

Recovering heavy oil/bitumen from naturally fractured carbonates is challenging due to unfavorable rock characteristics (fractures, vugs, tight matrix with low porosity, and oil wet nature). Gas, water or any other fluid injected for enhancement of oil production results in severe channelling through the fractures while the matrix tends to retain the oil due to unfavorable wettability. Therefore, oil displacement from tight matrix requires a long time for an effective transfer process by capillary imbibition or gravity drainage. To tackle these challenges, a feasible solution is to reduce the viscosity of heavy oil, which can be achieved in two ways: (1) heat transfer by steam or hot water injection, or (2) oil dilution by solvent injection. An alternative and more efficient way is to apply both as a hybrid process: hot solvent injection. In this technique, the combined effect of heat transfer and dilution yields a better result than the sole application of SAGD or cold solvent injection alone (Butler and Mokrys 1991, 1993; Pathak and Babadagli 2010; Pathak et al. 2011a-b; Edmunds et al. 2009). Due to the gas solvent injection, viscosity reduction effect was studied numerically by Kaneko et al. (2013). They demonstrated that higher recovery can be obtained with heavy gas solvent than with injecting light ones. This makes the process more expensive and requires effective retrieval of solvent for

an economically viable process. The efficiency of this process has been studied extensively but all these efforts were made using homogeneous sandpacks or highly permeable sandstones (Moreno and Babadagli 2013, 2014a; Haghghat and Maini 2013; Pathak and Babadagli 2010; Pathak et al. 2011a-b).

In the case of naturally fractured carbonate rock matrix, this kind of processes requires special attention due to poor interaction between matrix and solvent in fractures caused by unfavorable rock properties as listed above. Rostami et al. (2005) focused their studies on dual porosity systems and stated the necessity of establishing an optimum solvent injection rate. Rahnema et al. (2008) observed in their studies with low matrix permeability fractured systems that heavy-oil recovery can be efficiently enhanced by solvent diffusion process. Rezaei and Mohammadzadeh (2010) studied the VAPEX process on a vuggy porous media and concluded that the presence of vugs improves the efficiency of VAPEX. Later, Naderi et al. (2013) and Naderi and Babadagli (2014) experimentally analyzed the dynamics of heavy oil recovery from heterogeneous carbonates by solvent injection alternated by steam or hot-water. Their reported values of heavy oil recovery using different solvents were highly encouraging despite unfavorable matrix conditions (oil-wet sands and carbonates).

Leyva-Gomez and Babadagli (2014, 2016) performed experiments injecting hot heptane into artificially fractured sandstones saturated with heavy oil. They showed that temperature of injected solvent should be close to its vapour pressure in order to maximize oil recovery. The proper selection of solvent for this kind of recovery process becomes more important in low permeability rock matrix. Due to the solvent presence, effective permeability will be reduced by the blockage of the pores by the asphaltene precipitation. This effect was studied by Syed et al. (2012) and more recently by Moreno and Babadagli (2013, 2014a-b). The latter concluded that an optimum solvent selection not only depends on oil and rock characteristics, but also on the diffusion and mixing quality. On the basis of these observations, they recommended using different solvents throughout the recovery processes; i.e., lighter ones initially and switching to heavier ones later on.

5.3 Description of the problem and solution methodology

The aforementioned previous experiments either used homogenous samples with static conditions (Pathak et al. 2012, 2013), dynamic conditions (injection through the core) with homogeneous sandpacks (Moreno and Babadagli 2013, 2014a-b), or fractured sands under dynamic conditions (Leyva-Gomez and Babadagli 2014, 2016). The outcome of these studies was consistent: The maximum ultimate recovery is reached when the operating temperature is near the saturation temperature of the solvent injected for a given pressure. Also, it was observed that for a successful solvent retrieval by hot water injection, the temperature of water should be equal to or higher than the saturation temperature of liquid solvent retained in the rock matrix.

In carbonates, however, matrix-fracture interaction may differ due to tight and oil-wet nature of the rock matrix, which may significantly reduce the efficiency of the process. However, solvent injection is one of the limited options to heavy-oil recovery from fractured carbonates, especially in the deep reservoirs where effective heating may not be technically possible. On the basis of these, we adapted our earlier experimental design (continuous solvent injection -dynamic experiments- through fractured rock matrix) introduced in Leyva-Gomez and Babadagli (2014, 2016) and a parametric study was conducted considering a wide range of temperatures, pressures, solvents, and rock types.

The main objective of this study is to define the optimal injection rate and temperature when hot solvent is injected in a continuous way (dynamic conditions). To achieve this, hot solvent was injected through two types of carbonates rocks at different temperature and pressure conditions covering different thermodynamic conditions that yield a liquid or gas form of the solvent injected. The solvent phase was followed by hot water injection for solvent retrieval. During the experiments, operational conditions and properties of the fluids produced were measured continuously. The results were compared with the previous runs in which water and oil-wet sandstones samples were used as rock matrix and heptane as solvent.

5.4 Experimental setup and procedures

The first set of experiments was performed using Indiana limestone cores plugged out from the same block. A second set of experiments was performed with vuggy naturally fractured

carbonate (NFC) cores, obtained from a single long core, extracted from the outcrop of a producing formation in Mexico (**Figure 5-1**). All cores were cut along their longitudinal and transversal axes. Next, both sets of cores were placed inside a desiccator at a temperature of 140°C for 7 days and saturated with heavy oil obtained from a field in the Gulf of México, under vacuum at 74°C. The original oil-in-place (OOIP) of the cores was calculated on the basis of the weight of the core before and after saturation process and density of the heavy oil. Similarly, porosity was calculated using the weight and dimensions of the cores. Then, the core sections were joined using an epoxy (**Figure 5-2**). For the first set of cores, the final size of vertical fracture was 2 x 6 inches while the horizontal fracture had a 2-inch diameter. For the second set, the vertical fracture was 2.5 x 3 inches and the horizontal fracture had a 2.5-inch diameter. In all cases, the vertical and horizontal fracture thickness was approximately 1 mm. The fracture space was filled, unless otherwise stated, with the remaining oil after the saturation process. Rock and oil properties are listed in **Table 5-1**.

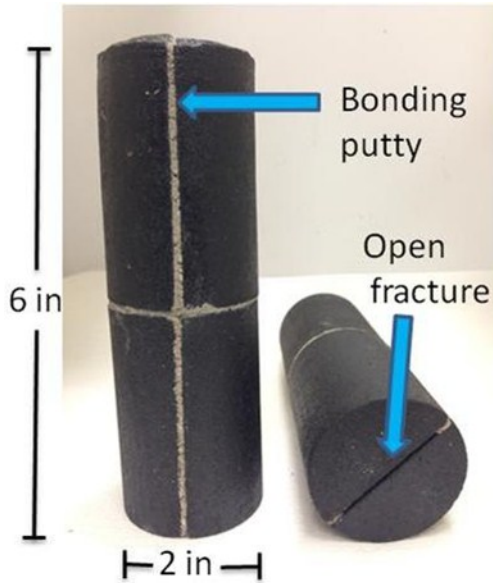


Core number 1

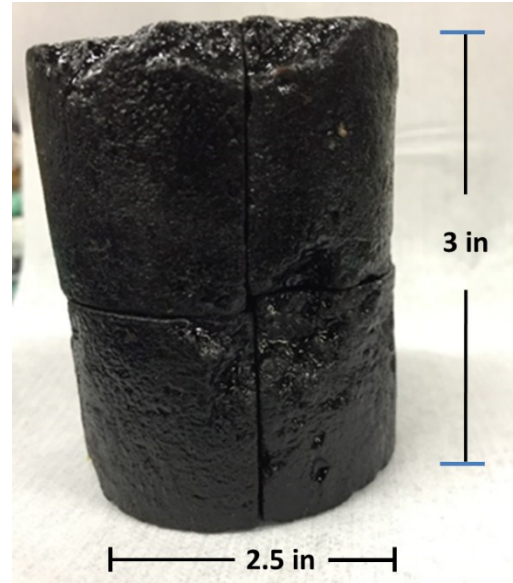


Core number 2

Figure 5-1. Bioclastic wackestone cores with moldic porosity, open fractures, and partially sealed from a Mexican outcrop field.



a) Indiana limestone core



b) Naturally fracture vuggy carbonate core

Figure 5-2. Cores after saturation processes: a) Indiana limestone core after joint the four sections with bonding putty; b) Naturally fractured carbonate core before joint the four sections with bonding putty.

Table 5-1. Oil and core properties.

Parameter	Value	Units	Parameter	Value	Units
Oil density	1.0003 @ 25°C 0.9903 @ 40°C 0.9772 @ 60°C	(g/cm ³)	Oil viscosity	136,000 @ 25°C 15,369 @ 40°C 2,097 @ 60°C	(cP)
Oil refractive index	1.57622 @ 25°C	(cP)	Artificial fracture thickness	1.0	(mm)
Porosity			Permeability		
• Indiana Limestone	17	(%)	• Indiana Limestone	27	(mD)
• Fracture carbonates	12		• Fracture carbonates	10	
Core height			Core diameter		
• Indiana Limestone	6	(in)	• Indiana Limestone	2	(in)
• Fracture carbonates	3		• Fracture carbonates	2.5	
SARA analysis			S_{wi}	0	(%)
Saturates	12.4				
Aromatic	30.7	(%)			
Resin	21.4				
Asphaltene	35.5				

**Table 5-2. Heptane composition
(Fisher Scientific data sheet).**

Heptane composition	Weight (%)
n-Heptane	>99
Methylciclohexane	0 – 0.2
Isooctane	0 – 0.1
Dimethylciclopentane	0 – 0.1

Table 5-3. Naphtha composition.

Carbon number	n-Paraffin (%wt)	Unknowns (%wt)
5	6.33	7.61
6	4.25	5.93
7	3.09	11.48
8	1.18	1.34
9	0.95	7.97
10	0.87	10.33
11	0.47	7.80
12	0.28	6.71
13	0.13	4.25
14	0.01	5.57
15	0.00	0.45
16	0.00	0.07
17	0.00	0.00
18-120	0.00	12.89
Total	17.56	82.44

To perform experiments with either heptane or distilled oil (naphtha) (Tables 5-2 and 5-3), individual cores were placed inside a rubber sleeve. Two sensors, one for pressure and one more for temperature, were positioned at the inlet of the sleeve while one more pressure sensor was placed at the outlet. A second temperature sensor was placed at the center of the core, through a previously drilled small hole practiced through the sleeve and the core (Figure 5-3). To increase the temperature of the fluid injected into the core, the tubing at the inlet was covered by heating tape connected in turn to a high precision temperature controller. Both the produced diluted oil and injected hot water were collected using a graduated glass tube. The entire system was placed inside a convection oven. Solvent was injected using a high precision syringe pump. Solvent produced in the form of vapour was taken out the oven and collected in two graduate glass tubes that were submerged into ice to cool the solvent vapour by condensation.

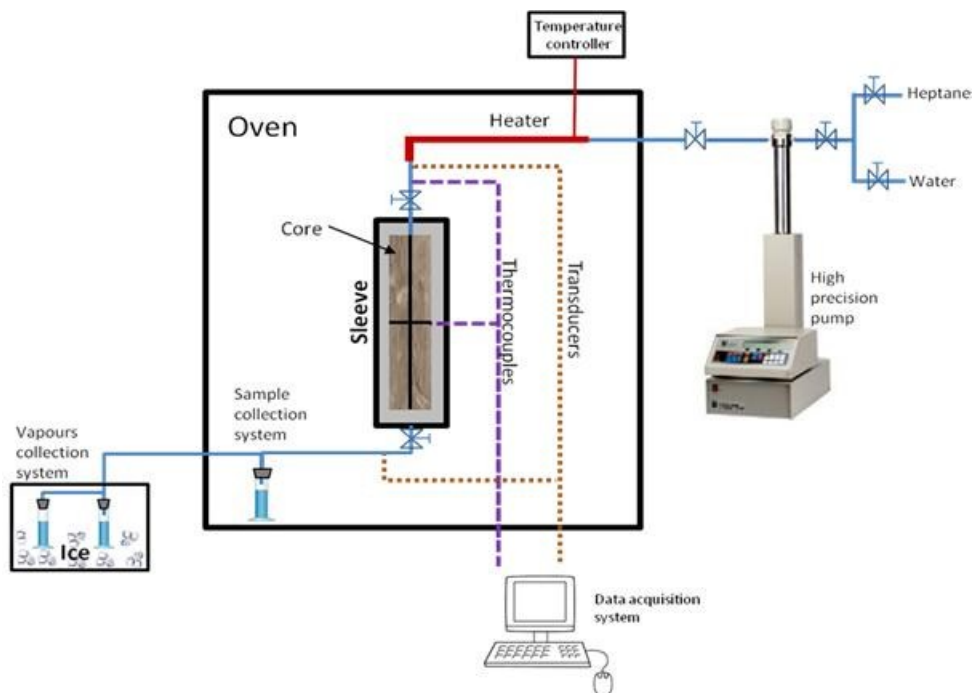


Figure 5-3. Experimental setup used to perform experiments with either heptane or naphtha at low pressure.

For the propane experiments, the rubber sleeve was placed inside a core holder; therefore, the second temperature sensor was omitted. In order to keep the propane in the liquid form, the sampler collection system was modified as follows: Two separated high pressure and high temperature transparent borosilicate tubes were connected immediately at the valve located at the exit of the core holder (**Figure 5-4**). One of the valves was used to collect the produced diluted oil while the other was used to collect the hot water produced. Solvent produced was in the gaseous form during the hot water injection stage. To maintain the solvent in liquid form and to avoid flooding the tubes with liquid solvent, nitrogen at high pressure was injected through a high precision syringe pump into both tubes. At the same time, both tubes were connected to a gas flowmeter for experiments with solvent injected in gaseous form.

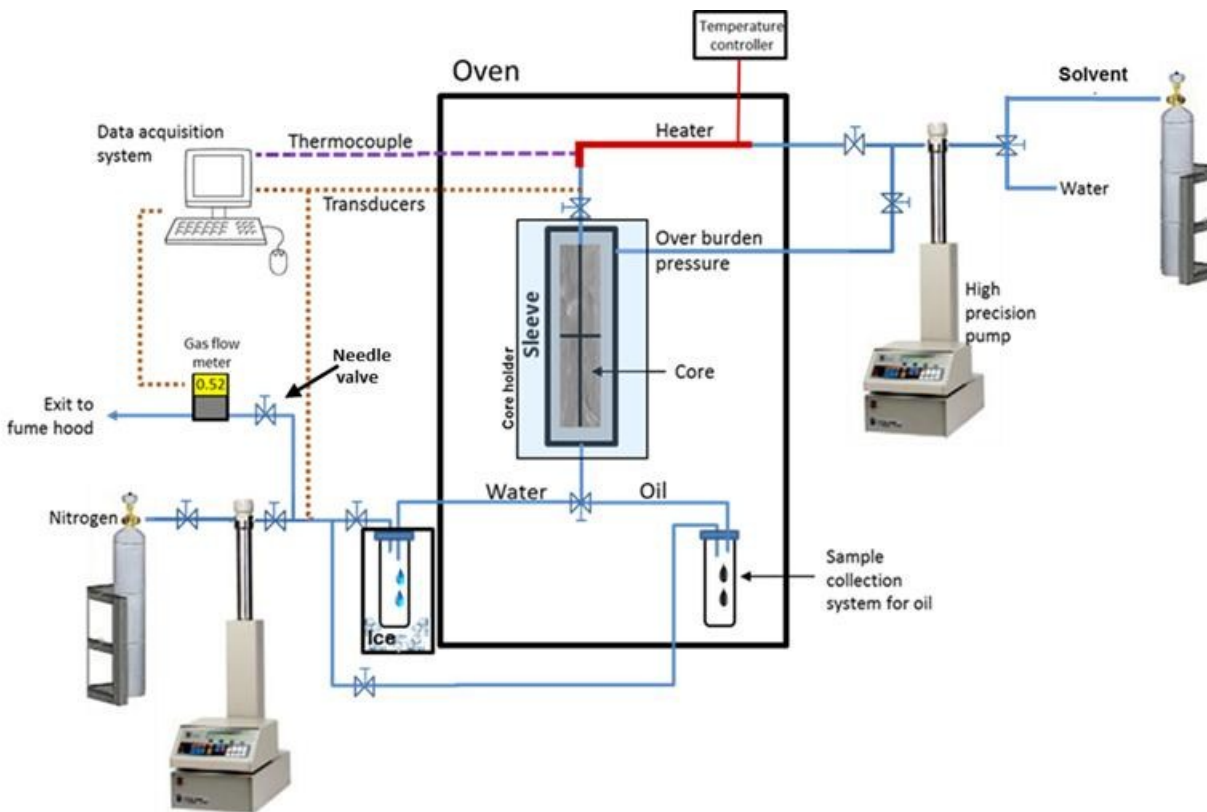


Figure 5-4. Experimental set up used to perform experiments with propane at high pressure.

A total of four experiments were performed for each of the two solvents (propane and heptane); two in the liquid phase and two in the gaseous phase. **Figure 5-5** shows the pressure and temperature conditions selected for each experiment and their relative position to the saturation curve of either propane or heptane. For naphtha, three experiments were performed injecting solvent in liquid phase and two more with solvent in two phases. To achieve this, a chromatographic analysis was performed to the naphtha sample. It was determined that its composition was mainly of hydrocarbons ranging from C_5 to C_{15} . With this composition, the two phase envelope was constructed using the phase behavior option of a commercial numerical simulator. **Figure 5-6** displays the two phase envelope as well as the pressure and temperature conditions proposed for each experiment, showing their relative position with respect to two phase region.

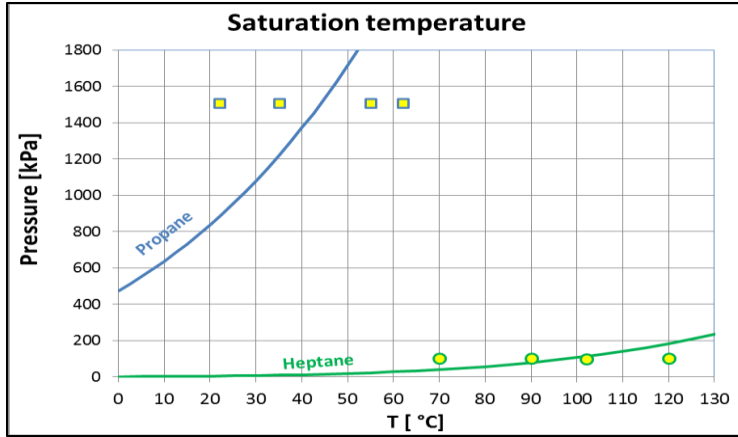


Figure 5-5. Pressure and temperature conditions for experiments performed with propane and heptane.

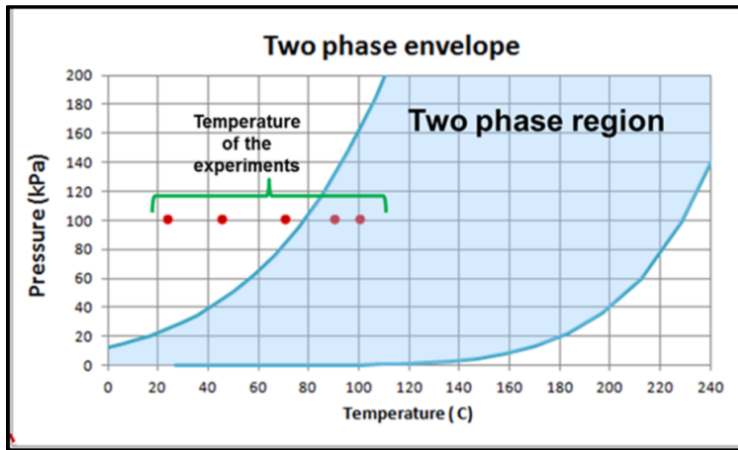


Figure 5-6. Pressure and temperature conditions for experiments performed with naphtha.

Each experiment began by placing the core, as described above, and preheating the oven for several hours until it reaches the desired temperature inside the core. All cores were preheated with both inlet and outlet valves closed. When the desired temperature was reached, the lower valve was opened and oil was allowed to be drained until no more oil was obtained after 30 minutes. The overburden pressure was maintained at atmospheric pressure for heptane and naphtha, and 150 psi (≈ 1034.2 kPa) above the programmed experimental pressure for the propane case.

Experiments performed with either heptane or distilled oil (naphtha). For these experiments, the setup shown in Figure 5-3 was used. After releasing the accumulated oil during the preheating stage, solvent was injected in liquid form at a constant rate of 0.1 mL/min. Oil diluted was collected in a glass tube while solvent vapours were collected through the vapour collection/condensation system. After 1 pore volume of solvent was injected, hot water was started at the same temperature of the solvent at a constant rate of 0.5 ml/min. Water injection continued until no more solvent was recovered at such temperature. At this point, temperature of water was increased to recover more solvent by boiling. The process was repeated until no more solvent was recovered or 100% of injected solvent was recovered. For the experiments with solvent in the gaseous form, the same procedure was followed. Solvent vapour was collected through the vapour collection system as explained above.

Experiments performed with propane. The setup employed for the propane experiments is shown in Figure 5-4. After releasing the cumulated oil during the preheating stage, nitrogen was injected to pressurize the entire system until it reached the programmed pressure. Next, the injection of liquid solvent at high pressure began at a constant rate of 0.1 ml/min and 0.05 ml/min in other cases. The pressure in the system was maintained at a constant pressure by means of the nitrogen pump, working at a constant pressure. From this point forward, the process was the same as in the heptane and naphtha experiments with solvent in liquid form. For experiments with solvent in gaseous form, the valve to the nitrogen pump was closed. After releasing the accumulated oil during the preheating stage, the system was filled up with the gaseous solvent until it reached the desired pressure. Then, solvent injection was started through the core at a constant pressure and the needle valve was regulated to control the gas flow at low rates. The rate oscillated between 0.5 and 1.5 ml/min. The volume of gas produced was recorded using a data acquisition system.

Pressure and temperature were recorded during experiments. Produced fluids were collected and density and RI measurements were performed periodically. The volume of oil diluted and liquid condensate were registered. Initially, a calibration process was carried out for the RI measurements to correlate the solvent concentration in the diluted oil. The calibration process and chart can be found in our previous publication (Leyva-Gomez and Babadagli 2014).

5.5 Results

Figure 5-7 shows the oil recovered from heavy oil saturated Indiana limestone rock matrix by heptane injection. The black dotted line corresponds to the oil recovered. On this line, the first point at 0.0 pore volumes injected correspond to the volume of oil drainage from the fracture after the preheating time and before the solvent injection. The solid brown line corresponds to the cumulative solvent injected at 0.1 ml/min at 70°C, while the dotted orange line represents the cumulative solvent recovered from the diluted oil and condensed vapour. Oil and solvent recovered volumes were periodically calculated based on the RI measurements. In the same figure, it is indicated that after 1.0 pore volume, solvent injection was stopped and hot water injection was started.

It can be seen that all the solvent injected was recovered by hot water injection after injecting 1.7 pore volumes. **Figure 5-8** shows the same experimental data as Figure 5-7 for cumulative solvent injected and recovered but, for simplicity, oil recovered was substituted by the temperature at the center of the core. In this figure, the temperature of water injected is also indicated. After 1.45 pore volumes injected, the temperature of water was increased to 98°C and an immediate increase in solvent recovery was observed. However, the temperature at the center of the core reached 98°C until 1.75 pore volume injected. It is worth mentioning that the temperature of the solvent injected was the same as the temperature of the core during the solvent injection stage. Injection pressure as well as overburden pressure was 1 atm. The same plots were constructed for every single experiment and they are shown in **Appendix A**.

Heptane experiments. Four experiments were performed at atmospheric pressure at 70, 90, 100 and 120°C. Injection rate was 0.1 mL/min in the Indiana limestone experiments. **Figures 5-9 and 5-10** show the RF and solvent retrieved, respectively, for each experiment. **Figures 5-A1 and 5-A2** correspond to the experiment performed at 90°C. As in the case for 70°C, solvent was injected in the liquid form. As seen, after 1.0 pore volumes of solvent injection, hot water injection was started. To increase the volume of solvent, temperature of water was increased to 100°C. **Figures 5-A3 and 5-A4** correspond to the experiment performed at 100°C. Again, at 1.0 pore volume injected hot water, injection began and increasing the temperature of the water was not necessary to recover all of the solvent retained in the rock matrix. **Figures 5-A5 and 5-A6**

correspond to the experiment performed at 120°C. Temperature of water injected was 120°C and it recovered all the solvent retained.

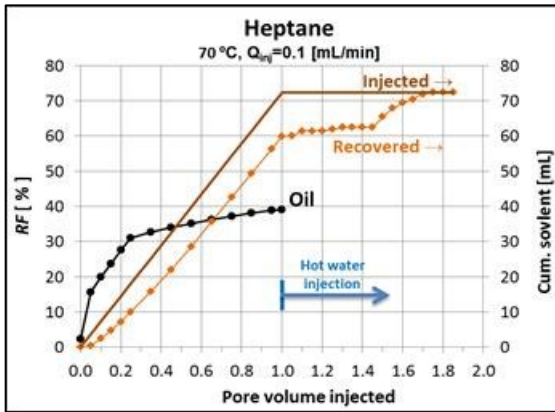


Figure 5-7. Oil produced from experiment performed at 70°C with Indiana limestone and heptane.

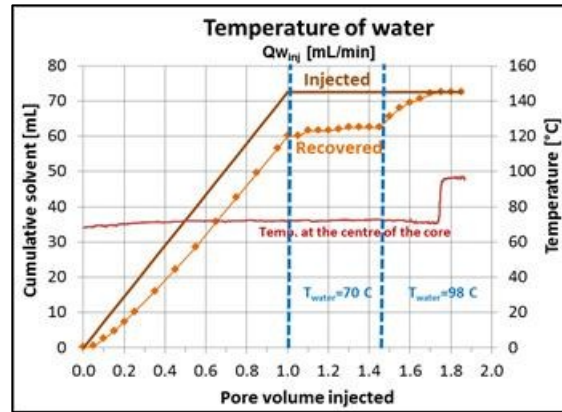


Figure 5-8. Solvent retrieval for experiment performed at 70°C with Indiana limestone and heptane.

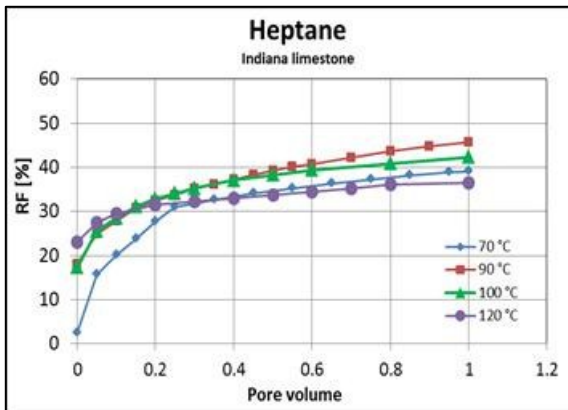


Figure 5-9. Oil recovered from experiments performed with heptane and Indiana limestone.

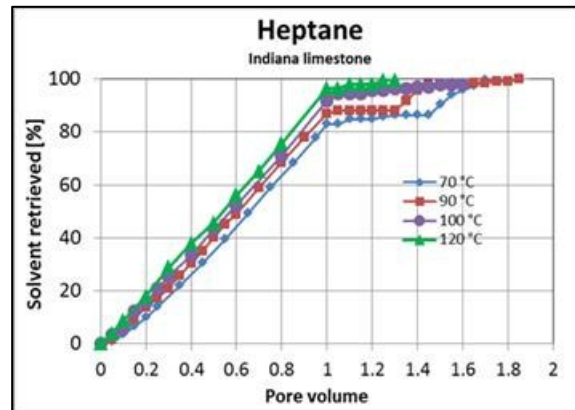


Figure 5-10. Solvent retrieved from experiments performed with heptane and Indiana limestone.

Naphtha experiments. Recovery factor and solvent retrieved for all experiments are shown in **Figures 5-11 and 5-12**. As in the previous case, the experiments were run at atmospheric pressure. Temperatures of the experiments were 21.5, 45, 70, 90, and 100°C. Injection rate was 0.1 [mL/min] through Indiana limestone cores. **Figures 5-A7 and 5-A8** correspond to the experiments performed at 21.5°C. With the water injection at room temperature, no more naphtha was recovered. For this reason, the temperature of water was increased to 100°C.

Experiment with naphtha performed at 45°C is shown in **Figures 5-A9 and 5-A10**. To recover the solvent, water temperature was increased to 100°C at 1.75 pore volumes injected. **Figures 5-A11 through 5-A16** show the results of the experiments performed at 70, 90, and 100°C, respectively. For the experiment at 100°C, almost all the solvent was retrieved without any need for temperature increase.

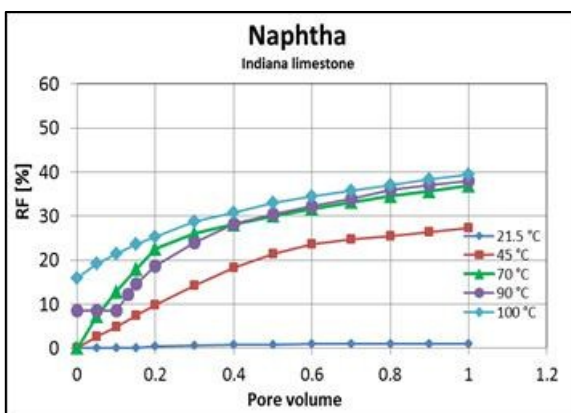


Figure 5-11. Oil recovered from experiments performed with naphtha and Indiana limestone.

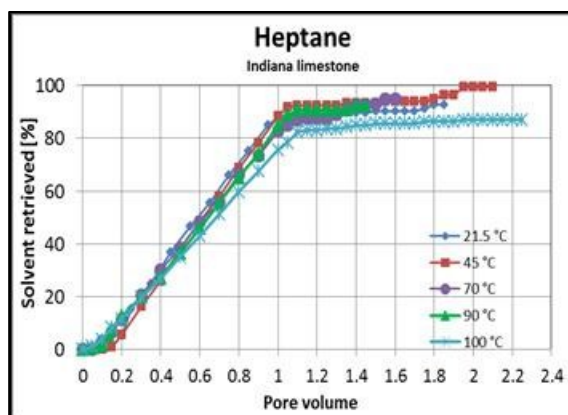


Figure 5-12. Solvent retrieved from experiments performed with naphtha and Indiana limestone.

Propane experiments. We performed experiments with propane at the pressures of 1483–1511 kPa (215.1–219.2 psi) and temperatures of 22, 35, 55, and 60°C. Injection rate was 0.1 ml/min. Due to the range of temperatures, propane was injected in liquid phase in the experiments performed at 22 and 35°C, while for the other two temperatures the solvent was injected in the gaseous form (**Figures 5-13 and 5-14**).

For the case in which solvent was injected in liquid phase (22°C), the fluid recovery was mainly propane. At 0.85 pore volumes, water was injected at 22°C (**Figure 5-A17**). Temperature of water was increased at 60°C when 1.7 pore volumes were reached. As a result of this, 2 ml more solvent was recovered. Only traces of oil were observed in the collection tubes. **Figure 5-15** shows the fluids recovered at the end of the experiment.

In the experiment performed at 35°C, the fluid recovery at the beginning of the experiment was dark, and as the injection continued, the color of the fluid produced became green and light brown (**Figure 5-16**). No water injection was performed in the experiment at 35°C due to low recovery of oil and solvent diffusion (**Figure 5-A18**). The analysis of the sample collected

indicated the existence of mainly propane with nitrogen and the presence of oil components like C7 and above. Due to the very low recovery of oil, the experiment at 35°C was repeated at an injection rate of 0.05 ml/min (**Figure 5-A19**). As in the previous experiment, the fluid recovered was mainly propane brown in color. Not all solvent was recovered and this may be attributed to the propane in the gaseous form, which might have been produced during the hot water injection stage. Asphaltene precipitation was observed when solvent was injected in liquid phase.

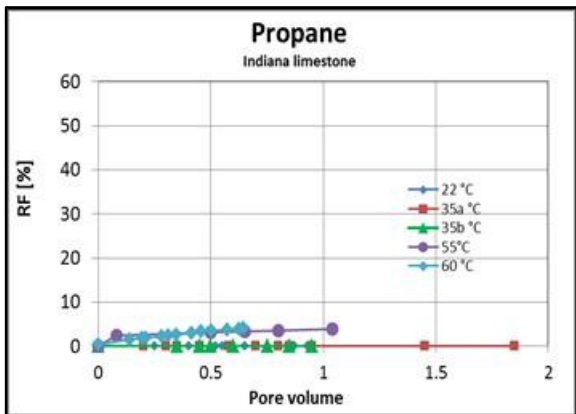


Figure 5-13. Oil recovered from experiments performed with propane and Indiana limestone.

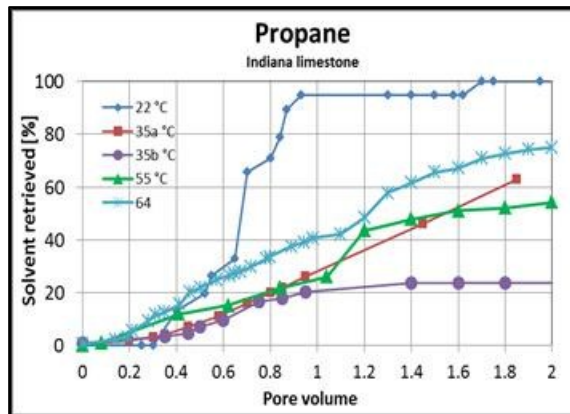


Figure 5-14. Solvent retrieved from experiments performed with propane and Indiana limestone.

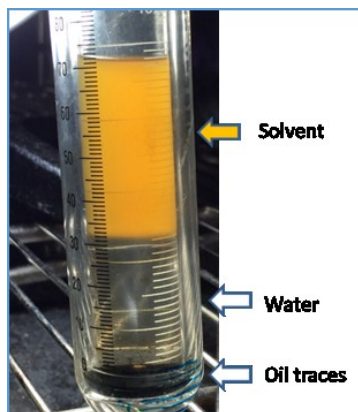


Figure 5-15. Fluid produced during experiment performed at 21°C at a lower injection rate and low temperature. Note the oil traces at the bottom of test tube.



Figure 5-16. Fluids produced during experiment performed at 35°C. Solvent injected in liquid form.

Results obtained from the experiments injecting solvent in gaseous phase are shown in **Figures 5-A20 and 5-A21**. In both experiments, the temperature of the water injected after the solvent

phase was the same as the temperature of injected propane. Water injection at higher temperature was not performed in both experiments due to the capacity of the test tubes.

One experiment was performed with heptane and one more with distillate oil at atmospheric pressure through vuggy naturally fractured carbonate cores (**Figures 5-17 and 5-18**). We injected heptane at 95°C through core No. 1 (**Figures 5-A22 and 5-A23**) and distillate oil at 73°C through core No. 2, just below the saturation temperature of solvent (**Figures 5-A24 and 5-A25**). In both cases, solvent was injected at atmospheric pressure. Temperature for both experiments was chosen close to the saturation temperature and two phase envelope because, as will be explained later, temperatures around the saturation point yielded the highest oil recovery.

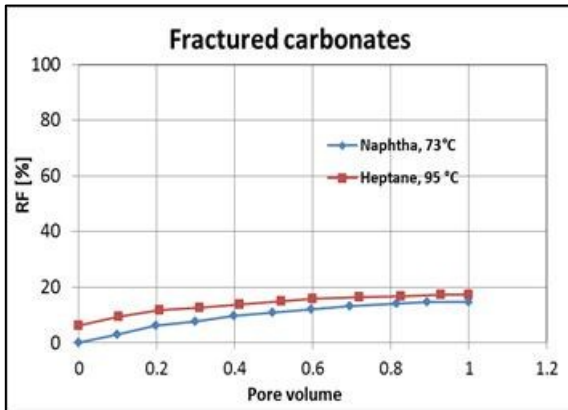


Figure 5-17. Oil recovered from experiments performed with heptane and distilled oil, naturally vuggy fracture carbonate cores.

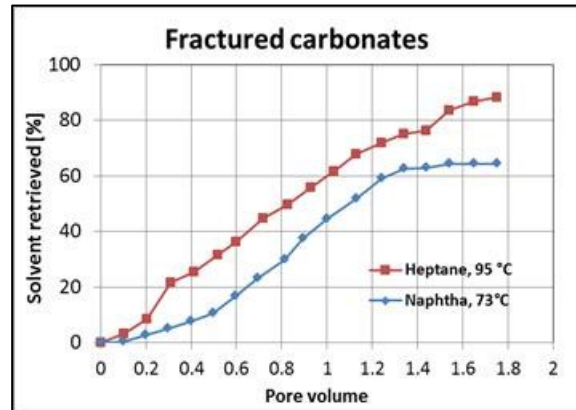


Figure 5-18. Solvent retrieved from experiments performed with heptane and distilled oil, naturally vuggy fracture carbonate cores.

5.6 Analysis of results

Based on the overall recovery from the heptane experiments, the highest recovery was obtained from the experiments that had a temperature closer to the boiling point. This corresponds to the liquid phase zone according to the phase diagram of heptane (**Figure 5-19**). Note, however, that phase behavior might be different due to the Thompson effect and lower saturation temperature is expected in porous media. In this case, one may expect gas-liquid mixture (transition) zone rather than pure liquid phase or even more “gas dominated” heptane phase at the temperature yielding the highest recovery.

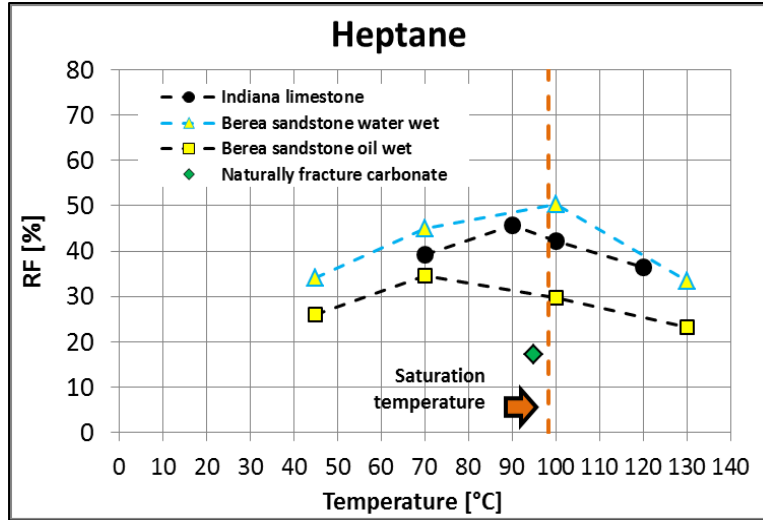


Figure 5-19. Oil recovery factor from experiments with heptane at different temperatures with Indiana limestone and naturally fractured carbonate samples and heptane. Previous results from Leyva and Babadagli (2014) for Berea sandstone are included for comparison.

After this peak point, oil recovery began to decrease as temperature increased, which is also in agreement with our previous observations on sandstone experiments using heptane as solvent (Leyva-Gomez and Babadagli 2014). These observations on the effect of temperature on ultimate recovery by hot-solvent injection need further explanations. As the temperature increases, intermolecular distance increases and the shear stress decreases. This results in a decrease in viscosity benefiting the gravity drainage mechanism. On the other hand, when solvent interacts with heavy oil, a mixing process occurs due to diffusion and dispersion processes. Then, oil becomes diluted and its viscosity also decreases. This in turn, also benefits the gravity drainage. Hayduk and Minhas (1982) proposed an expression for diffusion coefficient considering n-paraffin solutes from C₅ to C₃₂ and n-paraffin solvents from C₅ to C₁₆.

$$D_{AB}^o = 13.3 \times 10^{-8} \cdot T^{1.47} \cdot \left[\frac{\left(\frac{10.2}{V_A^{-0.791}} \right)}{V_A^{0.71}} \right] \quad (5-1)$$

Equation (5-1) suggests that the diffusion coefficient increases as temperature increases. Thus, higher temperature will result in more oil production enhanced by improved diffusion. However,

this process cannot continue indefinitely; as the temperature continues to increase, eventually the saturation conditions of the solvent will be reached. At this point, solvent is vapourized leaving more dense oil with higher viscosity. From this point, the diffusion liquid-liquid is replaced by the diffusion gas-liquid. While it is true that mass transfer between gas solvent and the heavy oil is more efficient, the solubility of gas in heavy oil at constant pressure decreases with increasing temperature. Henni and Shirif (2010) carried out extensive laboratory measurements of solubility and diffusion coefficients for CO₂, ethane, and propane in Lloydminster and Cactus Lake heavy oils. Their results clearly indicate how increasing temperature at a fixed pressure eventually results in a decrease in the fraction of solvent.

If temperature increase goes forward, not only will solvent leave the oil, but also eventually the lighter oil components will be vapourized. As a consequence, more dense and viscous oil will remain in the rock matrix. In such conditions the gravity drainage will slow down. In our experiments, the presence of light components was observed through unclear solvent condensed at temperatures beyond the boiling point. The chromatographic analysis performed at the gas stream and liquid condensed on these samples indicated the presence of lighter components in the produced fluids as well.

Figure 5-20 shows the recovery factor obtained when naphtha was injected through Indiana limestone cores for different temperatures. In contrast with the previous results, recovery is higher even in the gas phase. This was attributed to the multicomponent nature of the solvent (more aromatic content). As stated, its hydrocarbon composition ranges from C₅ to C₁₅. Therefore, its boiling point is higher than heptane and different components (saturates and aromatics) will also have different boiling points. Hence, although some components have been vapourized at 90°C, there will still be liquid solvents present in the mixture. Such components continue diluting the oil while high temperature decreases oil viscosity. Both effects in turn benefit the gravity drainage.

Heavy oil recovery factor obtained from propane injection was the lowest from all the solvents used. Recovery factor obtained at 22 and 35°C was nearly zero (**Figure 5-21**). In contrast with the heptane results, beyond the saturation temperature of propane, a higher oil recovery was obtained. Based on our previous analysis, viscosity reduction of the oil used at 22 and 35°C

would be fairly low to significantly reduce oil viscosity. Thus, the oil trapped in the rock matrix cannot be drained effectively by gravity. This also explains why the recovery factor obtained with naphtha at 21.5°C is so low. At such temperatures, propane is in liquid form and therefore there should be a dilution effect so that oil flows downward. However, this expected positive effect on the recovery was not obtained as similar to our earlier observations (Leyva and Babadagli 2014).

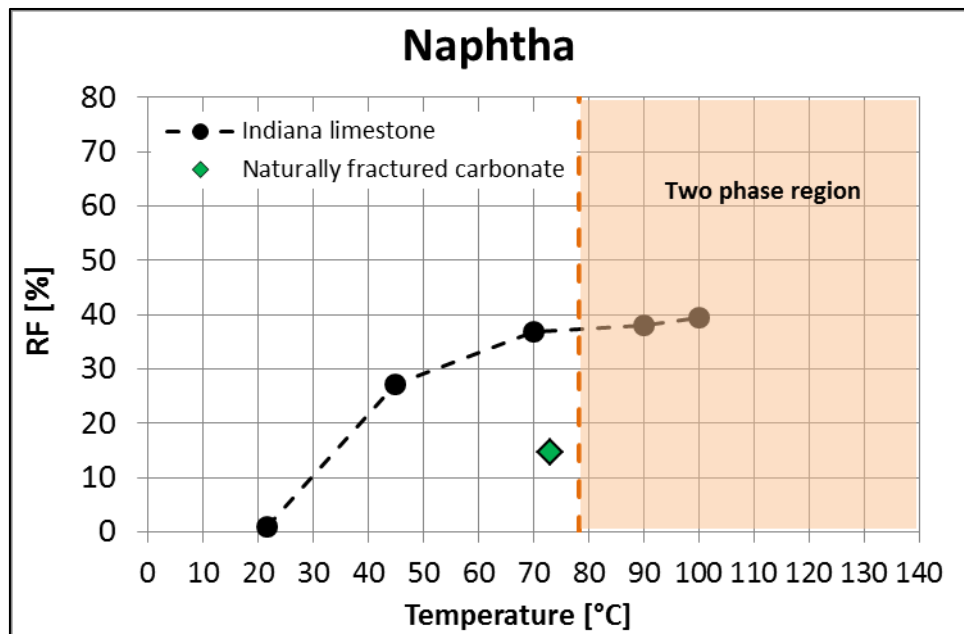


Figure 5-20. Oil recovery factor from experiments with naphtha at different temperatures. Indiana limestone, naturally fracture carbonate, and heptane.

Low recovery factor caused by increasing temperature beyond the saturation point can also be attributed to the pore plugging due to the asphaltene precipitation. Previous experiences show that asphaltene precipitation decreases as the carbon number of solvent increases (Rahimini et al. 1998; Papadimitriou et al. 2007; Moreno and Babadagli 2013). Moreno and Babadagli (2014a-b) performed high temperature solvent injection experiments using propane, n-hexane, n-decane, and distilled hydrocarbon through sand pack systems saturated with heavy oil. The experimental pressure and temperature ranges were 100-300 psi and 25-120°C, respectively. They demonstrated that for the propane case, the oil recovery was lower than for the other solvents used. Visual data on the sand packs' grains from an optical microscope showed that a reduction of the fluid pathways occurred. In our case, it would be reasonable to expect a lower

oil recovery with propane for the same reason. In fact, the core from the experiment at 35°C was cut through the vertical axis and no significant change from the original state of the core was observed. This can be an indication of a permeability reduction around the surface of the core where solvent is exposed to oil first. Consequently, this prevents any solvent diffusion into the matrix causing low oil recovery. The experiment at 35°C was repeated and a similar behavior was observed. A higher recovery was obtained at 55 and 60°C and one may conclude that a lower injection rate is needed along with a temperature range of greater than 50°C when propane is injected.

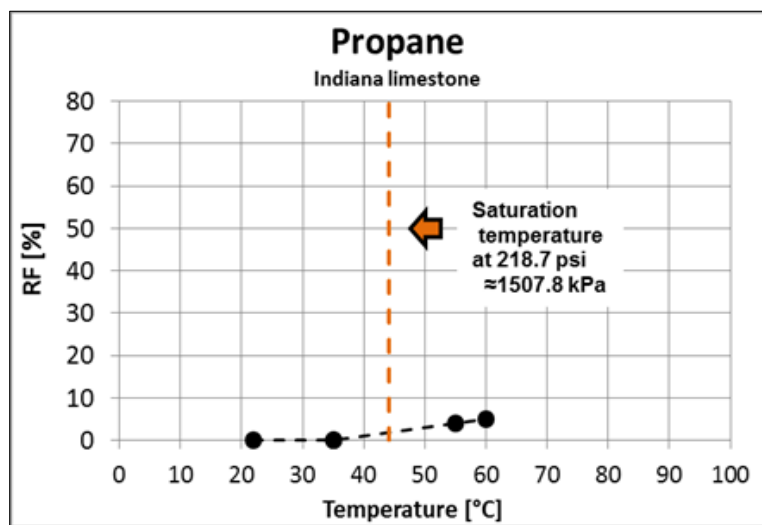


Figure 5-21. Oil recovery factor from experiments with propane at different temperatures with Indiana limestone.

Oil recovery factor from the carbonate rock matrix (obtained from an outcrop of a producing formation in Mexico) was lower than that of Berea sandstone and Indiana limestone. Figures 5-19 and 5-20 compare the recovery fractured carbonate with the other rock matrices. Visual inspection of the cores samples after experimentation unveils the lower recovery. **Figure 5-22** shows a section of core # 1 after the experiment. The heterogeneity of the rock and extremely tight portion of matrix did not allow for a full saturation in certain regions despite a long saturation process under vacuum. In other words, certain portions vuggy and fissured parts were well saturated whereas no oil could penetrate certain parts due to extremely tight (perhaps no permeability) segments of the core. **Figure 5-23** shows a section of core #2. After the experiment, some vugs were found still saturated with heavy oil. It was observed that asphaltene

was precipitated in the fractures. Some of the vugs, mainly the small ones, were found to be fully plugged (**Figure 5-24**). It is obvious that even the vugs were not fully drained due to asphaltene deposition and poor connectivity with the other parts of the rocks via fissures or so (matrix and other vugs).



Figure 5-22. Core after injecting heptane at 73°C showing zones that apparently were not saturated with heavy oil.



Figure 5-23. Trapped oil, after experiment with distillate oil at 90°C.

Solvent retrieval is also critical in this process. It was observed that as the temperature of the experiment was increased, less volume of solvent is retained in the rock matrix. More solvent is produced along with the oil (before hot water injection) and then in the gaseous form (during hot water injection). **Figure 5-25** shows the heptane recovered at different temperatures during the water injection processes from Indiana limestone and naturally fractured carbonate. One may observe that above the saturation temperature, all the solvent can be recovered with the exception of the naturally fractured carbonate. This can be attributed to heterogeneity and poor connectivity of this rock sample.

For naphtha, an increase in temperature until reaching the bubble point was not enough to recover the solvent retained in the rock matrix (**Figure 5-26**). Naphtha is a multicomponent liquid where each component has a different boiling temperature that increases as the carbon number increases (**Table 5-4**). Hence, it is necessary to reach higher temperatures to boil all the components for a better solvent retrieval. For example, for the retrieval of C5 to C10, it is necessary to increase the temperature of water to 174°C.

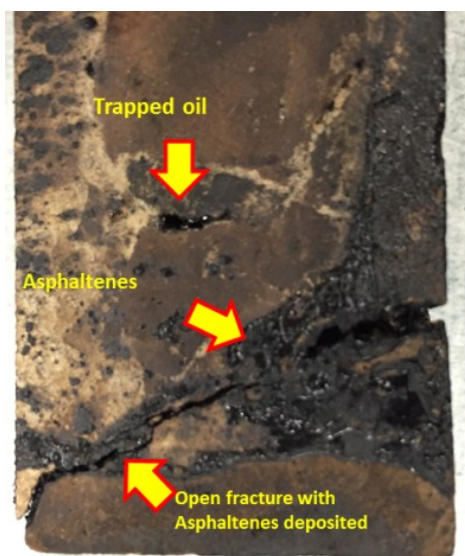


Figure 5-24. Core after injecting naphtha, showing asphaltene deposited on fractures.

Figure 27 shows the propane retrieved by hot water injection. At the end of the solvent injection stage of the experiment performed at 22 °C, nearly 94% of propane was recovered (blue diamond marks). This volume increased to 100 % with hot water injection at 60°C. In the experiment performed at 35°C, 82% of propane was recovered at the end of the solvent injection stage (red square mark). No water injection was done in this particular experiment. As commented before, this particular experiment was repeated at the same pressure and temperature but with an injection rate of 0.05 ml/min. During the experiment, an unquantified volume of propane was vaporized and produced along the experiment. In consequence, the volume of propane recovered during hot water injection was not recorded reliably and were not marked in Figure 27. The volume, however, is expected to be close to the previous lower temperature experiment.

For temperature above the saturation point, the propane was injected and retrieved as gas. Capturing the exact amount of gas through gas flow meter was not practically easy. In the experiment run at 55 °C, 26% of the propane injected was retrieved at the end of the solvent injection stage. In the next stage, hot water was injected at the same temperature, and the volume of solvent recovered reach 54% (purple circle mark). Water injection at higher temperatures was not performed because the test tubes were totally filled with water at 55°C. In the experiment at 60 °C, 41% of propane was recovered at the end of solvent injection, reaching 75% at the end of hot water injection stage. In this case, hot water was injected at 60 °C. Test tubes were filled with

water leaving no room for water injection at higher temperature. Although the amounts recorded are approximate due to experimental difficulties, the trends in Figure 27 indicate that the retrieval of propane while it is in the gas phase (right part of the red dashed line representing the saturation point) can be improved by increased temperature. However, oil recovery was significantly lower than liquid solvents (heptane and naphtha) and this makes this solvent an ineffective choice even if its full retrieval is achieved.

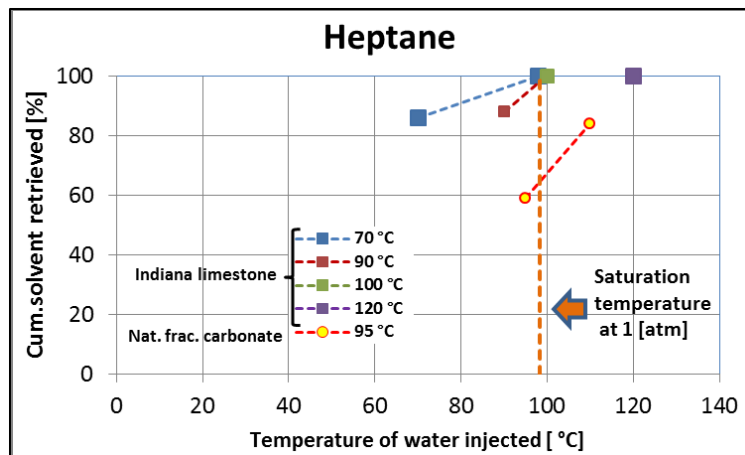


Figure 5-25. Heptane retrieved during the water injection processes. Colors correspond to the temperature of solvent injected previously. Experiments performed either with Indiana limestone and naturally fractured carbonate sample.

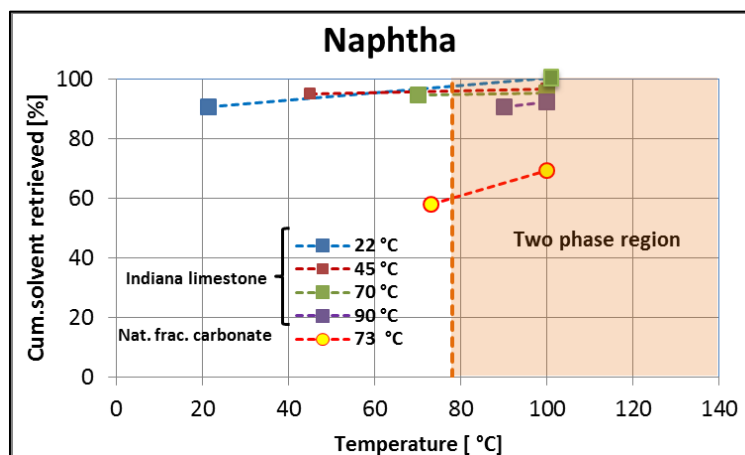


Figure 5-26. Naphtha retrieved during the water injection processes. Colors correspond to the temperature of solvent injected previously. Experiments performed either with Indiana limestone or naturally fractured carbonate.

Table 5-4. Normal boiling point for some alkanes (Ahmed 1989).

Alkane	Boiling point (°C)
C_3H_8	-42.1
C_5H_{12}	36.1
C_6H_{14}	68.7
C_7H_{16}	98.4
C_8H_{18}	125.7
C_9H_{20}	150.8
$C_{10}H_{22}$	174.0

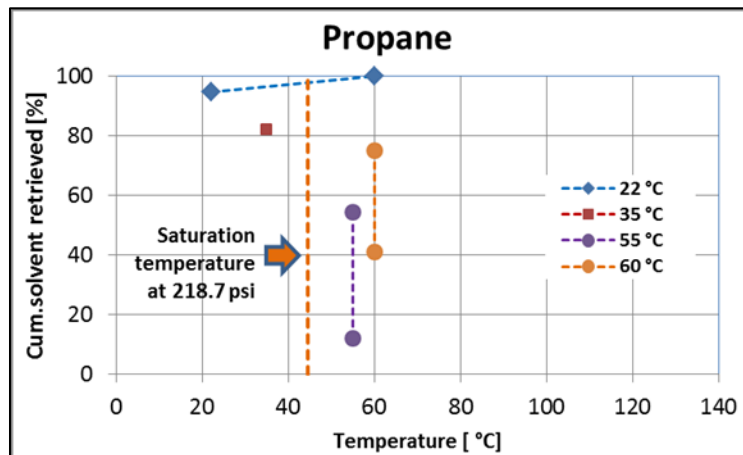


Figure 5-27. Solvent retrieved from propane experiments for Indiana limestone

5.7 Conclusions

Based on our results and observations, we can conclude the following:

1. For the solvent used in this research, the higher recovery was obtained when the operation pressure and temperature were located near to the saturation temperature of solvent, but in the liquid phase zone.
2. Beyond the saturation temperature, oil recovery factor decreased as the lighter components of heavy oil began to be dragged by the solvent gas stream.
3. Heavy oil recovery by propane required lower rates to enable diffusing time of the

solvent into the rock matrix. Skin damage was found on the surface of the cores caused by asphaltene precipitation, which limited solvent intrusion into matrix. With propane, higher temperatures were needed to reduce oil viscosity and accelerate oil gravity drainage. However, increasing temperature also caused an increase in pressure, which was unfavorable as it caused faster injection rates and solvent to remain in the liquid phase.

4. Higher recovery factors were obtained for the heptane case. This can be attributed to a lower asphaltene precipitation and higher temperatures applied. However, when recovery from Indiana limestone is compared with that obtained from Berea sandstone, the oil recovery results to be lower, which can be attributed to higher permeability and porosity of the sandstone sample than Indiana limestone. For the naphtha case, oil recovery trend was similar to that obtained with heptane. However, naphtha recovery resulted to be lower as the saturation temperature of heptane was reached to 98.4 °C, while it is at 78.4 °C for naphtha.
5. In the naturally fractured carbonate samples, the fracture/vug network facilitated solvent diffusion into the rock matrix; however, they may be obstructed by asphaltene precipitation. For this reason, it is important to choose a solvent with higher number of carbon to minimize this effect.
6. Naturally fractured carbonates had a lower recovery than Indiana limestone with naphtha, due to the heterogeneity and poor connectivity of fissures and vugs. Some parts of the rock were observed to be extremely tight (matrix) and no oil saturation was even possible.
7. Most of the heptane was recovered injecting hot water at the saturation temperature. For naphtha, it was necessary to consider higher temperatures due to its multicomponent nature.

5.8 Nomenclature

D_{AB}^0	Diffusivity at infinite dilution of A in B [cm^2/s]
T	Absolute temperature [$^{\circ}\text{K}$]
V_A	Molar volume at the normal boiling point of solute [cm^3/mol]
μ_B	Solvent viscosity [$\text{mPa}\cdot\text{seg}$]

5.9 References

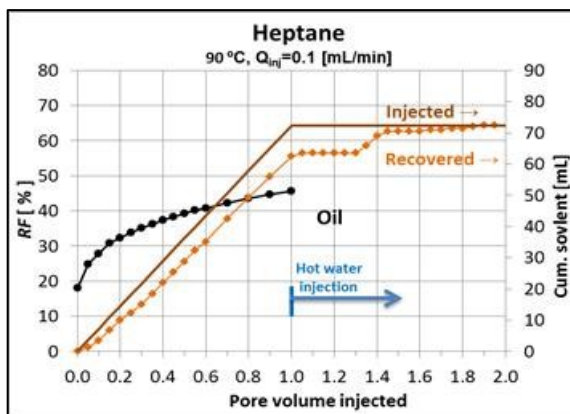
- Ahmed, T. 1989. *Hydrocarbon Phase Behaviour. Contributions on in Petroleum Geology and Engineering* 7 (6-8). Gulf Publishing Company.
- Butler, R.M. and Mokrys, I.J. 1991. A New Process (VAPEX) for Recovering Heavy Oils Using Hot Water and Hydrocarbon Vapour. *J. Cdn. Pet. Tech.* **30** (1): 97–110. <http://dx.doi.org/10.2118/91-01-09>.
- Butler, R.M. and Mokrys, I.J. 1993. Recovery of Heavy Oils Using Vapourized Hydrocarbon Solvents: Further Development of the VAPEX Process. *JCPT* **32** (6): 38–55. <http://dx.doi.org/10.2118/SS-92-7>.
- Edmunds, N., Barrett, K., Solanki, S., Cimolai, M. and Wong, A. 2009. Prospects for Commercial Bitumen Recovery from the Grosmont Carbonate, Alberta. **48** (9): 26–32. <http://dx.doi.org/10.2118/09-09-26>.
- Haghighat, P. and Maini, B.B. 2013. Effect of Temperature on VAPEX Performance. *JCPT* **52** (6). <http://dx.doi.org/10.2118/2009-115>.
- Hayduk, W. and Minhas, B. S. 1982. Correlations for Prediction of Molecular Diffusivities in Liquids. *Can. J. Chem. Eng.* **60**: 295–299. Doi:10.1002/cjce.5450600213.
- Henni, A. and Shirif, E. 2010. Solubility and Diffusion Coefficients of Gases in Heavy Oil and its Fractions. Petroleum Technology Research Centre. Available at the STEPS Research Library. http://steps.ptrc.ca/concrete/files/2714/0554/7521/D7_-_001-00148-UOR_Final_Report.pdf.
- Kaneko, F., Nakano, M., Imai, M., and Nishioka, I. 2013. How Heavy Gas solvents Reduce Heavy Oil Viscosity? SPE 165451, Heavy Oil Conference Canada, Calgary, Alberta, Canada, 11–13 June. <http://dx.doi.org/10.2118/165451-MS>.
- Leyva-Gomez, H. and Babadagli, T. 2014. Optimal Application Conditions for Heavy-Oil/Bitumen Recovery by Solvent Injection at Elevated Temperatures. SPE 172901, SPE Heavy Oil Conference and Exhibition, Mangaf, Kuwait, 8–10 December. <http://dx.doi.org/10.2118/172901-MS>.
- Leyva-Gomez, H. and Babadagli, T. 2016. Hot Solvent Injection for Heavy Oil/Bitumen Recovery from Fractured Reservoirs: An Experimental Approach to Determine Optimal Application Conditions. *Energy Fuels* **30** (4): 2780–2790. Doi: 10.1021/acs.energyfuels.6b00044
- Moreno, L. and Babadagli, T. 2013. Asphaltene Precipitation, Flocculation and Deposition During Solvent Injection at Elevated Temperatures for Heavy Oil Recovery. *Fuel* **124**: 202–211. <http://dx.doi.org/10.1016/j.fuel.2014.02.003>.
- Moreno, L. and Babadagli, T. 2014a. Selection of Optimal Solvent Type for High Temperature Solvent Applications in Heavy-Oil and Bitumen Recovery. SPE 170021, Oil Conference-Canada, Calgary, Alberta, Canada, 10–12 June. Doi:10.2118/170021-MS.

- Moreno, L. and Babadagli, T. 2014b. Optimal Application Conditions of Solvent Injection Into Oil Sands to Minimize the Effect of Asphaltene Deposition: An Experimental Approach. *SPE Res. Eval and Eng.* **17** (4): 530–546. Doi:10.2118/165531-PA.
- Naderi, K., Babadagli, T. and Coskuner, G. 2013. Bitumen Recovery by the SOS-FR (Steam-Over-Solvent Injection in Fractured Reservoirs) Method: An Experimental Study on Grosmont Carbonates. *Energy and Fuels* **27**: 6501–6517. Doi: 10.1021/ef401333u.
- Naderi, K. and Babadagli, T. 2014. Use of Carbon Dioxide and Hydrocarbon Solvents During the Method of Steam-Over-Solvent Injection in Fractured Reservoirs for Heavy-Oil Recovery From Sandstones and Carbonates. *SPE Res. Eval and Eng.* **17** (2): 286–301. Doi:10.2118/169815-PA.
- Pathak, V and Babadagli, T. 2010. Hot Solvent Injection for Heavy Oil/Bitumen Recovery: An Experimental Investigation. SPE 137440, Canadian Unconventional Resources & International Petroleum Conference, Calgary, Alberta, 19–21 October. <http://dx.doi.org/10.2118/137440-MS>.
- Pathak, V., Babadagli, T., and Edmunds, N.R. 2011a. Mechanics of Heavy Oil and Bitumen Recovery by Hot Solvent Injection. SPE 144546, Western North American Regional Meeting, Anchorage, Alaska, 7–11 May. Doi:10.2118/144546-PA.
- Pathak, V., Babadagli, T., and Edmunds, N.R. 2011b. Heavy Oil and Bitumen Recovery by Hot Solvent Injection. *J. Petr. Sci. and Eng.* **78**: 637-645. <http://dx.doi.org/10.1016/j.petrol.2011.08.002>.
- Pathak, V., Babadagli, T. and Edmunds, N.R. 2012. Mechanics of Heavy Oil and Bitumen Recovery by Hot Solvent Injection. *SPE Res. Eval. and Eng.* **15** (2): 182–194. Doi:10.2118/144546-PA
- Pathak, V., Babadagli, T. and Edmunds, N.R. 2013. Experimental Investigation of Bitumen Recovery from Fractured Carbonates Using Hot-Solvents. *JCPT* **52** (4): 289–295. Doi:10.2118/159439-PA.
- Papadimitriou, N., Romanos, G., Charalambopoulou, G., et al. 2007. Experimental Investigation on Asphaltene Deposition Mechanism During Oil Flow in Core Samples. *J. Pet. Sci. Eng.* **57** (3-4): 281–293. <http://dx.doy.org/10.1016/j.petrol.2006.10.007>.
- Rahimi, P., Ellenwood, R., Parker, R., et al. 1998. Partial Upgrading of Athabasca Bitumen Froth by Asphaltene Removal. Proc., 7th Unitar International Conference on Heavy Crude and Tar Sands, Beijing, China, Vol. 1998.074, 1–8.
- Rahnema, H., Kharrat, R., and Rostami, B. 2008. Experimental and Numerical Study of Vapor Extraction Process (VAPEX) in Heavy Oil Fractured Reservoir. Canadian International Petroleum Conference/SPE Gas Technology Symposium Joint Conference (Petroleum Society's 59th Annual Technical Meeting), Calgary, Alberta, Canada, 17–19 June. Doi:10.2118/2008-116.
- Rezaei, N. and Mohammadzadeh, O. 2010. Pore-Level Investigation of Heavy Oil and Bitumen Recovery Using Hybrid SAGD. SPE 130011, 2010 SPE Improved Oil Recovery Symposium, Tulsa, Oklahoma, 24–28 April. Doi:10.2118/130011-MS.

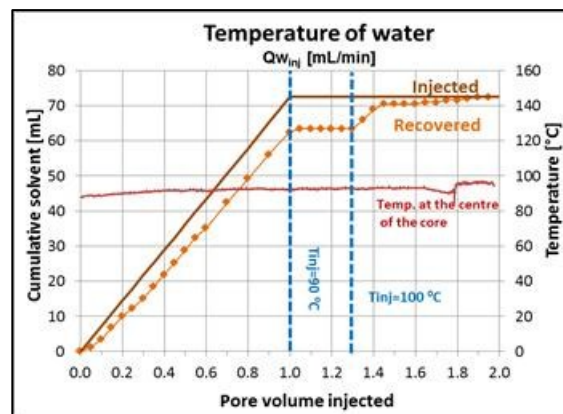
Rostami, B., Azin, R., and Kharrat, R. 2005. Investigation of the Vapex Process in High Pressure Fractured Heavy Oil Reservoirs. SPE 97766-MS, 2005 International Thermal Operations and heavy Oil Symposium, Calgary, Alberta, Canada, 1–3 November. <http://dx.doi.org/10.2118/97766-MS>.

Syed, F. I., Ghedan, S. G., Al-Hage, A. et al. 2012. Formation Flow Impairment in Carbonate Reservoirs Due to Asphaltene Precipitation and Deposition during Hydrocarbon Gas Flooding. SPE 160253, Abu Dhabi International Petroleum Conference and Exhibition, Abu Dhabi, UAE, 11–14 November. <http://dx.doi.org/10.2118/160253-MS>.

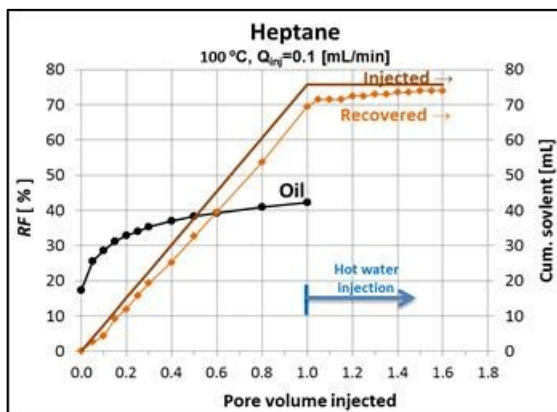
5.10 Appendix



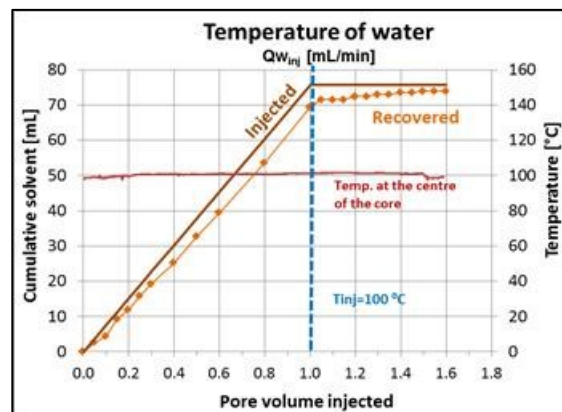
5-A1. Oil produced from experiment performed at 90°C with Indiana limestone and heptane.



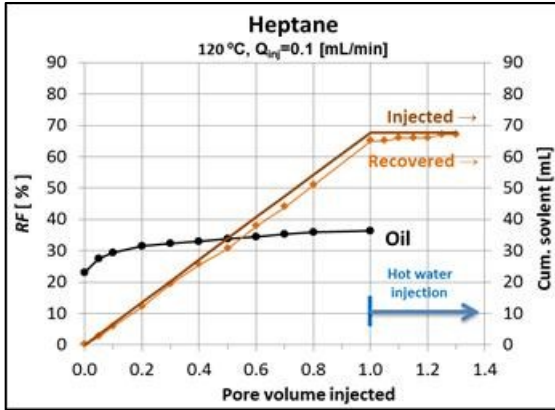
5-A2. Solvent retrieval for experiment performed at 90°C with Indiana limestone and heptane.



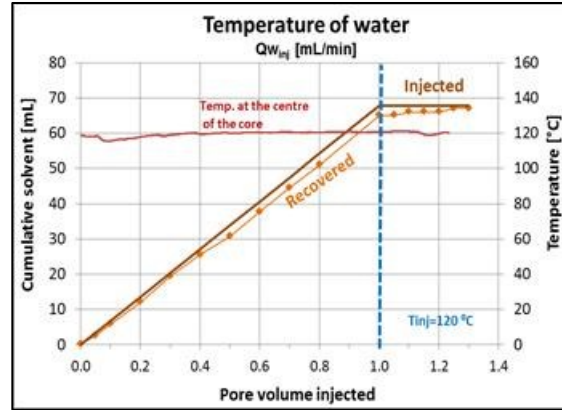
5-A3. Oil produced from experiment performed at 100°C with Indiana limestone and heptane.



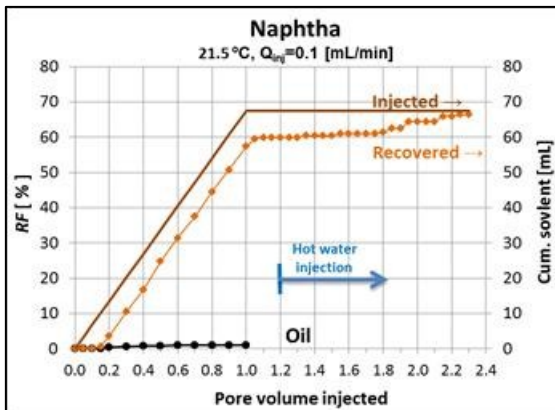
5-A4. Solvent retrieval for experiment performed at 100°C with Indiana limestone and heptane.



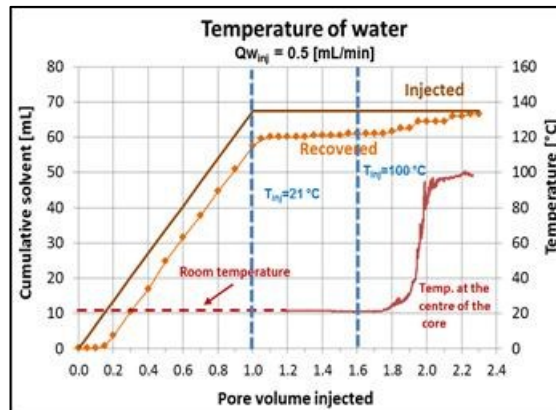
5-A5. Oil produced from experiment performed at 120°C with Indiana limestone and heptane.



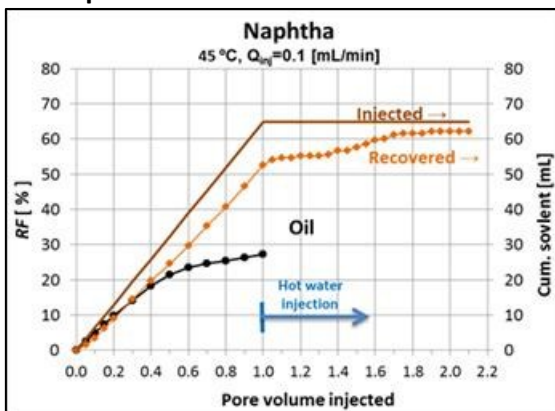
5-A6. Solvent retrieval for experiment performed at 120°C with Indiana limestone and heptane.



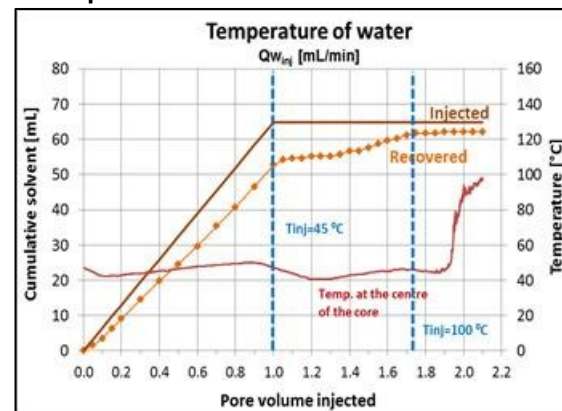
5-A7. Oil produced from experiment performed at 21.5°C with Indiana limestone and naphtha.



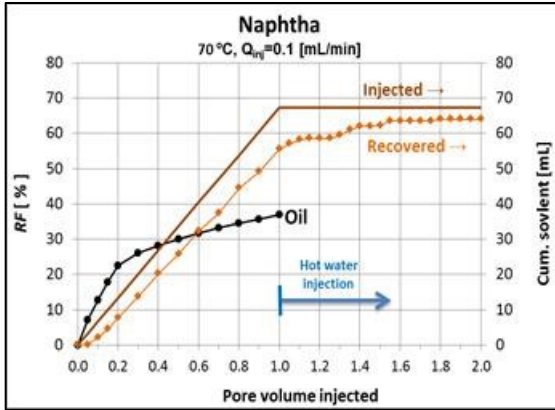
5-A8. Solvent retrieval for experiment performed at 21.5°C with Indiana limestone and naphtha.



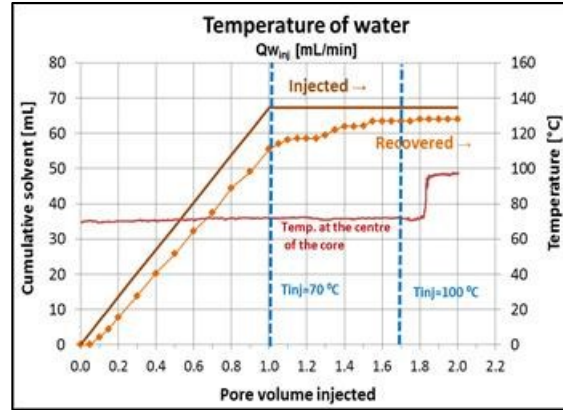
5-A9. Oil produced from experiment performed at 45°C with Indiana limestone and naphtha.



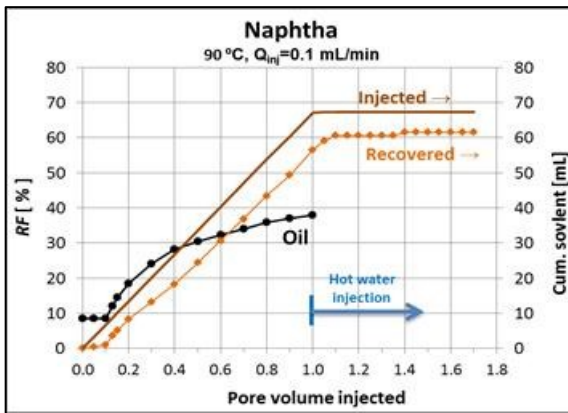
5-A10. Solvent retrieval for experiment performed at 45°C with Indiana limestone and naphtha.



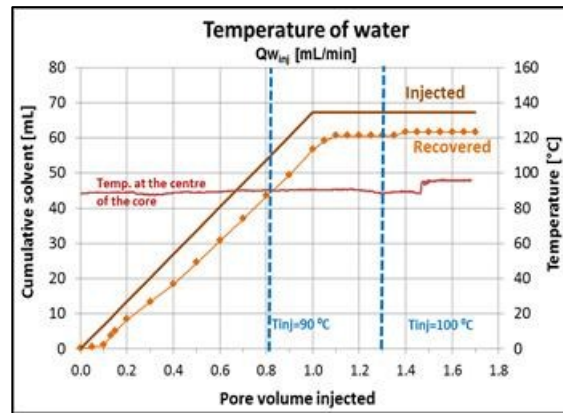
5-A11. Oil produced from experiment performed at 70°C with Indiana limestone and naphtha.



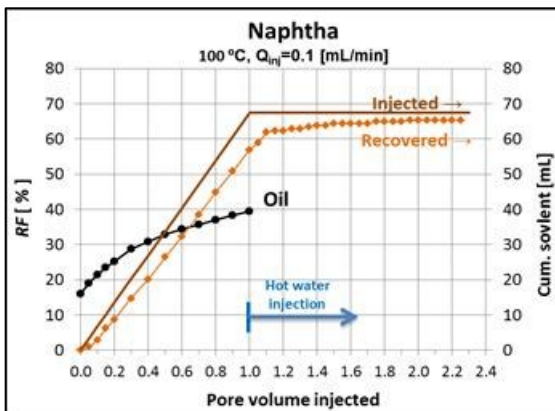
5-A12. Solvent retrieval for experiment performed at 70°C with Indiana limestone and naphtha.



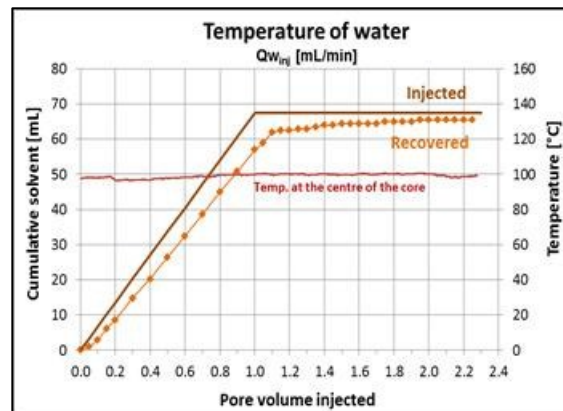
5-A13. Oil produced from experiment performed at 90°C with Indiana limestone and naphtha.



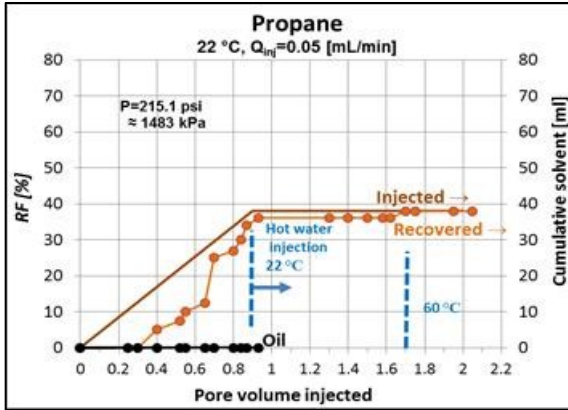
5-A14. Solvent retrieval for experiment performed at 90°C with Indiana limestone and naphtha.



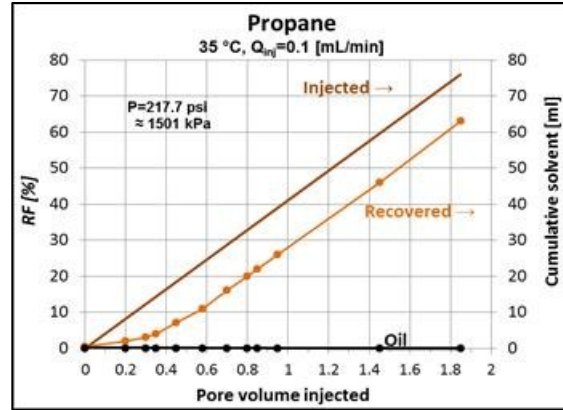
5-A15. Oil produced from experiment performed at 100°C with Indiana limestone and naphtha.



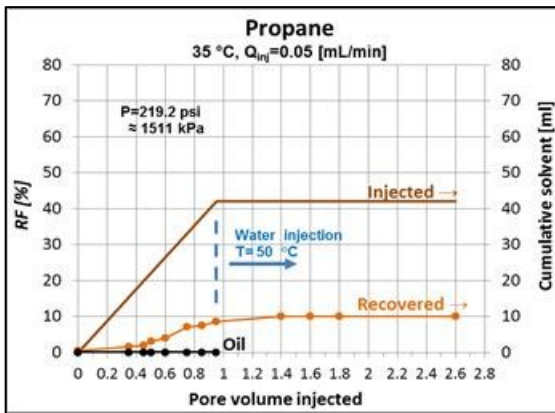
5-A16. Solvent retrieval for experiment performed at 100°C with Indiana limestone and naphtha.



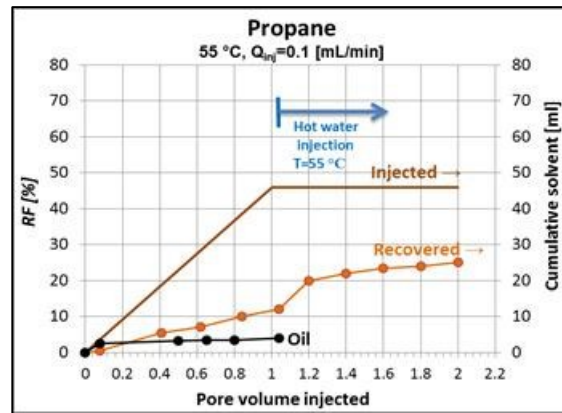
5-A17. Oil diluted and produced solvent retrieved from experiment performed at 22°C with Indiana limestone and liquid propane.



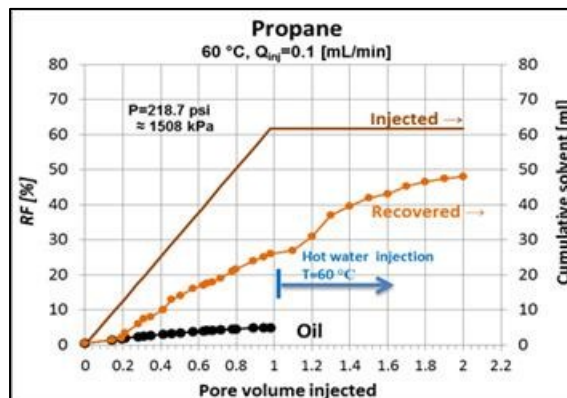
5-A18. Solvent retrieval for experiment performed at 35°C with Indiana limestone and liquid propane.



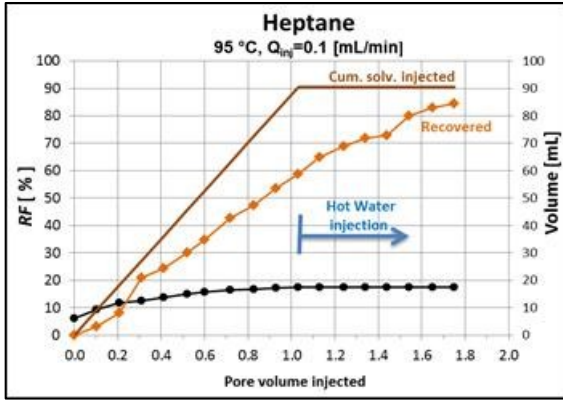
5-A19. Oil produced and solvent retrieved from experiment performed at 35°C with Indiana limestone and liquid propane.



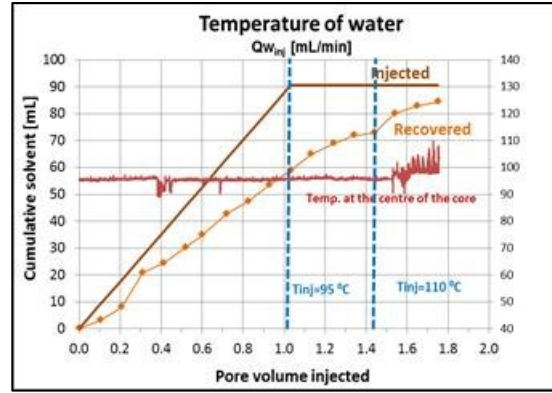
5-A20. Oil produced and solvent retrieval for experiment performed at 55°C with Indiana limestone and gaseous propane.



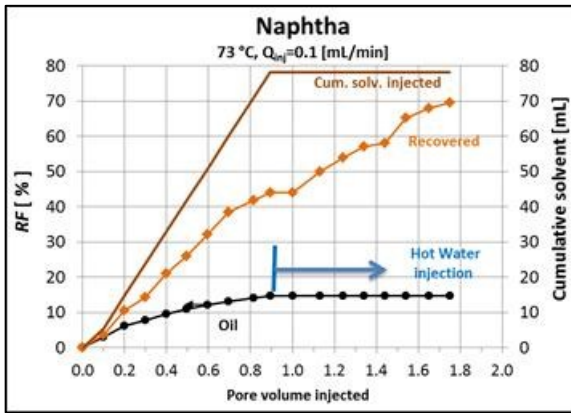
5-A21. Oil produced and solvent retrieved from experiment performed at 60°C with Indiana limestone and gaseous propane.



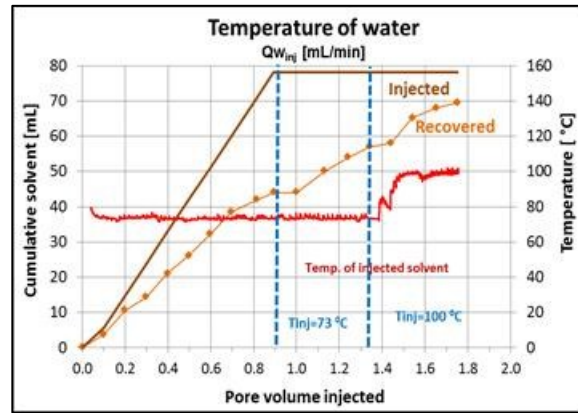
5-A22. Oil recovered from experiment performed at 95 °C with naturally fractured carbonate sample and heptane.



5-A23. Solvent retrieval for experiment performed at 95°C with naturally fractured carbonate sample and heptane.



5-A24. Oil produced from experiment performed at 73°C with naturally fractured carbonate sample and naphtha.



5-A25. Solvent retrieval for experiment performed at 73°C with naturally fractured carbonate sample and naphtha.

Chapter 6 : Summary, Contributions and recomendations

6.1 Summary of the research

Firstly, the injection of propane and butane through either sandstone or glass beads cores saturated with heavy oil/bitumen was simulated by radial 3D numerical model of $15 \times 1 \times 48$ cells to simulate this process. The results were matched to data from experiments in which heavy oil saturated either Berea sandstone or sand packs made of glass beads were exposed to solvent vapour at high temperature. A pressure-temperature sensitivity analysis was carried out for different core sizes to understand the dynamics of gravity drainage process associated with asphaltene precipitation. Asphaltene pore plugging behavior was modeled and the diffusion of solvent into heavy oil/bitumen was analyzed to determine both ideal solvent type and optimal operating conditions for solvent injection at high pressures and temperatures. Important key parameters such as the minimum solid concentration, flow restriction factor and reaction rate were identified.

Next, a hypothetical field scale numerical model was constructed and the key parameters identified through the aforementioned sensitivity analysis were incorporated. A rectangular 2D grid model of $70 \times 1 \times 50$ cells was constructed to simulate the hot solvent injection into a homogeneous sand reservoir. The model considered the asphaltene precipitation, the key parameters identified previously and the operational cost to produce the heavy oil. Then, injection process was simulated for a two-horizontal injection/production pattern. Four different injection/production schemes were studied for propane solvents. The optimal values of injection/production parameters that maximize the profit were obtained by genetic algorithms.

We also conducted a series of dynamic experiments in which solvent in liquid or gaseous form (propane, heptane, and distilled oil) was injected into heavy oil saturated artificially fractured Berea sandstone, Indiana limestone or naturally vuggy fracture carbonate samples with and without pre-thermal injection. To account for the effect of wettability on the process, experiments were repeated on the samples exposed to wettability alteration (more oil-wet) process. Cores were saturated with heavy crude oil and placed inside a rubber sleeve. Next, the system was placed into an oven and maintained at constant temperature conditions. Then, either hot solvent (superheated to be in vapour phase) or cold solvent was introduced into the system through the fracture at a constant rate. Pressure and temperature was continuously monitored at

the inlet and center of the core when it was possible. Properties of oil and liquid condensate from the gas produced were measured and analyzed. This scheme was repeated for a wide range of temperature conditions. The retrieval of the solvent during solvent injection phase and post-thermal method (steam or hot-water) injection performed for a wide range of temperature was monitored. The optimal temperatures for heavy oil recovery and solvent retrieval, in the subsequent hot water injection, for each kind of rock sample and type of solvent were determined.

6.2 Scientific and practical contributions to the literature and industry

- Heavy-oil recovery using solvent injection depends mainly on pressure and temperature. Simulation results showed that recovery is more sensitive to temperature than to pressure. The oil recovery is greater when the temperature is located near to the saturation curve of solvent but in the liquid phase region. Beyond the saturation temperature, oil recovery factor decreases and the lightest components of the heavy oil begin to be dragged by the solvent gas stream.
- Three parameters were identified as a result of the sensitivity analysis that depend on the type of solvent used and operating conditions (i.e., pressure, temperature):
 1. *Flow restriction factor* gives the restriction to effective permeability, applied to the oil liquid phase as the blockage of flow by the precipitation of solid components into the porous media;
 2. *Reaction rate factor*, which is the speed with which the reaction is proceeding; i.e. the velocity in which the precipitating component (reactant) reacts with the other hydrocarbon components;
 3. *Minimum Solid Concentration*, which is needed in order to start the blockage.
- Also, as a result of the sensitivity analysis was identified that there is a range of temperature in which a major quantity of solids is produced with the oil produced. Out of this range, a major quantity of solids remains inside the core; in a reservoir, it would cause a plugging of the pore throats. Consequentially, in a long core more time is needed to obtain the same

factor recovery than when using a short core. Similarly, more time is needed to obtain the same recovery factor when temperature is above the saturation temperature of the solvent used.

- Heavy oil recovery by injecting propane requires lower rates to allow diffusing the solvent into the rock matrix because the skin damage on the surface of the cores caused by asphaltene precipitation. With propane, higher temperatures are needed to reduce the oil viscosity and benefit the oil gravity drainage. However, rise in the temperature implies higher pressures to keep the solvent in liquid phase.
- Heavy oil recovery by injecting heptane was higher than that obtained using propane. Because of the higher temperature in the heptane experiments, viscosity was lowered, which in turn enhanced the recovery by gravity drainage. At the same time, asphaltene precipitation was lower in the heptane case, which results in less reduction in permeability due to asphaltene deposition than in the propane case.
- Naphtha and heptane yielded a similar amount of heavy oil recovery just below the bubble point and saturation temperature. Above these values, the behaviour was different. Lowered recoveries were obtained with heptane above the saturation temperature while it was higher with naphtha at the temperature range. Above the bubble point temperature, heavier components of naphtha remained in the liquid phase and as consequence of this, diluting process continued.
- In the naturally vuggy fracture carbonates, the fracture network benefits the solvent diffusion into the rock matrix. However, the size of the fracture matters because the smallest will be obstructed by the asphaltene precipitation. For this reason, it is important to choose a solvent with a higher number to reduce this phenomenon, enabling diluted oil to be drained.
- Most of the heptane was recovered injecting hot water at the saturation temperature. For naphtha, it is necessary to consider higher temperatures due to its multi-component nature.

- Heavy oil/bitumen recovery through hot solvent injection process is expensive and highly sensitive to the price of solvent, which entails robust optimization models. In this study, we selected the genetic algorithm to optimize the operational parameters during the exploitation of a reservoir.
- We considered four schemes of solvent injection and oil production. Only a pair of injection/production well system was considered in this study. For all the cases studied we got a negative profit. The most negative economic benefit was obtained from the continuous injection with simultaneous and continuous production scheme with propane or butane. For the other schemes with propane or butane, a less negative profit was obtained but it requires almost the entire life of the project. However, in these cases, the injection/production schemes applied leaves a considerable amount of oil and solvent in the reservoir. Hence, other production processes should be considered after hot solvent injection process to recover the remaining hydrocarbons to increase the profit.
- This paper dealt with complex problem and expensive process. Taking the laboratory scale experimental and simulations as the data base to a field scale optimization scheme, we showed that the inevitable solvent-heat injection combination (especially for extra heavy oil and bitumen cases) may result in a profitable project. The optimal application conditions were identified and critically analyzed to guide the practitioners for their field applications.

6.3 Suggested future work

Experimental studies can be extended to include:

- Perform more experiments with naturally fracture carbonate using other solvent than heptane and distilled oil for a wide range of temperatures.
- Perform some of the experiments above mentioned exclusively to quantify the volume of asphaltenes produced.
- Perform more experiments alternating different types of solvents on a same core.

Numerical simulation modeling can be extended to include:

- Modeling hot solvent injection using a dual porosity model.
- Repeating the numerical simulation using different types of solvent in an alternated way.
- Carrying out the optimization of the hot solvent injection processes of the dual porosity model, using a stochastic model, followed by an additional process to recover the solvent from the reservoir.